



# *Institute of Paper Science and Technology*

## **KRAFT BLACK LIQUOR DELIVERY SYSTEMS**

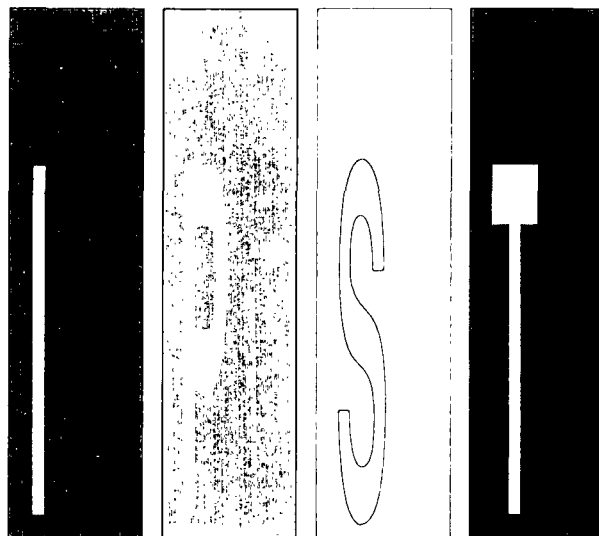
**Project 3657-2**

**Report 4**

**to**

**U.S. DEPARTMENT OF ENERGY  
AND THE  
MEMBER COMPANIES OF THE INSTITUTE OF PAPER SCIENCE AND TECHNOLOGY**

**January 1993**



*Atlanta, Georgia*

## INSTITUTE OF PAPER SCIENCE AND TECHNOLOGY PURPOSE AND MISSION STATEMENT

The Institute of Paper Science and Technology is a unique organization whose charitable, educational, and scientific purpose evolves from the singular relationship between the Institute and the pulp and paper industry which has existed since 1929. The purpose of the Institute is fulfilled through three missions, which are:

- to provide high quality students with a multidisciplinary graduate educational experience which is of the highest standard of excellence recognized by the national academic community and which enables them to perform to their maximum potential in a society with a technological base; and
- to sustain an international position of leadership in dynamic scientific research which is participated in by both students and faculty and which is focused on areas of significance to the pulp and paper industry; and
- to contribute to the economic and technical well-being of the nation through innovative educational, informational, and technical services.

## ACCREDITATION

The Institute of Paper Science and Technology is accredited by the Commission on Colleges of the Southern Association of Colleges and Schools to award the Master of Science and Doctor of Philosophy degrees.

## NOTICE AND DISCLAIMER

The Institute of Paper Science and Technology (IPST) has provided a high standard of professional service and has put forth its best efforts within the time and funds available for this project. The information and conclusions are advisory and are intended only for internal use by any company who may receive this report. Each company must decide for itself the best approach to solving any problems it may have and how, or whether, this reported information should be considered in its approach.

IPST does not recommend particular products, procedures, materials, or service. These are included only in the interest of completeness within a laboratory context and budgetary constraint. Actual products, procedures, materials, and services used may differ and are peculiar to the operations of each company.

In no event shall IPST or its employees and agents have any obligation or liability for damages including, but not limited to, consequential damages arising out of or in connection with any company's use of or inability to use the reported information. IPST provides no warranty or guaranty of results.

The Institute of Paper Science and Technology assures equal opportunity to all qualified persons without regard to race, color, religion, sex, national origin, age, handicap, marital status, or Vietnam era veterans status in the admission to, participation in, treatment of, or employment in the programs and activities which the Institute operates.

INSTITUTE OF PAPER SCIENCE AND TECHNOLOGY

Atlanta, Georgia

KRAFT BLACK LIQUOR DELIVERY SYSTEMS

Project 3657-2

Report 4

A Progress Report

to

U.S. DEPARTMENT OF ENERGY  
AND THE  
MEMBER COMPANIES OF THE INSTITUTE OF PAPER SCIENCE AND TECHNOLOGY

By

H.J. Empie, S.J. Lien, W. Yang, and D.B. Samuels

January 1993

## Kraft Black Liquor Delivery Systems - Report No. 4

### TABLE OF CONTENTS

Abstract . . . . .	i
Acknowledgments . . . . .	ii
Executive Summary . . . . .	iii
1.0 Introduction . . . . .	1
1.1 Objective . . . . .	1
1.2 Deliverables . . . . .	1
1.3 Benefits . . . . .	1
1.4 Organization . . . . .	2
1.5 Schedule . . . . .	3
1.6 Summary of Previous Results . . . . .	3
2.0 Experimental Design for Black Liquor Spraying . . . . .	5
2.1 Black Liquor Spraying Equipment . . . . .	5
2.2 Test Plan . . . . .	6
2.2.1 Previous Work . . . . .	6
2.2.2 Year 4 Test Plan . . . . .	7
2.2.3 Year 5 Test Plan . . . . .	9
2.3 Black Liquor Properties . . . . .	11
2.3.1 Black Liquor Viscosity . . . . .	12
2.3.2 Chemical Analysis . . . . .	14
3.0 Black Liquor Spraying Results . . . . .	16
3.1 Effect of Nozzle Diameter . . . . .	16
3.2 Effect of Black Liquor Variability . . . . .	19
3.2.1 Test Conditions . . . . .	19
3.2.2 Results . . . . .	19
3.2.3 Drop Size Correlations . . . . .	23
3.2.4 Conclusions . . . . .	24
3.3 High Temperature Black Liquor Spraying . . . . .	26
3.3.1 Experimental Test Plan . . . . .	26
3.3.2 Flashing Behavior . . . . .	28
3.3.3 Transition Temperature . . . . .	28
3.3.4 Droplet Diameter . . . . .	31
3.3.5 Flow Coefficients . . . . .	35
3.3.6 Conclusions . . . . .	40

## TABLE OF CONTENTS CONTINUED

3.4	Alternative Commercial Nozzles . . . . .	42
3.4.1	Screening of Nozzle Types . . . . .	42
3.4.2	Drop Formation Test Results . . . . .	42
3.4.3	Conclusions . . . . .	45
3.5	Developmental Nozzles . . . . .	45
3.5.1	Dual Splashplate Nozzle . . . . .	45
3.5.2	Modified Splashplate Nozzles . . . . .	52
3.5.3	Vibratory Assist . . . . .	61
3.5.3.1	Frequency of a Vibrating Nozzle . . . . .	67
3.5.2.2	Transverse Vibrations . . . . .	68
3.5.3.3	Axial Vibrations . . . . .	70
4.0	Conclusions . . . . .	73
5.0	References . . . . .	74

## ABSTRACT

Improvement of spray nozzles for black liquor injection into kraft recovery boilers is expected to result from obtaining a controlled, well-defined droplet size distribution. An environmentally-sound spray facility capable of delivering black liquor at normal firing temperatures has been installed and operated at the Institute of Paper Science and Technology. Drop size data have been obtained under a wide range of process conditions, including liquor type, temperature, and pressure. Traditional splashplate, V-jet, and swirl cone nozzles, along with alternative commercial nozzles, have been investigated. A number of alternative developmental nozzles have been fabricated and their operating characteristics determined. Early results with vibratory-assisted nozzles are also presented.

## ACKNOWLEDGMENTS

The authors thank Stanley F. Sobczynski, Program Manager, Office of Industrial Processes, U.S. Department of Energy, for providing guidance and critical support. The authors would like to acknowledge others who have provided invaluable input and services. Included are the support staff at IPST and industrial contributions from A. Ahlstrom Corp. (Roswell, GA), ABB Combustion Engineering Sys. (Windsor, CT), Babcock & Wilcox (Alliance, OH), Champion International Corporation (Quinnesec, MI), Delavan-Delta, Inc. (W. Des Moines, IA), Inland-Rome, Inc. (Rome, GA), The Mead Corporation (Phenix City, AL), Packaging Corporation of America (Valdosta, GA), Tampella Power Machinery, Inc. (Brunswick, GA), and Union Camp Corporation (Pratteville, AL).

## EXECUTIVE SUMMARY

The research work described in this report represents the results of the fourth year of a four-year project; now extended to five, and designed specifically to develop the optimum black liquor delivery system for the current recovery boiler. Black liquor obtained from normal mill operation is being used in this study.

The primary objectives of the research program have been:

- \* To develop laboratory equipment and methods for quantitatively studying commercial black liquor nozzle designs when spraying kraft liquors at typical operating conditions;
- \* To quantify droplet size distribution, velocity, and mass distribution for commercial nozzles spraying kraft liquors at typical boiler conditions;
- \* To develop techniques currently envisioned for improving the control of black liquor spray droplet size distribution with commercial nozzles; and
- \* To extend current liquor spraying technology by testing several fundamentally different, but commercially viable, delivery systems.

Success with this program should yield benefits in increased thermal efficiency and process productivity, as well as have potential for improvements in equipment design and process control. Coupled with the recovery boiler modeling project currently under way at IPST, the potential value of these programs to the industry is approximately \$93MM/year for increased thermal efficiency and \$240MM/year for increased productivity.

Spraying tests on five different black liquors from four kraft mills were conducted to determine the effect of liquor type on droplet size and size distribution. A wide range of spraying conditions was examined with the finding that liquor type was not important at comparable viscosities; mean drop diameter depended primarily on nozzle type and diameter, pressure, temperature, and liquor viscosity.

The effect on drop size of liquor temperature is complex. Generally, as temperature increased, median drop diameter decreased slightly; eventually a transition temperature was reached at which a sharp decrease of at least 20% occurred. This was accompanied by a change in the sheet cross-section from planar to oval and was attributed to flashing within the nozzle prior to the liquor escaping to the atmosphere. Interestingly, the width of the distribution did not change when the transition temperature was passed. Flow coefficient correlations were established for predicting nozzle pressure drop based on the liquor vapor pressure, which gave a better fit to the data than previous correlations based on atmospheric pressure.



Alternative commercial nozzles were surveyed, including two-phase, sonic, and rotary atomizers and full cone nozzles with and without swirl. Most of these strive to give very fine droplets or mists, which are unsuitable for recovery boiler operation. Ultimately, three of these nozzles were tested, and only one, the Delavan Raindrop<sup>®</sup>, exhibited any noticeable difference in performance. It gave a coarser-than-normal droplet size, but did not result in a different distribution width. None demonstrated any ability to give independent control over drop size distribution.

Development of new nozzle concepts had to recognize the need to accommodate typical mill liquor flow rates and maintain 99%+ reliability. Hence, developmental nozzle activity centered on modified splashplate nozzles with no moving parts. Making various physical changes to the surface of the splashplate (e.g., grooves, slots) resulted in 25% smaller median drop diameters with no change in the distribution width. One design in which small cylindrical pegs were mounted normal to the splashplate surface around its outer periphery also gave smaller drops, but with a larger normalized standard deviation, characteristic of a bimodal distribution. A different design specifically aimed at generating a bimodal distribution employed two different sized orifices back-to-back using the same splashplate. The two liquor sheets formed tended to interact during break-up, giving larger-than-normal droplets with the usual distribution width. The two orifice conditions tested were not different enough to give component median diameters far enough apart that would provide a recognizable bimodal distribution.

It is apparent that gaining any degree of control over drop size distribution is going to require some external force, independent of the viscous, momentum, and surface tension forces which naturally control the droplet formation process. The concept of vibratory assist should provide an independently controlled means of influencing the sheet formation/break-up process. Application of vibrations transverse to the plane of the sheet gave a 15-30% increase in median diameter and distribution width using an air vibrator, but no change in either parameter using a mechanical vibrator. Vibration in the direction of flow (i.e., pulsation) is expected to be more effective for reducing the randomness of the sheet break-up process, and this is presently under investigation. Unfortunately, high frequency pulsation of flow is more difficult to accomplish experimentally and may require an "invention."

#### MAJOR ACTIVITIES FOR YEAR FIVE:

- \* Develop and test a high frequency vibratory device to induce a pulsed liquor flow in an attempt to reduce the randomness of the liquor sheet break-up process.
- \* Collect improved drop size data at temperatures above the transition point using improved droplet imaging techniques.
- \* Conduct mill scale testing of a vibratory-assisted prototype nozzle for performance comparison with existing nozzles.
- \* Propose follow-up implementation study and close out present project (DOE contract expires 9/30/93).

## **Black Liquor Delivery Systems Report No. 4**

### **1.0 INTRODUCTION**

#### **1.1 OBJECTIVE**

This research program was initiated as an applied effort to identify the optimum black liquor delivery system for the kraft recovery boiler and to present it to the industry in a timely fashion. Because it is not known what the preferred conditions for optimum recovery boiler operation are, the fundamental objective has to be to develop ways to control the formation of black liquor droplets such that, once the optimum conditions are actually known, the specified drop size and size distribution can be obtained and the optimum achieved. The recovery boiler modeling program currently under way at IPST may ultimately be the best way to establish what are the preferred operating conditions for optimum operation.

#### **1.2 DELIVERABLES**

This research effort has delivered or will deliver the following:

- a) A test facility capable of quantitatively assessing the performance of commercially viable spray systems while processing kraft black liquors at typical furnace feed conditions.
- b) The best commercial spray delivery system available with current technology.
- c) An appraisal of the commercial viability of several fundamentally different black liquor delivery systems.

The first two items have been accomplished, and the third will be in the coming year.

#### **1.3 BENEFITS**

The objective of this program can be viewed as delivering the tools which will help to realize the benefits of several other research activities in the black liquor area. Primary among these is the fundamental recovery boiler modeling research currently underway at IPST under DOE sponsorship. This basic work will determine the optimum black liquor droplet size and velocity distribution to maximize effective use of the furnace volume. Development of a system to achieve this desired liquor distribution is the objective of the present program. Potential benefits from this applied study are the same as projected in last year's report on this project; they are reproduced verbatim from last year's report in Table 1.1 below (1).

The increased thermal efficiency value for the industry is approximately \$93 million/year; the incremental value of a 1% increase in process productivity for the industry is estimated at \$240 million/year. These estimates reflect savings increments above the state-of-the-art recovery boiler technology that is available.

Table 1.1 Benefits from Proposed Research

- Goals:
1. Increased thermal efficiency
  2. Increased process productivity
  3. Improved equipment design potential
  4. Improved process control potential

- Targets:
1. Increased thermal efficiency

Element	Value		
	Improvement	10 <sup>5</sup> Btu/adt	\$/adt
Increased fired per cent solids	70 to 75%	2.3	0.69
Reduced flue gas temperature	350 to 325F	1.2	0.36
Reduced carbon in smelt	1.5 to 1.0%	0.86	0.27
Reduced sootblowing steam	3.0 to 2.5%	0.72	0.21
(Total)	5.1	3.2	

## 2. Increased process productivity

Incremental production                      1%                      400

### Industry

Value:

1. Increased thermal efficiency  
 $5.1 \times 10^5 \text{ Btu/adt} \times 60 \times 10^6 \text{ adt/yr} = 3.1 \times 10^{13} \text{ Btu/yr}$   
 $3.1 \times 10^{13} \text{ Btu/yr} \times \$3.00/10^6 \text{ Btu} = \$93,000,000/\text{yr}$

2. Increased process productivity (1%)  
 $60 \times 10^6 \text{ adt/yr} \times \$400/\text{adt} \times 0.01 = \$240,000,000/\text{yr}$

---

Thermal efficiency and process productivity goals are not independent. The recovery boiler is often the bottleneck in the entire pulping process. Thermal efficiency is often sacrificed for high productivity. Hence, thermal efficiency and productivity increases may not be realized simultaneously. On the other hand, the recovery boiler is the only pulp mill operation which can often claim that improved unit productivity will result in increased millwide productivity.

The in-place capital investment in recovery boiler technology is so large (\$10 billion) that radical changes, expansions, and replacements will be rare for the foreseeable future. Barring a significant departure from the kraft process in the near term, the industry will be firing black liquor in conventional recovery boilers well beyond the year 2000.

## 1.4 ORGANIZATION

Organizational and technical responsibility for the Delivery Systems Project has remained with Dr. H. Jeff Empie, Professor, in the Chemical and Biological Sciences Division. Mr. Steven J.

Lien, Associate Engineer, in the Chemical Recovery Group continues responsibility for equipment operation and data gathering/analysis. Dr. Wenrui Yang, post-doctoral appointee in the Chemical Recovery Group, was responsible for droplet image analyses, but transferred to the recovery boiler modeling project in July. Mr. Douglas B. Samuels, Sr. Technician in the Chemical Recovery Group, maintains responsibility for equipment installation and operation and has assumed the responsibility for image analysis.

## **1.5 SCHEDULE**

The work reported here covers the fourth year of the project. Because of the interruption caused by the 1989 move from Appleton, WI to Atlanta, GA by IPST, the project has been extended one year by DOE so that the remaining tasks can be successfully completed.

## **1.6 SUMMARY OF PREVIOUS RESULTS**

Early results were obtained on the performance of the three basic types of black liquor spray nozzles: the splashplate, the swirl cone, and the U- and V-jets. Data were reported on the flow and pressure drop characteristics of the B&W splashplate and the Spraying Systems U- and V-jets. Flow coefficient correlations for hot and cold black liquor were developed. The correlating parameter was Reynolds Number based upon the minimum flow diameter.

The formation of droplets from a black liquor stream require the formation of a fluid sheet by the nozzle. The ultimate drop size can be directly related to the initial sheet thickness and velocity. Sheet thickness, and therefore liquor droplet size, was found to increase with liquor viscosity (and hence black liquor solids) for the B&W splashplate nozzle.

Data on droplet size distributions from a B&W splashplate nozzle and a CE swirl cone nozzle were obtained. Droplet size showed a weak dependence on liquor velocity and fluid physical properties. Furthermore, the size distribution was almost the same for all nozzles when the size data were normalized by dividing the actual droplet size by the square root of the mass median diameter.

A series of trials was conducted at James River's Camas Mill to study black liquor sprays in a recovery furnace environment. High-speed video images of sprays were taken through a gun port on Camas' No.4 recovery boiler. Three different nozzles were operated at two levels of liquor flow and fired liquor temperature. Analysis of furnace response data and the video images of the sprays led to several interesting conclusions. Changing one nozzle and/or firing conditions for a short period of time did not produce significant changes in furnace operation as indicated by particulate count or lower furnace temperatures. There was evidence of liquor sheet breakup by perforation which agrees with the findings of the present study. Differences in sheet breakup between nozzles were seen in the video images; however, it was not possible to detect variation due to firing conditions. The video images were optically too dense to determine droplet size distribution by image analysis.

At IPST a test series with the B&W splashplate, CE swirl cone, and SS V-jet nozzles was completed, using a 3x3x3 matrix (solids of 50, 60, and 70%; viscosities of 270, 90, and 30 cP;

and nozzle pressures of 15, 30, and 45 psig). Pressure vs. flow rate correlations were derived as a function of Reynolds Number. For the three tests at high viscosity (270 cP) and low pressure (15 psig), the flow rate was too low to produce sheet breakup. Another three tests at 70% solids and low viscosity could not be completed because the heat exchanger did not have the capacity to heat liquor to well over the boiling point (130° C) in a single pass.

Video recordings of the spray pattern were made at four positions at distances of 34 to 44 inches from the nozzle. From the visual analysis of the video tape, it was apparent that the solids concentration of the black liquor had a strong effect on droplet formation. At low solids (50%), the majority of the drops were spherical, but at high solids (70%), most of the images were large, irregularly shaped drops connected to strings and filaments.

Several drop size distribution models were tested to fit the experimental data; the best one continued to be the square root-normal distribution. It was shown that the ratio of the standard deviation to the square root of the mass median diameter has a constant value of 0.2, and therefore only one parameter is necessary to characterize the square root-normal distribution for black liquor.

The ratio of mass median droplet diameter to nozzle diameter was related to the product of Reynolds Number and Euler Number, each raised to some experimentally determined non-integral power; similarly, Euler and Schmidt Numbers also correlated well. Both dimensionless correlations were broken down into a product of the individual physical parameters, each raised to some experimentally determined power. It was shown that the parameters which most strongly influenced mass median drop diameter were nozzle diameter, and liquor density and velocity. At high solids levels, liquor viscosity became important. When droplet diameter was empirically correlated with velocity and temperature raised to appropriate exponents, drop size was shown to decrease as either operating parameter was increased.

A study of the behavior of spray nozzles at liquor temperatures above the atmospheric boiling point was performed. Three different nozzles were tested at temperatures ranging from 200° to 270° F using 65% solids liquor. As temperature was increased, drop diameter gradually decreased until a transition temperature was reached where the drop size abruptly decreased by about a factor of two. This transition temperature was several degrees above the atmospheric boiling point of the liquor, suggesting that the sharp decrease in drop size was due to flashing at the nozzle. This effect would result in a several-fold increase in the number of drops being fired into the furnace, increasing burning rates and possibly carryover rates.

Measurements were made of the local distribution of liquor flow in the spray pattern as a function of the angle from the sheet centerline. Results for both the splashplate and V-jet nozzles showed the mass flow distribution to be parabolic, with the maximum mass flow at the centerline and decreasing with increasing angle. Limited analysis of drop size as a function of the angle from the sheet centerline showed no significant difference.

Present commercial black liquor nozzles do not provide a means for independently controlling droplet size distribution. The fluid dynamics of the droplet formation process is the main determining force; any significant change will require some externally applied, independent forcing mechanism.

## 2.0 EXPERIMENTAL DESIGN FOR BLACK LIQUOR SPRAYING

A spray facility has been constructed which makes it possible to test both commercial spray nozzles and new experimental nozzle designs, over a wide range of conditions. The system was designed to be large enough that realistic nozzle sizes (comparable to those used in recovery boilers) can be tested. This design includes the capability of recording the spray pattern and measuring the drop sizes. This spray facility is being used to determine how the major operating variables affect the resulting drop size distribution.

### 2.1 BLACK LIQUOR SPRAYING EQUIPMENT

The spray is contained in a large spray chamber with windows to allow video-tape recordings of the spray pattern and drop distribution (Figure 2.1). Black liquor flowrates as high as 50 gpm can be tested. A spiral heat exchanger and a direct steam injection system provide the capability to run liquor temperatures as high as 275° F (135° C). Instrumentation and data acquisition hardware and software record an accurate measure of the operating conditions for each test, including the temperature and viscosity of the liquor, nozzle pressure and flowrate, and solids content (Figure 2.2).

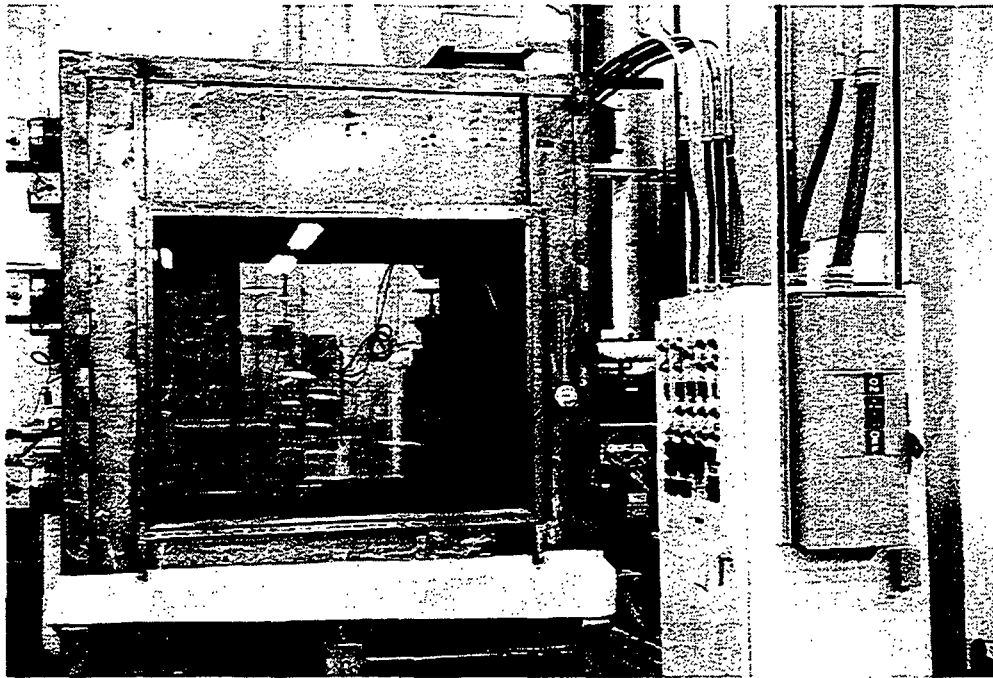


**Figure 2.1** Black Liquor Spraying Facility at IPST

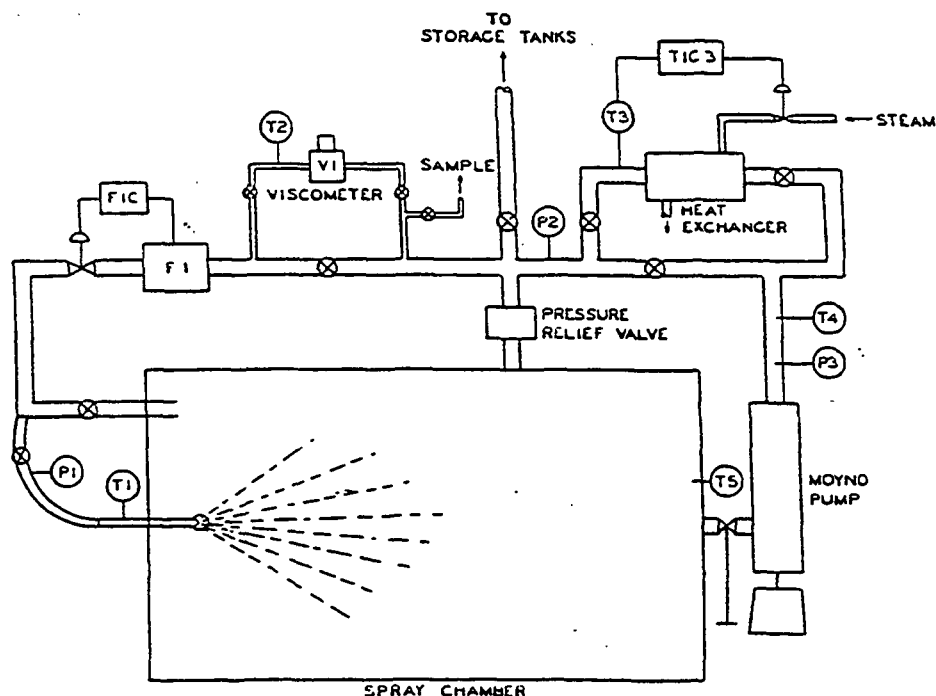


**Figure 2.2** Schematic of Piping Arrangement for Black Liquor Spray System.

The entire spraying process is performed in an enclosed chamber with an off-gas scrubber system to prevent the release of odor due to sulfur compounds from the black liquor. An induced draft fan maintains a vacuum on the chamber and the exhaust gas is drawn through an activated carbon adsorber before being released to the atmosphere.

A high speed video camera is used to record the spray pattern and the drops which form. The images are recorded on a VCR and later transferred to an image analyzer. On the image analyzer the image is filtered and converted from a gray-level image to a binary format. Each drop is then measured from the enhanced final image, and the results from several images are combined to perform a statistical analysis of the drop distribution.

A detailed description of the entire experimental apparatus can be found in previous DOE progress reports #2 and #3 (2,1).

## 2.2 TEST PLAN

### 2.2.1 Previous Work

Results of earlier work performed during years one through three of this five year study are described in Progress Reports #1, #2 and #3 (3,2,1). A summary of this work is also contained in Table 2.1.



During year one a spray chamber was constructed and preliminary testing was performed. This work was extremely important to the success of later testing, because it defined the conditions required for consistent operation of the spray facility. Some drop sizing data were collected and analyzed. Several drop distribution correlations were studied using data obtained, and the square-root normal distribution was found to provide the best correlation. Measurements of the sheet thickness and sheet velocity at the splashplate of a B&W nozzle were also made and analyzed.

During the second year of the project a new spray facility was built in conjunction with the move of the Institute from Appleton to Atlanta. Because of the experience obtained during early testing, it was possible to eliminate most of the problem areas during the system reconstruction. The new equipment allowed for safer and more consistent operation, reduced spillage of black liquor, and prevented the foul odor of the black liquor from escaping the chamber.

During the third year of the black liquor delivery systems project, a large amount of experimental work was performed. The main test series during the third year was designed to produce drop size data over a wide range of test conditions. The variables studied include, type of nozzle, solids content, liquor viscosity, and pressure at the nozzle. Three different nozzles were used in these tests, a Babcock & Wilcox 12/45 splashplate, a Combustion Engineering swirl-cone, and a Spraying Systems V-jet 11/65 nozzle.

Additional testing was performed to determine the correlation between the pressure drop and the liquor velocity through the nozzle. This equation allows the nozzle flowrate to be estimated if the pressure and liquor conditions are known. This analysis used data from both test series I and additional experimental work.

Next, tests were performed to determine the variations in flowrate around the spray angle of the nozzle. A sampling system was devised to collect liquor samples at 20 degree intervals around the perimeter of the nozzle. These data were measured for both the B&W splashplate and the SS V-jet at various nozzle pressures and viscosities. The data provides useful information on the initial trajectory of the black liquor droplets.

### **2.2.2 Year 4 Testing**

The experimental work during the past year of testing focused on four main areas. Test series III studied the effect of nozzle size on the resulting drop size. At least two different sizes of a given nozzle type were tested to determine the change in drop size. This provides data for extrapolation of drop size predictions from the small test nozzles to larger nozzles which are more common in mill use. Similarly different spray angles for a V-jet nozzle were tested.

A series of tests was performed to determine how important liquor variations are in influencing drop size distributions (Test Series IV). Several liquors were tested at standard conditions. These mill liquors represent a range of wood sources and pulping conditions. This data base provides an indication of the variation in drop size that can be expected between different mills.

**Table 2.1 Four Year Experimental Test Plan**

---

**Black Liquor Spray Project**

<u>Location</u>	<u>Equipment, Experimental and Analytical</u>
Year 1	
<u>Appleton, WI</u>	<ul style="list-style-type: none"><li>• Construction of Spray Chamber Facility</li><li>• Preliminary Testing with Water, Corn Syrup, and Black Liquor</li><li>• Measurement of Sheet Thickness and Sheet Velocity</li><li>• Determination of Pressure vs. Flow Correlations</li><li>• Preliminary Drop Sizing</li><li>• Comparison of Methods - Flash X-ray vs. High Speed Video</li></ul>
Year 2	
<u>Camas, WA</u>	<ul style="list-style-type: none"><li>• Mill Trial - High Speed Video Camera Recordings of Spray Pattern in a High Temperature Environment</li></ul>
<u>Atlanta, GA</u>	<ul style="list-style-type: none"><li>• Design and Construction of Revised Spray Chamber Facility</li></ul>
Year 3	
<u>Atlanta, GA</u>	<ul style="list-style-type: none"><li>• Preliminary Testing with Water and Black Liquor</li><li>• Test Series I Effect of Nozzle Type, Solids %, Viscosity and Flow</li><li>• Pressure vs Flowrate Correlations</li><li>• Black Liquor - Chemical Analysis and Viscosity Correlation</li><li>• Test Series II Black Liquor Spraying at High Temperatures</li><li>• Analysis of Drop Size and Shape</li><li>• Mass Flow Distribution vs. Spray Angle</li></ul>
Year 4	
<u>Atlanta, GA</u>	<ul style="list-style-type: none"><li>• Test Series III Nozzle Variations (size and spray angle)</li><li>• Test Series IV Effect of Liquor Variations - Five Liquors from Different Mills</li><li>• Additional High Temperature Testing</li><li>• Test Series V Alternative Nozzle Techniques, eg. Vibratory Assist</li></ul>

---

Additional work was also performed involving black liquor spraying at temperatures above 230° F. The analysis of these data, along with previous high temperature data, is included in this report. This work extends the results from test series I (PR #3), by adding the high solids and high temperature work. The correlation between nozzle pressure and flowrate was also studied as a part of this work at temperatures above the boiling point of the black liquor.

The final part of this study is to look at alternative technologies for producing black liquor drops. Since all of the preceding results showed a wide drop size distribution, these tests were directed at controlling the width of the drop size distribution rather than the median drop size. Although the question of what is the best drop size distribution has not been answered, it appears reasonable to assume that a narrow drop size distribution could improve recovery boiler operation.

A number of commercial nozzles were tested to determine if the drop distribution could be modified using any existing nozzle designs. Several developmental nozzles (primarily modified splashplates) were also tested.

The current experimental work is focused on the use of vibratory assist to modify the sheet break-up process in such a way that a more controlled drop size is produced. Although this work is continuing, the preliminary results are presented in this report.

### **2.2.3 Year 5 Test Plan**

In the final year of the project the work will continue on the investigation of techniques using vibratory assist as a method to produce a more controlled drop size distribution. Additional testing is also planned to more accurately determine the drop size distribution for high temperature operation above the transition temperature. Although data have been collected at high temperatures, the drop sizing was less accurate due to the smaller average drop size.

If time permits additional testing will be performed to try and measure the drop size for those conditions which previously resulted in the formation of strands rather than spherical drops. This includes the region at greater than 65% solids and temperatures less than the boiling point. This test plan is summarized in Table 2.2.

**Table 2.2 Test Plan for the Final Year of the Spray Project**

---

**Black Liquor Spray Project**

**Test Plan - Year 5**

**A. Vibratory Assisted Drop Formation**

**Objective**

Continuing work in testing and development of a high frequency driving device to induce a regular wavelength in the liquor flow and to modify the sheet breakup process. The eventual goal is to produce a more controlled drop size distribution.

**B. High Temperature Testing**

**Objective**

By using a smaller field of view for the video image of the black liquor, the accuracy of the calculated drop size will be greatly improved especially for the smaller drops. Additional accuracy can be achieved by constructing a view tube apparatus that will narrow the depth of field.

**Test Conditions**

<b>Nozzles:</b>	1. B&W 12/45	2. B&W 17/52	3. SS V-11/65
	4. SS V-16/50	3. CE Swirl-cone	
<b>Nozzle Pressure:</b>	1. 15 psi	2. 30 psi	
<b>Solids:</b>	1. 60%	2. 70%	
<b>Temperature:</b>	1. 108 C	1. 115 C	
	2. 113 C	2. 120 C	
	3. 118 C	3. 125 C	
	4. 123 C	4. 130 C	
		5. 135 C	

**C. High Solids Testing**

**Objective**

Determine drop size distribution for black liquors at greater than 65 % solids, at temperatures below the transition temperature. The previous work has determined drop size for a wide range of conditions, but with the exception of the tests at very high temperatures (above the transition temp) drop sizes have not been measured for black liquor at solids greater than 65%.

---

### 2.3.1 Black Liquor Viscosity

Despite the fact that most of the mills were using a similar wood supply and operating at similar pulping conditions, a wide variation in liquor viscosity was seen.

For each of the liquors used in the spray testing, the relation between viscosity, temperature and solids content was analyzed. The same correlation equation has been used for each liquor, with different coefficients calculated. This has been found to accurately describe the viscosity behavior over a wide range of temperatures and solids levels. The correlation equation used for each of the different black liquors is:

$$\text{Log}\left(\frac{u}{u_w}\right) = \frac{1}{\left(A * \left(\frac{T}{S\% \times T^*}\right) - B\right)}$$

where  $u$  = liquor viscosity (cP)  
 $u_w$  = water viscosity at  $T$  (cP)  
 $= 1000 / (36.6 \times T - 10090)$   
 $S\%$  = percent solids (%)  
 $T$  = liquor temperature (K)  
 $T^*$  = reference temperature (K)  
 $= 373 \text{ K}$

The values of the coefficients A and B in the equation have been calculated and are tabulated in the Table 2.4.

**Table 2.4** Coefficients for the Viscosity Correlation Equation.

BL Number	A=	B=
#1	65.62	.6682
#2	69.667	.6890
#3	46.485	.3480
#5	47.525	.3589
#6	38.482	.2806
#7	46.857	.3378
#8	63.371	.5725
#4	37.546	.2206

The table also includes the liquors from earlier work as a part of this entire project, (i.e. BL #1, #2, #3). The significance of these coefficients can be seen more easily in Figure 2.3 where the data and the correlation equations for black liquors #4, #5, #6, #7, #8 are graphed. The viscosity is plotted as the log of reduced viscosity (viscosity over the viscosity of water at the same temperature) versus the ratio ( $S\%T^*/T$ ) which can be considered the temperature adjusted solids level.

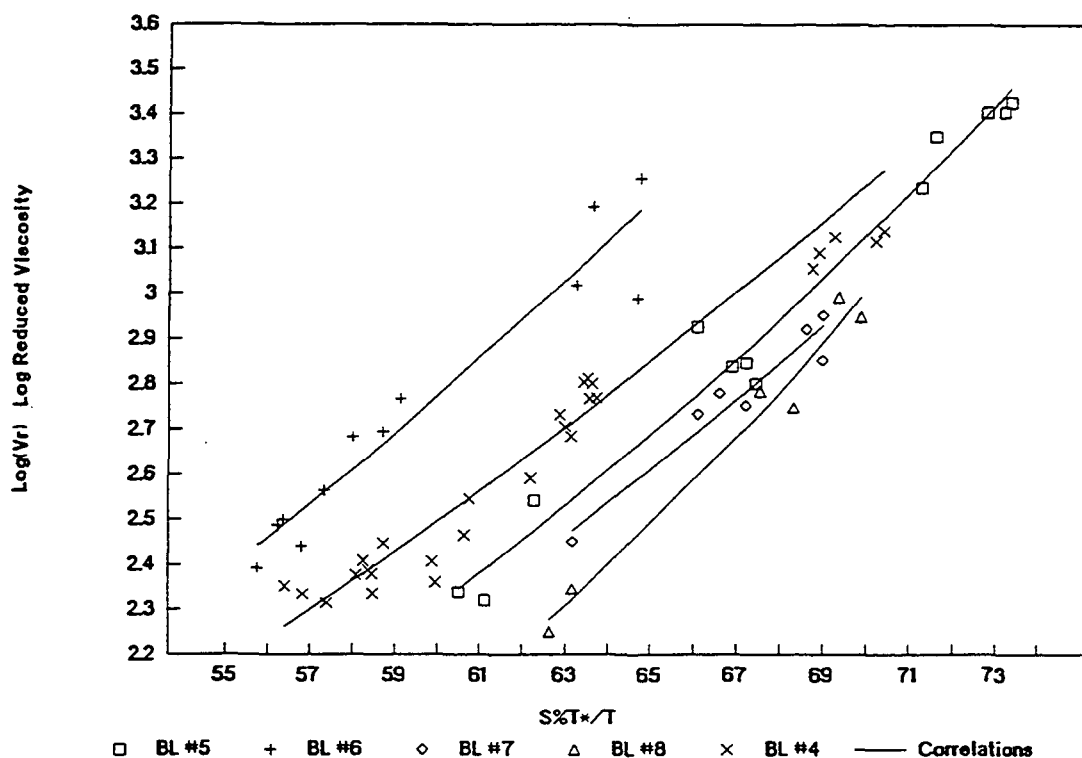


**Figure 2.3** Viscosity Data for Black Liquors Tested.

The effect of black liquor oxidation can be seen in the difference in viscosities of black liquors #5 and #6 which were obtained from the same mill on the same date. BL #5 was obtained from the concentrator at an initial solids level of 67.5% and was tested as delivered. BL #6 was collected at the outlet of the evaporators at 48.7% and was oxidized before testing.

As a result of black liquor oxidation (BLO), the viscosity of the liquor increased significantly. Before oxidation, at the same solids and temperature, the viscosity of BL #6 was the same as BL #5. After oxidation the viscosity was approximately three times higher. The viscosity of BL #5 at 100° C and 65% solids was 136 cP while BL #6 was 450 cP at the same conditions. The change in viscosity was also equivalent to an increase in the solids level of 6%. After oxidation, BL #6 had the highest viscosity of any of the black liquors we tested.

Since BL #7 was derived from hardwood, it might have been expected to show a different

viscosity behavior, but this was not the case. This liquor shows the same type of viscosity correlation and is within the typical range for southern softwood liquors. Based on this liquor, it appears that the viscosity depends more on mill operating variables than on differences in the wood supply.

### **2.3.2 Chemical Analysis**

Samples of all five liquors were submitted for chemical analysis to determine if there were any major differences. In addition to measuring the major elemental components, the sulfur ion species and carbonate were assessed, along with the heating value of the liquor. The results are listed below in Table 2.5.

Most of the values are within the range of typical values for black liquors, and the sum of the elements provides reasonably good closure (99.5 to 103%). These analyses do not indicate any large differences between the liquors.

The sulfur ion analysis shows the result of black liquor oxidation on BL #6. The sulfide level is decreased by conversion to thiosulfate. Although the sulfide level in BL #6 had been decreased to almost zero (.02%) immediately after oxidation, reversion to sulfide apparently had occurred in this sample taken at the end of testing.

All of the heating values appear to be slightly low, since reported values are generally in the range of 5400 to 6600 BTU/lb (A+F). For black liquor #7 the heating value is well below these values and appears to be erroneous despite the fact that the analysis was repeated and a similar result was obtained. Generally the heating value correlates well with carbon content, but for BL #7 this same relationship does not hold true.

**Table 2.5 Chemical Analysis of Black Liquor Supplies.**

Liquor Number	BLS #5	BLS #6	BLS #7	BLS #8	BLS #4
Elemental Analysis					
Carbon (C) %	37.94	38.49	34.34	36.11	37.11
Hydrogen (H) %	3.36	3.26	3.82	3.51	3.55
Oxygen (O) %	34.11	32.54	36.76	32.53	31.78
Sulfur (S) %	3.41	3.22	5.21	4.31	3.51
Sodium (Na) %	21.43	23.89	18.70	20.89	21.87
Potassium (K) %	0.85	0.80	1.95	1.56	2.15
Chlorine (Cl) %	0.63	0.68	0.61	0.69	0.49
Total(%)	101.7	102.9	101.4	99.6	100.5
Sulfur ions					
Na <sub>2</sub> SO <sub>4</sub> as S%	1.05	0.50	1.99	1.34	0.89
Na <sub>2</sub> SO <sub>3</sub> as S%	0.30	0.45	0.09	0.33	0.13
Na <sub>2</sub> S <sub>2</sub> O <sub>3</sub> as S%	1.34	1.79	1.96	1.96	1.77
Na <sub>2</sub> S as S%	0.77	0.27	1.43	0.76	0.87
Sulfur ions as S%	3.47	3.01	5.46	4.38	3.65
Elemental S %	3.41	3.22	5.21	4.31	3.51
Carbonate - as CO <sub>3</sub> %	6.90	5.98	3.40	4.03	3.95
HHV (BTU/lb)	5462	5414	4413	5490	5393
Sample Solids (%)	58.6	55.3	64.7	69.1	69.1



### 3.0 BLACK LIQUOR SPRAYING RESULTS

Several tests series were performed during the past year (year 4) to determine which variables have an important influence on the mass median drop diameter, and how these variables alter the drop size. The effect of increasing nozzle diameter is analyzed in the following section. Several different mill liquors were tested to determine whether differences between black liquors affected the median drop diameter (3.2). The importance of liquor temperature, especially above the boiling point, has been analyzed (3.3). Additional work was also performed to extend the correlation between flowrate and nozzle pressure to high temperature operation. Finally, in sections 3.4 and 3.5, alternative spray nozzles were tested, both commercially available nozzles, modified nozzles and new nozzle designs.

#### 3.1 EFFECT OF NOZZLE DIAMETER

A limited number of tests were performed to determine the effect of increasing the size of the spray nozzle orifice. Most of the previous work was performed with nozzles which had an equivalent orifice diameter of about 1 cm. In mill recovery boilers, typical nozzle diameters range from 1 cm up to 3 cm, so it is important to know how the mean drop size will change with increasing nozzle size.

Table 3.1 Nozzle Diameter Tests

Test	Nozzle	Diam.	Temp	Pres.	Visc.	Solids	Dm
		mm	C	psi	cP	%	mm
38A	B+W 12/45	9.5	81.5	20.1	136	55.0	2.6
38B	B+W 12/45	9.5	83.7	35.2	137	55.5	2.18
38C	B+W 15/52	11.9	83.8	19.4	150	56.0	2.53
38D	B+W 15/52	11.9	85.0	34.6	151	56.3	2.38
38E	B-Tamp 18	18.0	84.9	19.2	179	57.2	3.16
38F	B-Tamp 18	18.0	85.2	31.4	173	57.0	2.13

It was difficult to obtain data over the entire spray nozzle size range because of capacity limitations in the spray equipment and also because the sheet break-up process occurs more slowly for the larger nozzles. A small set of data were collected for three different splashplate nozzles (shown in Table 3.1). All of the tests were performed at essentially the same percent solids, temperature and viscosity. Two different nozzle pressures (20 and 35 psi) were used.

pattern has a greater initial sheet thickness and as shown in Table 3.2 below it produces slightly larger drops.

**Table 3.2 Effect of Spray Angle from V-jet Nozzles**

Test	Nozzle	Spray Angle	Temp C	Pres. psi	Visc. cP	Solids %	Dm mm
38G	SS V-11/65	65	80.8	15.0	106	53.5	1.87
38H	SS V-11/65	65	82.4	24.5	103	53.7	1.86
38I	SS V-11/25	25	82.3	14.7	103	53.6	1.97
38J	SS V-11/25	25	80.6	24.8	110	53.6	2.17

Using the average mass median drop diameters (2.07 mm @ 25° and 1.87 @ 65°) to calculate an exponential dependence of drop size on spray angle produces an exponential constant of -0.109.

$$D_m = 2.94 * SA^{-0.109}$$

It is likely that for both of the cases described above, the change in mass median drop diameter is due to a change in the initial thickness of the sheet formed at the outlet of the nozzle (or more accurately, the sheet thickness at a given distance from the nozzle). Both the nozzle diameter and the spray angle influence the initial thickness of the sheet leaving the nozzle. The initial sheet thickness is proportional to the nozzle diameter squared and is inversely proportional to the spray angle.

The fact that the exponent term for the nozzle diameter is roughly twice the magnitude of the exponent term for the spray angle (which is negative as expected) appears to confirm that sheet thickness is the critical variable. It is not surprising that the sheet thickness does not have a stronger influence on drop size, if the sheet thickness is increased, the sheet breakup process will simply be delayed until further thinning has occurred.

Because of the limited amount of data, it is difficult to draw conclusions from these results but there does appear to be a slight increase in the mass median drop diameter with increasing nozzle diameter. If the two values for each nozzle size are averaged together to reduce the variability in the data, this trend is more apparent. The test values, along with the average values for each nozzle are plotted in Figure 3.1 as a function of nozzle diameter.

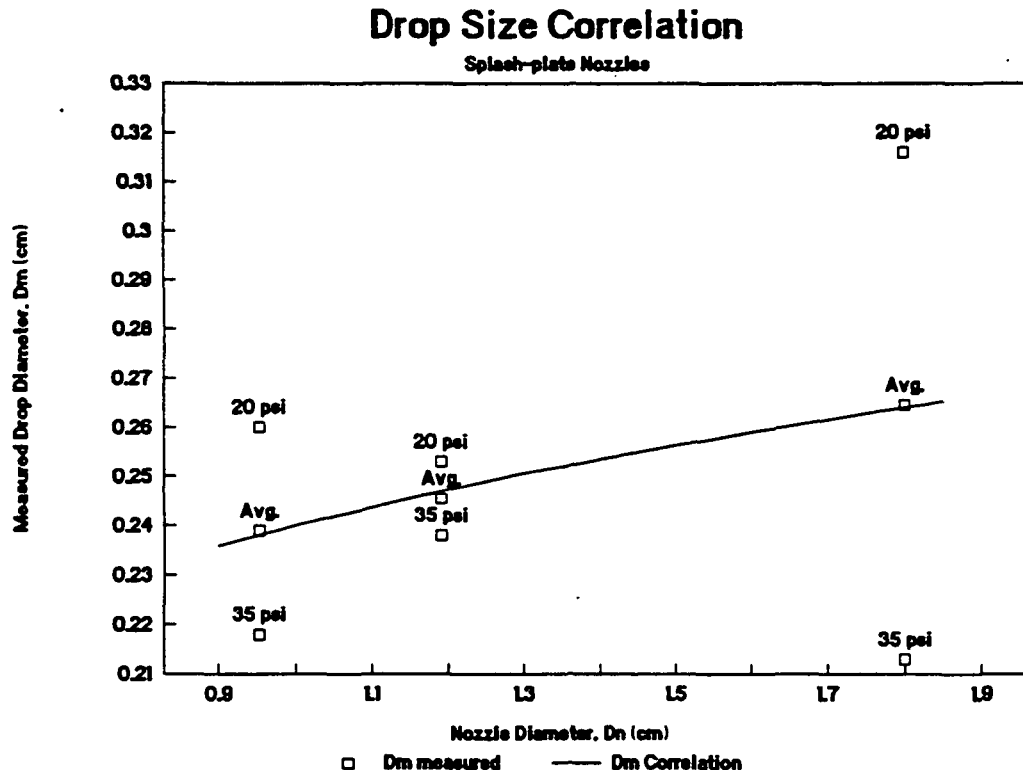


Figure 3.1 Mass Median Drop Diameter vs Nozzle Diameter

In previous analysis of drop size data, the mean drop size  $D_m$  was described as an exponential function of dimensionless variables. This type of function can also be used to correlate drop size to nozzle diameter. The following equation was determined by linear regression analysis.

$$D_m = 0.240 * D_n^{0.162}$$

The predicted values of  $D_m$  are also shown in Figure 3.1. The relatively low value of the exponent in this equation (0.162) indicate that the drop size is not strongly dependent on nozzle diameter. An increase in nozzle diameter from 1 cm to 3 cm would only result in an increase in drop size by a factor of 1.2.

Four additional data points were obtained using two different V-jet nozzles. In this case the nozzle diameter is the same for the the Spraying Systems V-jet 11/65 and 11/25 but the spray angle of the sheet is different. The first nozzle forms a sheet which spreads over a 65 degree angle, while the sheet leaving the second nozzle is much narrower (only 25°). The narrower

## **3.2 EFFECT OF BLACK LIQUOR VARIABILITY**

In this part of the project, a test series was performed to determine whether the variations in liquor properties from mill to mill have an important effect on the drop size distribution produced by spray nozzles. In earlier work the mass median drop diameter was correlated to operating variables such as nozzle type, nozzle pressure, liquor temperature, viscosity and solids concentration. Most of this work was performed using only two different mill-supplied black liquors. There are large differences in black liquors from different mills, especially in their burning and swelling behavior. Because of this, a test series was designed to determine how these liquor variations influence the drop size distribution produced by spray nozzles.

### **3.2.1 Test Conditions**

In order to test a range of conditions, the tests for each liquor were performed with two different nozzles (a CE swirl-cone and a B&W splashplate), two different nozzle pressures (20 and 35 psi), two different solids levels (60 and 70%), and two different viscosities (60 and 200 cP).

These two nozzles have been used in much of the earlier work and are both about the same size (approximately 3/8 inch orifice diameter). The pressure and viscosities selected represent a range of typical values for this type of nozzle. The test plan consisted of 12 different conditions for each black liquor supply (Table 3.3).

Five different mill black liquors were obtained from 4 different kraft pulp mills and used in these tests. An analysis of the viscosity and chemical makeup of these liquors was performed and the results are reported in section 2.3 of this report.

### **3.2.2 Results**

Image analysis revealed that for tests performed at high solids (70%), the drop formation process is not complete within the limited distance available in the spray chamber. At the point where video recordings are made, the liquor is in the form of long strands and other irregular shapes. It is impossible to determine a drop size from these images; therefore drop-size data, are not available for the tests at 70% solids. The effect of solids level was neglected in the analysis of the remaining data since all of these tests were performed at approximately 60% solids.

Of the variables studied, nozzle type, nozzle pressure and viscosity were all statistically significant in their effect on the drop size. The change in drop size with liquor type was not statistically significant. The mass median drop diameter ( $D_m$ ) is plotted in Figure 3.2 for each of the liquors. All of the liquors show about the same range of data except for BL #4 which has less variation and a slightly smaller average value.

**Table 3.3** Test Conditions for each Black Liquor.

Solids	Viscosity	Nozzle	Pressure
(%)	(cP)		(psi)
60	200	CE Swirl-cone	20
60	200	CE Swirl-cone	35
60	200	B+W Splash-plate	20
60	200	B+W Splash-plate	35
60	50	CE Swirl-cone	20
60	50	CE Swirl-cone	35
60	50	B+W Splash-plate	20
60	50	B+W Splash-plate	35
70	200	CE Swirl-cone	20
70	200	CE Swirl-cone	35
70	200	B+W Splash-plate	20
70	200	B+W Splash-plate	35

The effect of nozzle type, operating pressure and viscosity are shown in Figure 3.3. Although there is a range of drop diameters for each test condition, the trends are clear. The four groups on the right side of the graph are for the B&W splashplate nozzle, which has a larger median drop size than the CE swirl-cone. For both nozzles, increasing the nozzle pressure works to reduce the mass median drop size  $D_m$  and higher liquor viscosity results in a higher median drop size. These trends confirm what has been seen in all of the earlier tests.

An analysis of variance (ANOVA) technique was used to evaluate the test data from this study and the results are listed in Table 3.4. The F-ratio is an indication of the influence a given variable has on the mass median diameter. It is clear that the type of nozzle has the largest influence on the drop diameter. The mean drop size for the CE Swirl-cone nozzle was 2.04 mm and for the B&W splashplate it was 2.48 mm.

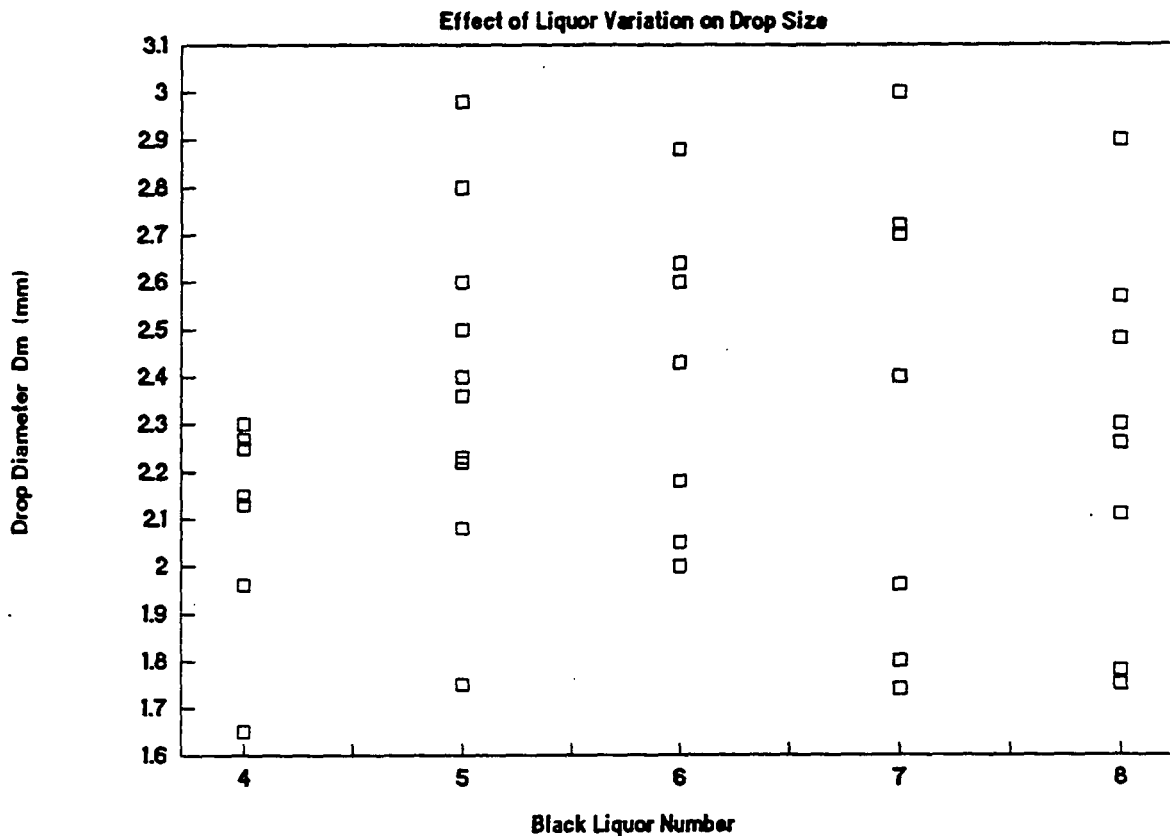


Figure 3.2 Drop Size does not correlate with Black Liquor Supply.

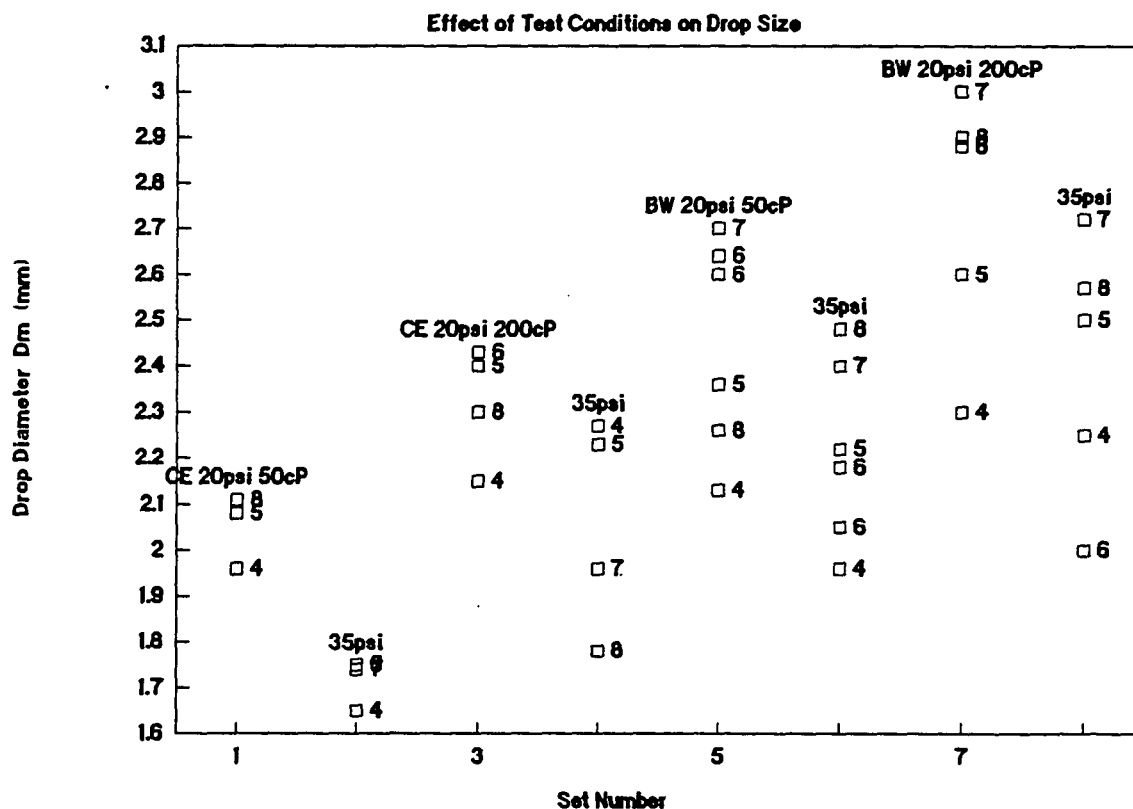


Figure 3.3 Mass Median Drop Diameter is Dependent on Nozzle Type and Pressure.

**Table 3.4 Analysis of Variance Results for Liquor Variation Tests.**

Source	Degrees of Freedom	Sum of Squares	Mean Squares	F-Ratio	Signif.
B NOZZLE	1	2.08213	2.08213	33.696	YES
D PRESSURE	1	0.76311	0.76311	12.350	YES
C VISCOSITY	1	0.65921	0.65921	10.668	YES
A BL	4	0.40273	0.10068	1.629	no
AB	4	0.36832	0.09208	1.490	no
AC	4	0.02479	0.00620	0.100	no
BC	1	0.04144	0.04144	0.671	no
AD	4	0.19300	0.04825	0.781	no
BD	1	0.00199	0.00199	0.032	no
CD	1	0.00645	0.00645	0.104	no
ERROR	16	0.98867	0.06179		
TOTAL	38	5.53184	0.14557		

The nozzle operating pressure was the next most important variable. At 20 psi the mean drop size was 2.46 mm, and increasing the pressure to 35 psi reduced the average drop size to 2.16 mm. The higher nozzle pressure increases the liquor velocity through the nozzle, so that more kinetic energy is available to break up the liquor spray into finer drops.

The viscosity of the liquor also changed the drop size. At 50 cP the mean drop diameter was 2.23 mm, and it increased to 2.40 mm at 200 cP. Again this is the same trend that was seen in previous work and it is the result of the higher viscosity liquor having more resistance to the process of sheet break-up.

All three of these test variables (nozzle type, nozzle pressure, and liquor viscosity) are statistically significant at a 99% confidence limit (F-ratio > 8.53). In contrast, the effect of liquor type is not significant, even at a 90% confidence limit (F-ratio < 2.33). Average values of the mass median diameter for each of the liquors are listed in the table below:

<u>BL #</u>	<u>Number Samples</u>	<u>Drop Diameter</u>		<u>Standard Error</u>
		<u>Median (mm)</u>	<u>Adjusted (mm)</u>	
# 4	8	2.08	2.08	0.102
# 5	10	2.39	2.36	0.092
# 6	7	2.40	2.17	0.109
# 7	6	2.42	2.39	0.118
# 8	8	2.27	2.27	0.102

The first value of median drop diameter is calculated based on the data available. Because there were some missing values and a couple of duplicate values in the factorial test sequence, the drop diameter is over-estimated for three of the liquors (#5, #6, and #7). The second value for drop diameter is derived from the ANOVA results and corrects for these missing values. The standard error also provides an indication that the differences are not meaningful.

All of the liquors are within a fairly close range of values. Only BL #4 differs by a slightly wider margin. There was nothing in the analysis of the liquor properties (section 2.3) to explain this difference. The smaller drop size with BL #4 may be at least partly due to the problems with the viscometer readings during the tests on this liquor. If the viscometer was reading higher than the true viscosity, this would tend to produce smaller drops.

In the ANOVA evaluation, the third order interactions were used to calculate the error term. This was necessary to obtain a good estimate of the error, because replicate tests were only performed at three of the 40 test conditions. Because all of the second order terms were insignificant, this is a reasonable assumption.

### 3.2.3 Drop Size Correlations

Using the data from these tests, a multiple linear regression analysis was performed to determine the correlation between drop size and nozzle operating conditions. The correlation was calculated using the ratio of mass median drop size over nozzle orifice diameter ( $D_m/D_n$ ) as the dependent variable, and the liquor viscosity ( $V_1$  @ TC1) and the nozzle velocity ( $V_n$ ) as the independent variables. These variables were correlated as shown in the equation below based on previous drop sizing analysis.

These results (Table 3.5) agree reasonably well with earlier correlations of this type. For the CE Swirl-cone nozzle the coefficient for viscosity of 0.14 is within the range of 0.07 to 0.17 calculated in progress report #3. The velocity coefficient of -0.47 is slightly higher than the reported value of -0.32 calculated in that earlier analysis.



For the CE Swirl-cone Nozzle:

$$\frac{D_m}{D_n} = 0.409 \times V_1^{0.141} \times V_n^{-0.470}$$

For the B+W 12/45 Splash-plate Nozzle

$$\frac{D_m}{D_n} = 0.588 \times V_1^{0.0256} \times V_n^{-0.386}$$

**Table 3.5 Multiple Linear Regression Analysis of Drop Size.**

Dependent Variable: LN-D <sub>m</sub> /D <sub>n</sub>				
Independent Variable	Parameter Estimate	Standard Error	Seq. R-Sqr	Simple R-Sqr
CE Swirl-cone Nozzle (Filter: AVG =0)				
Intercept	-0.89367	0.40434		
LN-V <sub>1</sub>	0.14072	0.03433	0.3789	0.3789
LN-V <sub>n</sub>	-0.47044	0.15178	0.6551	0.1721
B&W 12/45 Splash-plate (Filter: AVG =1)				
Intercept	-0.53132	0.36245		
LN-V <sub>1</sub>	0.02557	0.03675	0.1522	0.1522
LN-V <sub>n</sub>	-0.38595	0.10030	0.5235	0.5114
Both CE + B&W Nozzle (Filter: AVG <2)				
Intercept	-0.83174	0.25553		
LN-V <sub>1</sub>	0.07737	0.02560	0.2215	0.2215
LN-V <sub>n</sub>	-0.37047	0.07855	0.5294	0.4030

For the B&W 12/45 splashplate nozzle the influence of viscosity appears to be much less significant, since the coefficient is only 0.026. However the velocity coefficient of -0.39 does agree reasonably well with the values obtained from the swirl-cone (-0.47).

### 3.2.4 Conclusions

The data obtained indicate that differences in liquor properties do not have a significant effect on the drop size distribution produced by standard spray nozzles. The controlling variables were viscosity, nozzle type and size, and nozzle pressure. When these primary variables are held constant the variation in mean drop size from one liquor to another can be explained entirely by the random nature of the drop formation process and by the relatively high error in measuring the drop sizes.

Since the variations in liquor type from mill to mill do not cause a significant difference in the median drop size, the correlations determined above can be used for the prediction of median drop diameter from a nozzle at known operating conditions. The biggest measurable difference between these liquors, was the variation in viscosity. Since the testing was performed at constant viscosity, the influence of this variable did not appear as a difference between the liquors.

In order to apply these correlations and to accurately predict the drop size from correlations of this type, it is necessary to have data on the liquor viscosity. Since this can vary widely from mill to mill, it cannot be accurately predicted a priori from the firing solids and temperature. Using the widest range of viscosity found in our testing, the viscosity would vary by a factor of three. This would result in a difference in median drop size of 17% (e.g. the drop size could increase from 2.1 to 2.45).

In addition, all of the results obtained to-date indicate that the drop size distribution fits a square root-normal correlation where the standard deviation depends only on the mean drop size:

$$s = 0.2*(D_m)^{.5}.$$

Therefore, by knowing the liquor firing conditions at the nozzle, it is possible to produce an estimate of both the mean drop size and the width of the drop size distribution entering the recovery boiler.

### 3.3 High Temperature Black Liquor Spraying

During earlier experimental tests with black liquor spray nozzles, a dramatic change in the behavior of the spray discharge from the nozzle was noticed, above certain temperatures. Operating above this limit resulted in much smaller drops. This transition temperature was found at the upper end of the normal operating region for black liquor spraying, and the phenomena appeared to be due to operation above the boiling point, resulting in flash vaporization of water from the black liquor occurring at the nozzle.

The initial drop size from a pressure nozzle is crucial to the proper operation of a kraft recovery boiler and will significantly affect the subsequent recovery of energy and pulping chemicals. In traditional mill practice, black liquor was sprayed at temperatures below the boiling point, and some mills reported unstable boiler operation at higher temperatures (12). Over the past two decades the fraction of water in the liquor going to the boiler has been gradually reduced, with the average solids content increasing from 60 % to over 70%. As a result, the liquor viscosity has also increased and many mills have gone to higher firing temperatures. Typical viscosity values are listed in Table 3.6. Some mills are now firing at temperatures well above the boiling point. Little or no data are available on spray nozzle operation at high temperatures.

**Table 3.6 Typical Black Liquor Viscosity and Boiling Point Data.**

Solids (%)	Viscosity		Boiling Point (C)
	@100 C (cP)	@115 C (cP)	
60	65	39	111
70	535	242	118

#### 3.3.1 Experimental Test Plan

A test plan was developed to study the behavior of the black liquor spraying above the transition temperature, but before these tests could be performed, the experimental apparatus had to be modified for high temperature operation. The equipment was revised to allow for direct injection of steam into the liquor, greatly increasing the heating capacity and allowing for operation at higher solids levels. A schematic of the revised system is shown in Figure 2.2.

Three nozzles were used for this experimental work. The nozzles are representative of the types being used in recovery boilers. The three nozzles are a Babcock and Wilcox 12/45 splashplate nozzle, a Spraying Systems V-jet 65200 (11/65), and a Combustion Engineering Swirl-cone nozzle. All three are approximately the same size and are at the small end of the size range that can be considered industrial scale (nozzle orifice = 3/8", flowrates = 12 gpm at 25 psi).

For each nozzle, data were collected at two solids concentrations and two nozzle pressures (nominally 60 and 70% solids and at 20 and 30 psi). The use of direct steam reduces the solids concentration by about 3 or 4%, so the initial solids had to be raised by 3 to 4% above the target operating concentration.

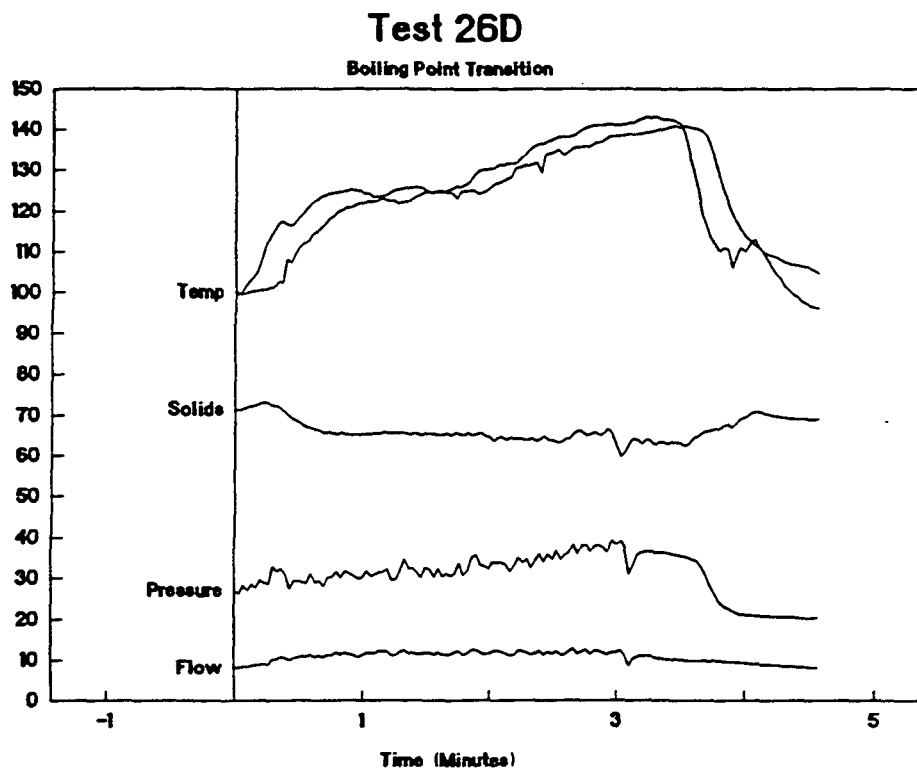


**Figure 3.4** Test 26D with B+W 12/45 Splashplate Nozzle

The tests were performed by adjusting the nozzle pressure to a given flow level at a relatively low initial temperature (about 200 F); then the liquor temperature was gradually increased by using the heat exchanger and the direct steam injection, until the transition in spray behavior was observed. The steam was then shut-off and the temperature was allowed to fall back below the transition temperature. Typical data from a test run are shown in Figure 3.4.

A high speed video camera was used to record the drops in a section of the spray pattern at a position approximately 4 ft from the end of the spray nozzle. A light source is located behind the spray, with the video-camera on the opposite side of the spray pattern, resulting in a high contrast image. The camera, manufactured by Xybion, uses an image intensifier and electronic gating to obtain images at very high shutter speeds (about 50 micro-seconds for all of these tests). The video images are recorded on a VHS video recorder and later transferred to a Tracor Northern Image Analyzer for determination of mass median drop diameter.

### 3.3.2 Flashing Behavior

The procedure used for most of these tests was to spray the black liquor continuously while the temperature was raised by the direct injection of steam. There is a temperature at which the behavior of the spray changes noticeably. Above this transition temperature, the drop size appears to decrease dramatically when viewed with the high speed video camera.

There is also a change in the shape and direction of the spray pattern. With a V-jet nozzle the flat spray pattern opens up into an oval-shaped spray cone, and with a splashplate nozzle the flat spray pattern moves away from the nozzle plate. Apparently this change in direction of the spray is due to the vaporization of water, with the steam then contributing a momentum component perpendicular to the spray direction. There is also an apparent increase in the velocity of the black liquor drops above the transition temperature, although no quantitative data are available.

The flashing phenomena can be analyzed by considering the flow of black liquor through the nozzle. Although the specific design of the nozzles are quite different, they are all similar in that the black liquor flows through a narrowed restriction before the spray is ejected from the nozzle. Initially the liquor velocity is relatively low, but as the cross-sectional area of the nozzle decreases, the velocity increases. An energy balance on the black liquor shows that as the kinetic energy of the liquor increases, the pressure decreases.

This acceleration of the liquor is the cause of most of the pressure difference required to move the liquor through the nozzle. Because the pressure at the inlet of the nozzle is higher than the vapor pressure of the liquor (even above the transition temperature), vapor formation cannot occur at this point. As the liquor flows through the orifice of the nozzle and the pressure decreases, a point is reached where vapor pressure exceeds the liquor pressure and vaporization can occur. This can only occur when the liquor is at a temperature above the boiling point.

### 3.3.3 Transition Temperature

The liquor temperature where the transition to flashing occurs is not easy to determine precisely. An estimated value was manually recorded in a lab notebook during these tests, but because the temperature is increasing rapidly during the tests, it is only accurate to a value of  $\pm 5^{\circ}\text{F}$ . Although the temperature and other data are recorded on a continuous basis with a PC based data acquisition system, there is no obvious change in this data set to indicate when the transition occurs.

From these data (Figure 3.4) it is apparent when the steam flow to the nozzle is on, because the steam flow creates pressure fluctuations in the liquor pressure. The point when the steam is shut off provides an upper limit on the transition temperature, since the transition had already been reached before this point. But in general this upper-limit is well above the estimated transition temperature.

Because of the rapid heating rate during most of the tests, the temperature as indicated by the thermocouple is lagging behind the true liquor temperature. A correction for this error was made for those tests with the highest heating rates, as indicated by a difference between thermocouples TC1 and TC2. When this difference exceeded 2.5°C then a correction was made to adjust  $T_T$  by:

$$T_{tr} = T_T + (TC1 - TC2)/3$$

where:

$T_{tr}$  = Adjusted Estimate of Transition Temperature

$T_T$  = Initial Estimate of Transition Temperature

TC1 = Temperature at Thermocouple TC-1 (C)

TC2 = Temperature at Thermocouple TC-2 (C)

It is expected that the transition temperature will be higher than the atmospheric boiling point of the black liquor, since the pressure at the nozzle will tend to suppress flashing. The atmospheric boiling point of the liquor was not determined experimentally for this liquor, but an estimate can be made using a standard equation (Ref 13, p. 18). Typical values of  $K_{bp}$  range from 5 to 9°C, and for BL #3.5 and #4 the estimates were made with a  $K_{bp}$  value of 7°C.

$$T_{bp} = 100 + K_{bp} * \left( \frac{S\%}{100 - S\%} \right)$$

A comparison of the estimated boiling point with the experimentally determined transition temperature in Figure 3.5 confirms that the transition temperature follows the same trend with increasing solids. This transition temperature ( $T_{tr}$ ) is about 7.5°C higher than the calculated atmospheric boiling point and can be correlated to the solids level using the same type of equation as used for boiling point. The calculated value of  $K_{tr}$  in this equation is 11°C.

$$T_{tr} = 100 + K_{tr} * \left( \frac{S\%}{100 - S\%} \right)$$

For BL #9 the coefficients in these equations are slightly different. An estimate of  $K_{bp} = 6^\circ\text{C}$  for the boiling point coefficient was derived from an analysis of the effect of vapor pressure on the pressure versus flow-rate correlations. Similarly, the transition temperature coefficient ( $K_{tr} = 9^\circ\text{C}$ ) is slightly lower for this black liquor. Once again the difference between these two estimates is about 7.5°C (Figure 3.6). The transition temperature for both liquors is plotted in Figure 3.7.

Since the transition phenomena appears to be due to the formation of water vapor in the nozzle, it is not surprising that simply heating to the atmospheric boiling point temperature is not adequate to trigger these changes. Additional super-heating is required to provide energy for the formation of water vapor at a line pressure slightly above atmospheric.

## Black Liquors #3 and #3.5

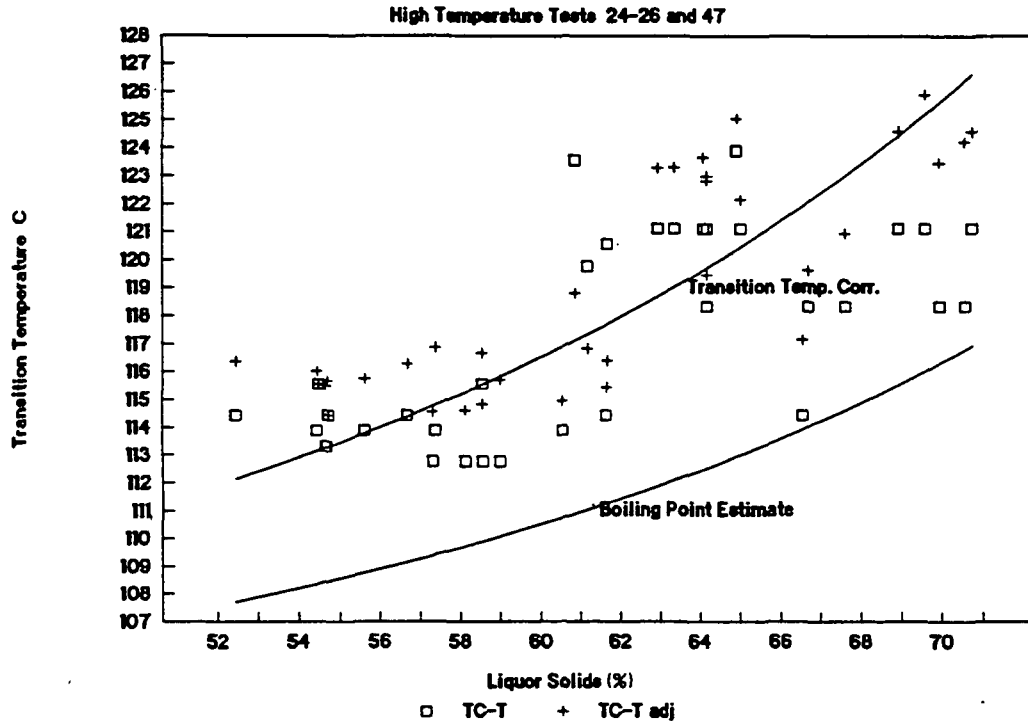


**Figure 3.5** Flashing Transition Temperature is Above the Boiling Point for Black Liquor #3.5.

Other research suggests that part of the difference between the boiling point and the transition temperature may be due to the finite growth rate of bubbles in a superheated liquid (14, Brown+York AIChE 1962). Even though liquor vaporization can occur at a temperature below the transition temperature, the rate is apparently too slow to trigger the changes in the sheet breakup process. Observations made during the heat-up would tend to confirm this. It appears that some change in the droplet size and shape occurs at a lower temperature (near the boiling point), but the most dramatic change only occurs after several more degrees of super-heating.

Using the Clausius-Clapeyron Equation it is also possible to estimate the vapor pressure of the black liquor at a given temperature. This value was calculated for the measured transition temperatures. As expected, the vapor pressure lies below the inlet pressure of the spray nozzle (Figure 3.8), which simply confirms that the flashing is initiated somewhere in between the inlet and outlet of the nozzle. The average value of the vapor pressure at the measured transition temperature is 3.8 psig and these values range from a minimum of 1.6 to a maximum of 6.7 psig. The fact that the vapor pressure is relatively low is an indication that the vaporization does not occur until the liquor is almost to the outlet of the nozzle.

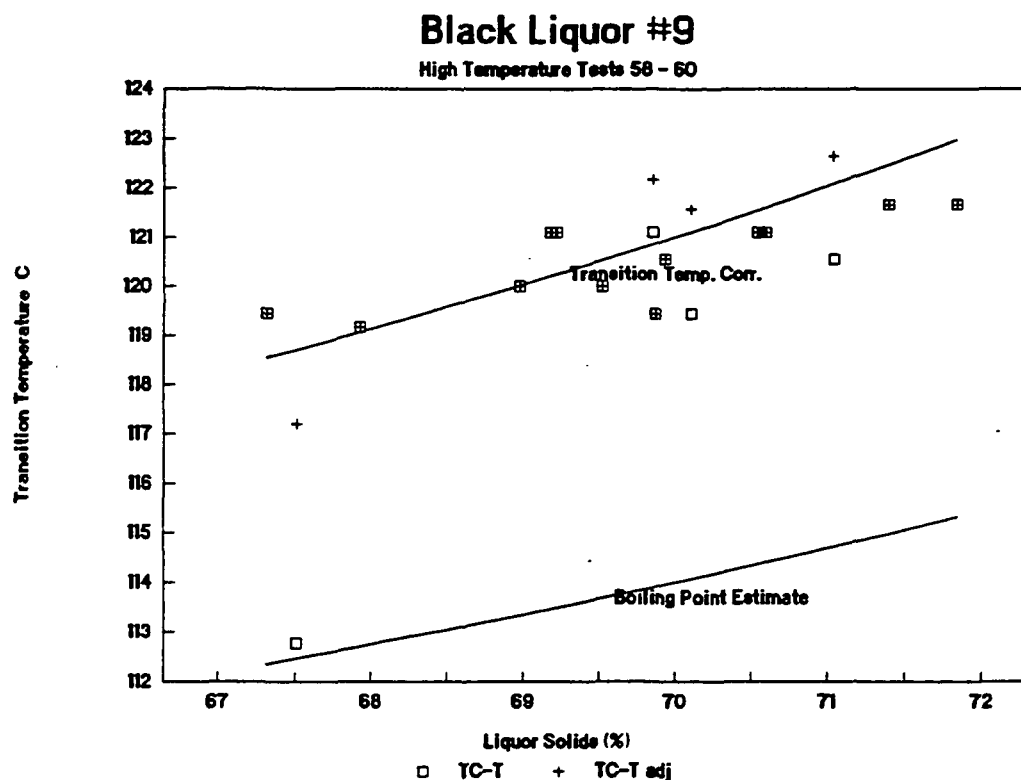


**Figure 3.6** Flashing Transition Temperature is slightly lower for Black Liquor #9.

### 3.3.4 Drop Diameter

Increasing the liquor temperature above the transition temperature results in a significant change in the appearance of the spray pattern and the median size of the drops produced. The average median drop size after this transition was about 80% of the size before the change, but because of the difficulty in obtaining accurate data at high temperatures, the actual ratio may be even lower.

In addition to the normal amount of error associated with drop size measurements, there is additional variability in these high temperature data, because the video recordings were made during non-steady-state conditions in which the liquor was being rapidly heated. Also, since the minimum drop diameter which can be measured on the image analyzer is fixed at about 0.3 mm, as the mean drop size decreases the absolute error increases. Finally, the movement of the spray pattern toward the camera, which changes the calibration, is not accounted for in these values.

The last two errors described above will both tend to result in over-estimating the drop size at temperatures above the transition point. No attempt has been made to correct these effects in the estimated drop size, therefore the actual drop size at high temperatures may be even smaller than reported.



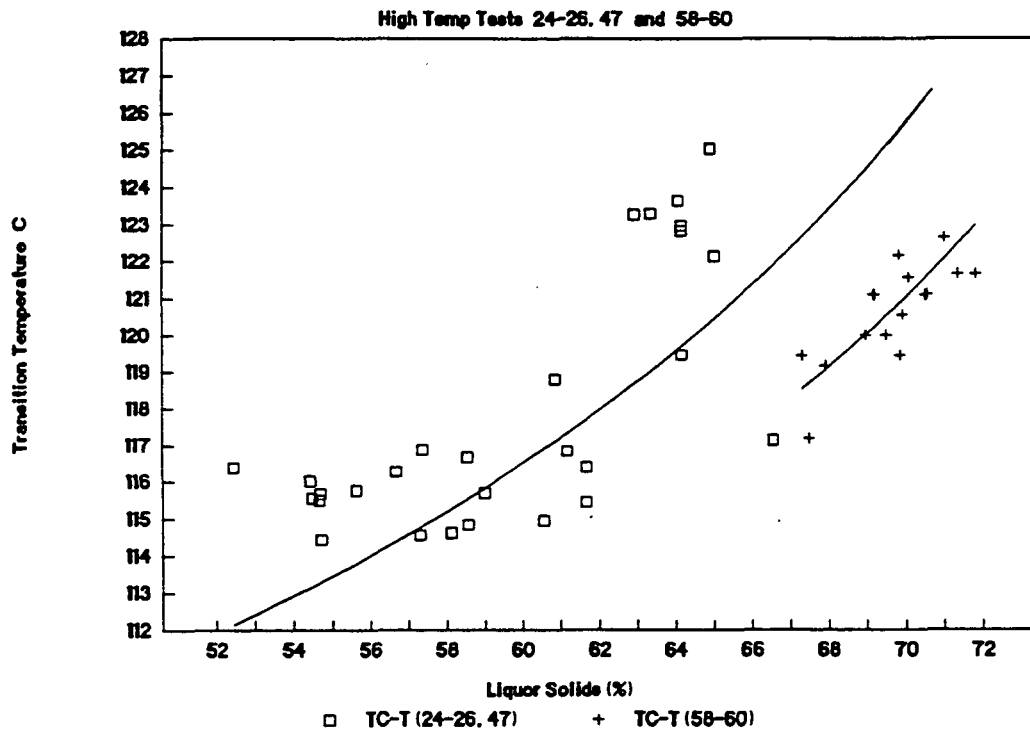


**Figure 3.7** A Comparison of the Estimated Transition temperature  $T_r$  for BL #3.5 and #9.

As the spray tests were performed and the temperature was gradually increased, a continuous video tape of the spray pattern was recorded. Image analysis of these tapes was performed by first analyzing the segment of the tape which appeared to have a minimum drop size (i.e. above the transition temperature). Next two points on the video recording before the transition temperature were also analyzed to measure the mass median drop size and standard deviation. In some cases two additional points were analyzed after the transition as the temperature was allowed to fall.

For each test, three to five drop diameters were measured, corresponding to different times and temperatures during the test. Because the time of the video tape is not known with respect to the data collection, it is difficult to accurately correlate these drop sizes with the exact operating conditions at a given point in time, but a best estimate has been made to determine the liquor temperature. A graph of the measured median drop size is plotted against the estimated nozzle temperature in Figure 3.9 below. It is obvious from this graph that the median drop size is decreasing as the temperature increases.

To reduce some of the variability in this graph and to account for differences in the liquor solids, an excess liquor temperature ( $T_x$ ) was defined as the difference between the liquor temperature (TC1) and the estimated transition temperature ( $T_r$ ). For  $T_x$  greater than zero, the nozzle is operating above the transition temperature. The change in  $D_m$  is more obvious when plotted on this scale (Figure 3.10).

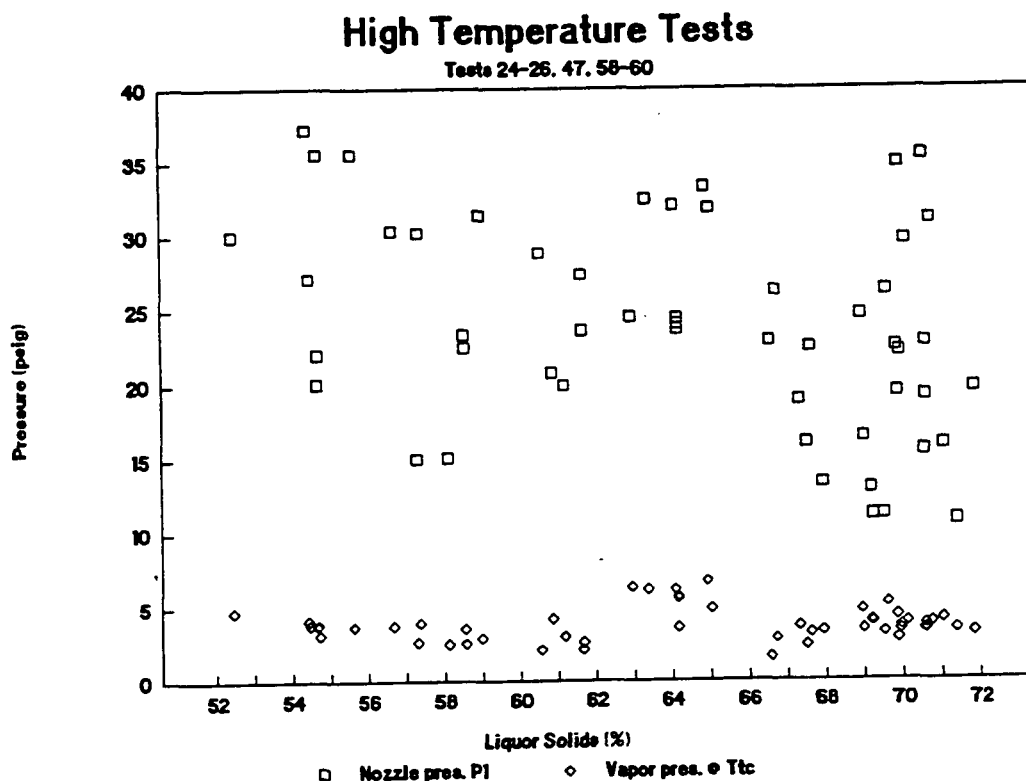


**Figure 3.8** The estimated Vapor Pressure at the Transition Temperature.

An average drop size was calculated for temperatures below and then above the transition temperature. For  $T_x < -2.5$  there were 35 data points with an average  $D_m = 1.99$  mm at an average  $T_x$  of  $-14.4$  C. For  $T_x > 2.5$ ,  $D_m$  averaged 1.63 mm at  $T_x = 11.0$  C.

A t-test analysis demonstrated that the difference between these average values is statistically significant at a 99% confidence limit. The ratio of drop size above and below the transition temperature is 82%, although as noted earlier, the actual drop size above the transition temperature may be even smaller.

In addition to measuring the median drop size, the standard deviation of a square-root normal distribution is also calculated for each test. Other work has shown that the standard deviation is strongly correlated to the median drop size so that  $s/D_m^{.5}$  is on average equal to about 0.20. For these high temperature tests, similar values of  $s/D_m^{.5}$  were measured with an average value of 0.193.

# High Temp Tests 24-26, 47 and 58-60

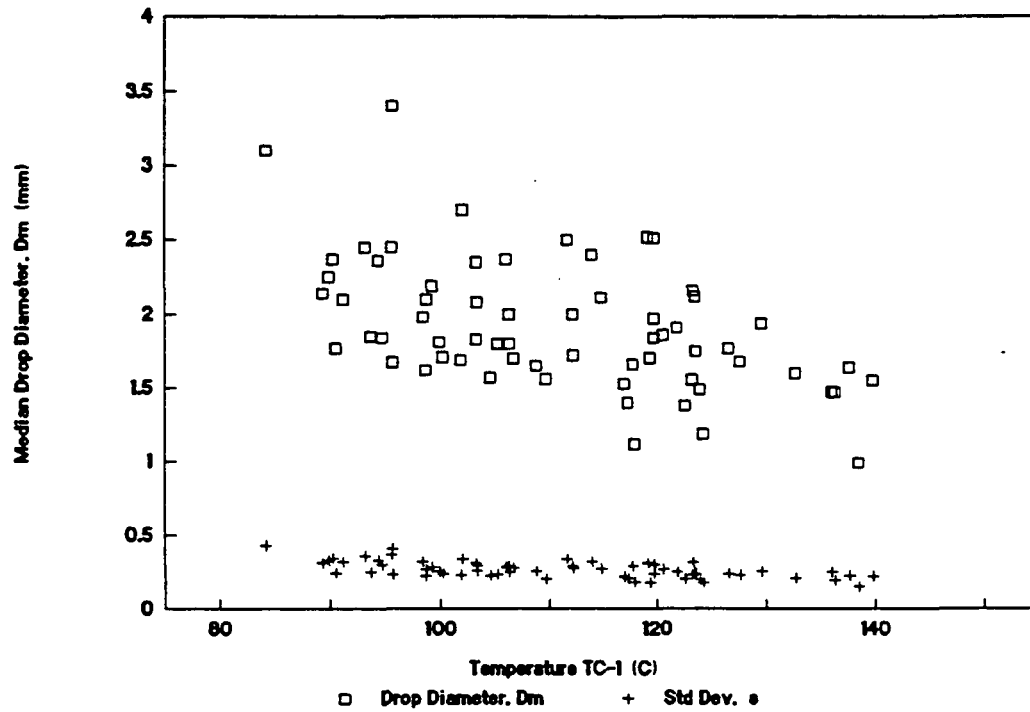
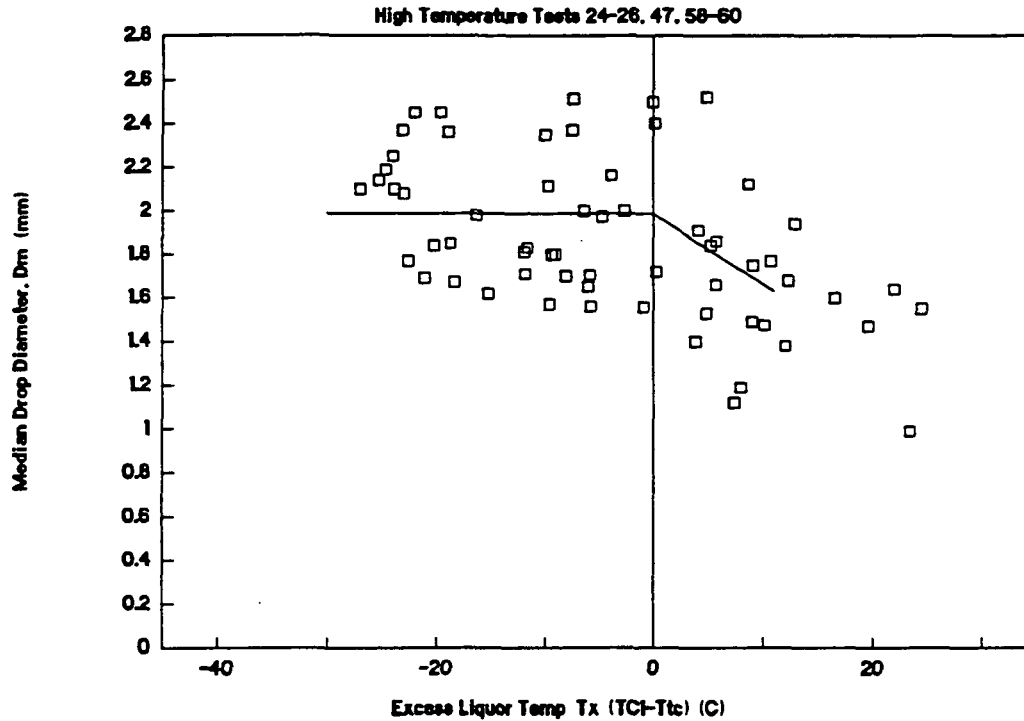


Figure 3.9 Median Drop Diameter vs Nozzle Temperature (TC1).



**Figure 3.10** Median Drop Diameter Drops when  $T_x$  is greater than zero.

### 3.3.5 Flow Coefficients

In previous work (Progress Report #3) the correlation between the average nozzle velocity and the pressure drop was calculated as a flow coefficient  $C_f$  where:

$$\Delta P = C_f \rho \frac{V_n^2}{2}$$

where:

$\Delta P$  = Pressure Drop (Pa)

$\rho$  = Density ( $\text{kg/m}^3$ )

$V_n$  = Nozzle Velocity (m/sec)

$C_f$  = Flow Coefficient

$C_f$  in turn is a function of the Reynolds Number and the nozzle type. For all splashplate nozzles tested, the data agreed with the following correlation.

$$C_f = 1.24 + \frac{458}{Re^{0.9}}$$

A similar correlation was derived for a Spraying Systems V-jet nozzle.

$$C_f = 1.09 + \frac{540}{Re^{1.35}}$$

However, in more recent work for operating conditions near the flashing temperature, the flow coefficients were found to deviate from the predicted values. The experimentally determined values of  $C_f$  were found to be higher than the correlation would predict; that is, the pressure drop across the nozzle was higher than expected.

In the original calculations the pressure drop across the spray nozzle was assumed to be equal to the gauge pressure at the nozzle inlet ( $P_1$ ) because the outlet of the nozzle was at atmospheric pressure. For the high temperature tests where the temperature is above the boiling point temperature, a simple correction can be made by using the difference between the inlet pressure and the vapor pressure of the black liquor for  $\Delta P$ . The flow coefficients calculated using this method agree closely with the correlations calculated earlier at low temperatures, for all of the nozzles tested.

The explanation for this is that the minimum pressure in the nozzle occurs near the outlet at the vena contracta. The pressure at this point cannot drop below the vapor pressure of the black liquor. The pressure is regulated by the vaporization of water from the black liquor which will counteract any pressure drop. The result is that the outlet pressure is maintained at  $P_{vap}$  for temperatures above the boiling point ( $P_{vap}$  is greater than 1 atmosphere). Ruiz and others have studied this behavior (#15) and he has compared the effect to that of compressible flow through a nozzle at critical pressure where a decrease in the outlet pressure does not increase the flow rate through the nozzle.

Using this corrected method, the analysis of flow coefficients was reevaluated for all of the pressure vs. flow data which has been collected during this spray project. The effect of using this correction is shown below in Figure 3.11 for the B+W 12/45 splashplate nozzle. The amount of scatter in the flow coefficient data is reduced significantly after the vapor pressure is accounted for ( $C_{fadj}$ ).

All of the splashplate nozzles tested produce the same correlation with Reynolds Number (Figure 3.12) and a regression analysis of these data produced the following equation.

$$C_f = 1.35 + \frac{371}{Re^{0.9}}$$

## B+W 12/45 Splash-plate Nozzle

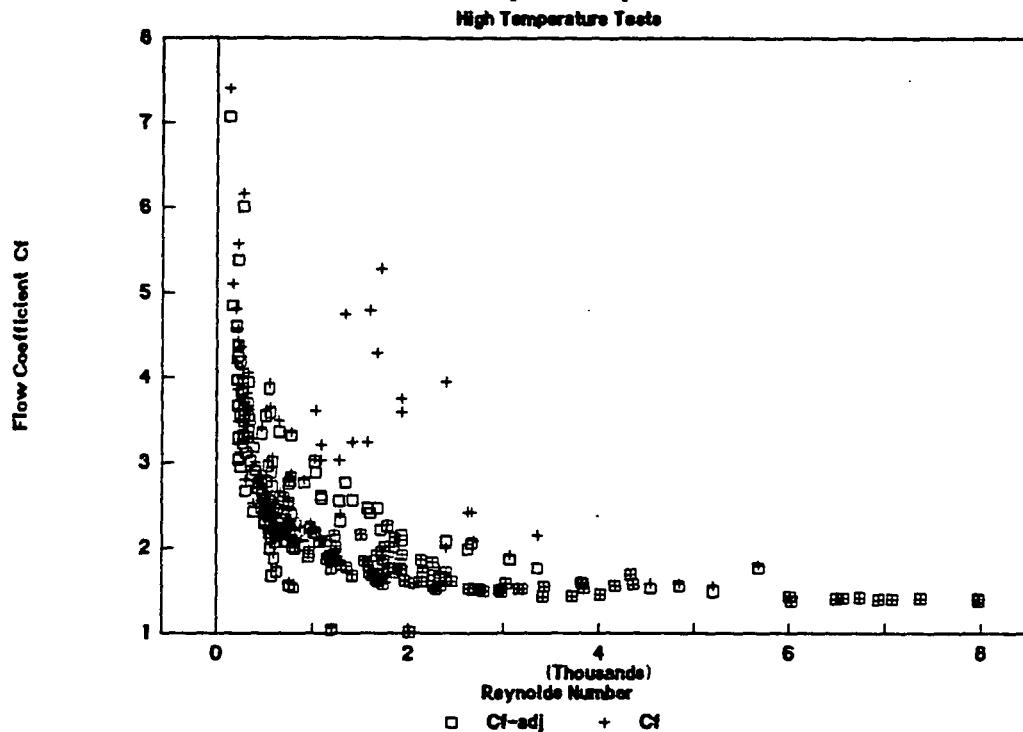


**Figure 3.11** Correct Calculation of the Flow Coefficient requires the Liquor Vapor Pressure.

The tested nozzles included two B+W nozzles, one Gotaverken and one Tampella splashplate nozzle. Despite differences in the nozzle design which could affect flow patterns, all the results appeared to lie on the same curve. The result is slightly higher but very similar to the earlier correlation obtained at low temperatures.

Similarly three different sizes of V-jet nozzles produced by Spraying Systems Inc. were tested and all followed the same curve independent of nozzle diameter (Figure 3.13). The resulting equation is also very comparable to that reported earlier and was independent of nozzle diameter for all of the Spraying System V-jets. The exponent term for the Reynolds Number has decreased from 1.35 to 1.0, which simplified the equation. The value of this exponent can be varied somewhat without changing the  $R^2$  value of the correlation significantly.

$$C_f = 1.057 + \frac{66.4}{Re}$$

Some data were also collected for a V-jet nozzle manufactured by Combustion Engineering. The flow coefficients were significantly higher for this nozzle (about 20% higher) than for the Spraying Systems V-jets. Therefore unlike the splashplate correlation, this equation does not apply universally to all V-jet nozzles.

## All Splash-plate Nozzle

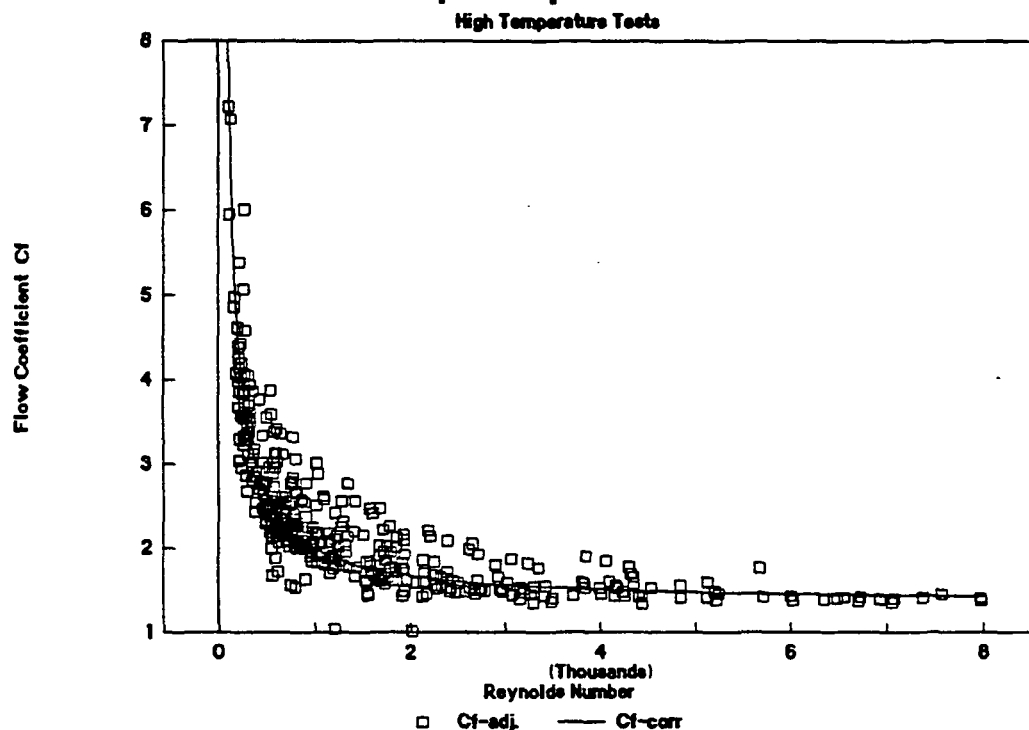


**Figure 3.12** Flow Coefficients follow the same trend for all splashplate nozzles tested.

As in the previous work, this technique does not yield a clear correlation between  $C_f$  and  $Re$  for the swirl-cone nozzle. In the previous analysis of flow coefficients at low temperatures, the average value of  $C_f$  was 1.11, almost identical to the current averaged value of 1.12 (Figure 3.14). The geometry of the swirl-cone nozzle is more complex, with the liquor passing through two separate restrictions before discharge.

The differences in the flow coefficient correlations for the three types of nozzles tested may be due to differences in the geometry of the nozzles which effect when the transition from laminar to turbulent flow occurs. Since the high values of  $C_f$  are associated with low Reynolds number, it is logical to assume that in general the value of  $C_f$  is higher for laminar flow.

For the swirl-cone nozzles the range of  $C_f$  values is much lower than that measured for the splashplate nozzles (Figure 3.15). This may be due to the tortuous flow path through the swirl-cone, resulting in turbulent flow regardless of the Reynolds number. In contrast, for most splashplates there is a gradual transition to the orifice diameter which would be more likely to produce a laminar flow pattern. These nozzles also show the highest values of  $C_f$  at Reynolds Numbers less than 1000.

### All SS V-jet Nozzles (11, 21 and 24)

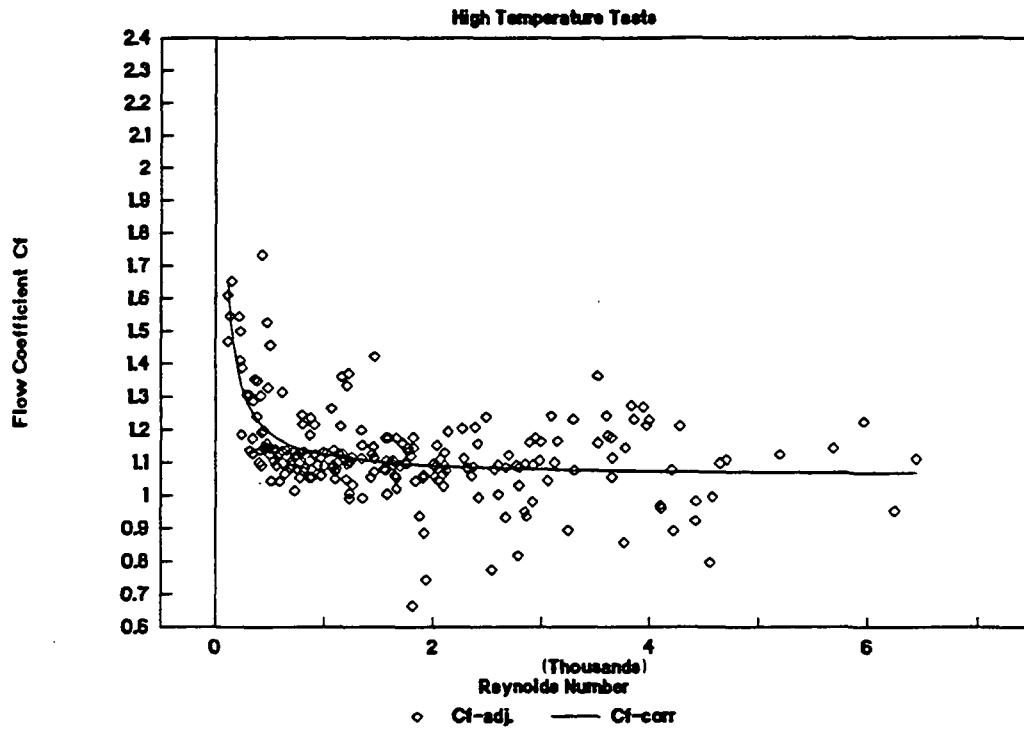


**Figure 3.13** Flow Coefficients for three sizes of SS V-jet Nozzles.

### CE Swirl-cone Nozzle

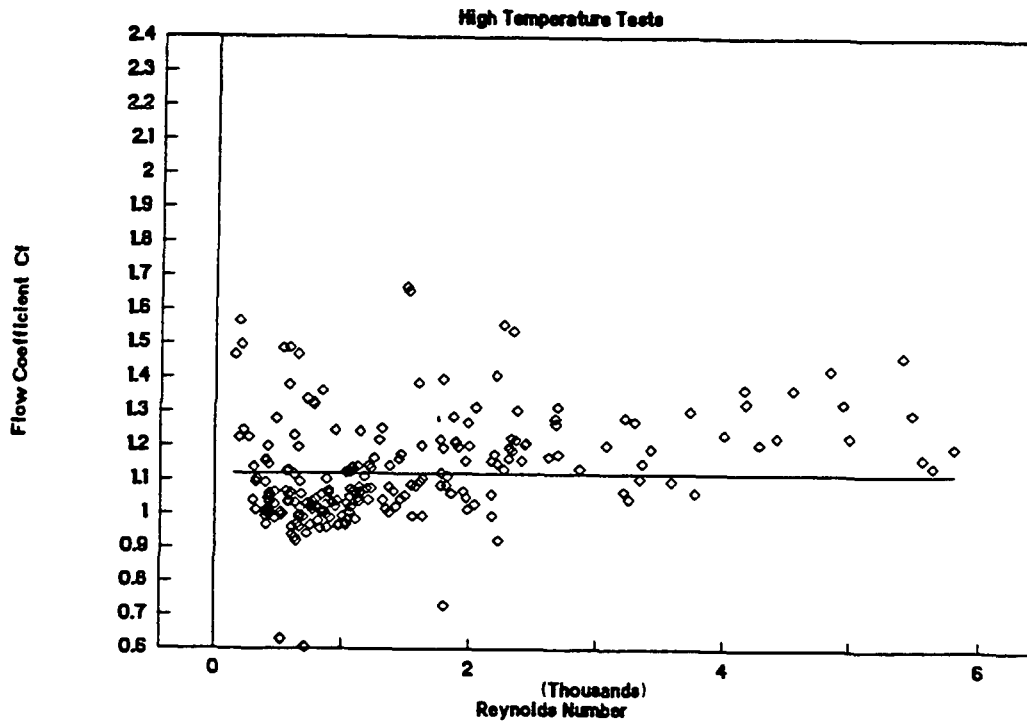


**Figure 3.14** There is no clear trend of  $C_f$  with  $Re$  for the CE Swirl-cone Nozzle.



## Flow Coefficient Correlations

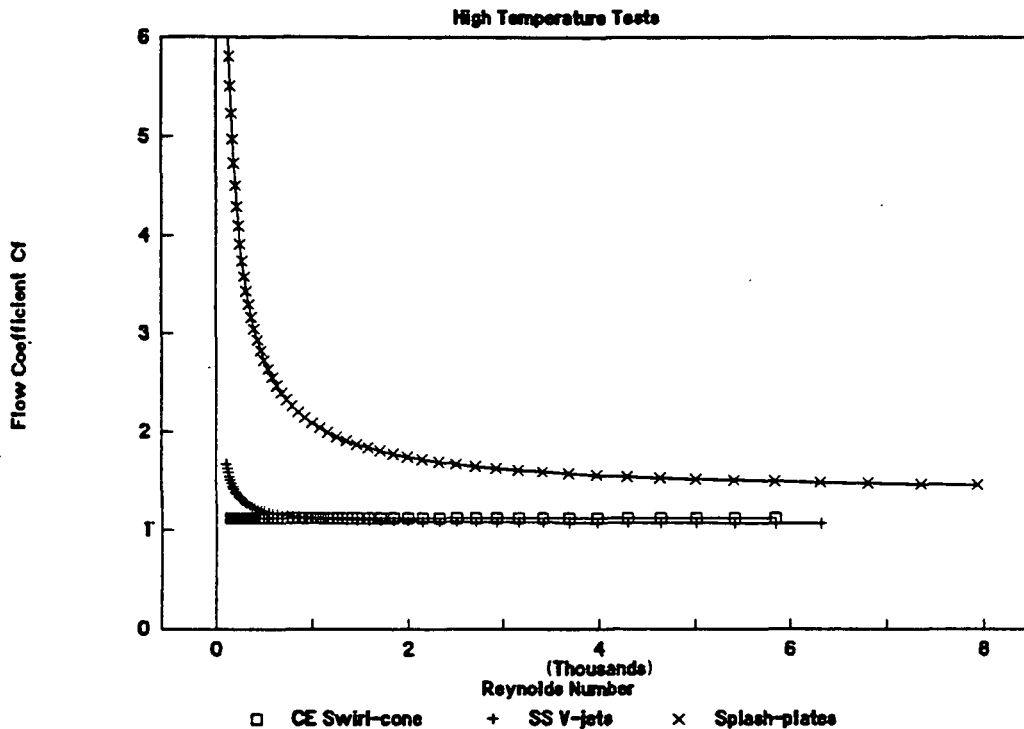


**Figure 3.15** The splashplate nozzles show the highest dependence on the Reynolds Number.

The V-jet nozzles also show less dependence of  $C_f$  on Reynolds number, implying that transition to laminar flow occurs at a lower Reynolds number. The design of V-jet nozzles is such that the transition to the orifice is much more abrupt than the splashplates. The value of  $C_f$  is also much lower for the V-jet than the splashplate at the same Reynolds number (at  $Re = 500$ , V-jet  $C_f = 1.19$ , splashplate  $C_f = 2.73$ ).

### 3.3.6 Conclusions

1. Flashing occurs at a point approximately 6 to 9 C above the atmospheric boiling temperature of black liquor (at 60 to 70% solids). The transition temperature can be correlated to solids using a boiling point rise equation.
2. The average change in droplet size as the consequence of operation above the transition temperature was a decrease in droplet diameter from 1.99 to 1.63 mm. This would result in almost doubling the number of drops being fired into the boiler. The smaller drops would also result in an increase in the total droplet surface area and have a significant effect on the operation of the boiler. The standard deviation of the drop size distribution shows the same correlation with drop diameter as all previous tests.

3. Spraying black liquor above the transition temperature generates steam which results in increased velocity through the nozzle. This additional energy release causes increased sheet break-up and smaller median droplet formation. It also results in a change in the initial direction of the droplets.
4. For splashplate and V-jet nozzles operating above the boiling point but below the flashing temperature of the black liquor, the relation between pressure and flowrate can be predicted from previously derived correlations. The pressure drop required for these calculations at high temperature operation is based on the difference between the inlet nozzle pressure and the vapor pressure of the black liquor.

### 3.4 ALTERNATIVE COMMERCIAL NOZZLES

#### 3.4.1 Screening of Nozzle Types

Commercially available spray nozzles exist in many types for a myriad of different applications ranging from spray coating to aerial application of pesticides for agricultural crops. Common commercial nozzle types not presently used with black liquor include: sonically assisted atomizers; two-phase atomizers; rotary disc atomizers; and full-cone nozzles. All but the last one are generally designed to provide fine droplets (under 100 microns) for such typical uses as uniform surface coatings, dust suppression, or humidification of various substrates including paper.

The nozzles we chose to test were the Bete Spiral, Bete Whirl, and Delavan Raindrop (c.f. Fig. 3.16). All are basically full cone nozzles with design features (internal or external) that give a tangential velocity component to the liquor flow; all are claimed to give coarse, uniform conical sprays. Table 3.7 summarizes specifications for the three alternative commercial nozzles, along with the three conventional nozzles used for comparison.

Table 3.7 - Nozzle Specifications

<u>Vendor</u>	<u>Nozzle Type</u>	<u>Desig.</u>	<u>Rating ( gpm @ psig)</u>	<u>Cone Angle ( degrees)</u>	<u>Orifice Diam. (inches)</u>
Bete	Spiral	ST24FCN	17 @ 20	90	3/8
Bete	Whirl	NCM1520N	35 @ 20	60	9/16
Delavan	Raindrop	RA200/140	14 @ 20	140	5/16
B&W	Splashplate	12/45	12 @ 20	sheet	3/8
Spray Sys.	Full-jet	SS F-12	19.4 @ 20	70	27/64
Comb. Eng.	Swirl Cone	Sw-10			5/16

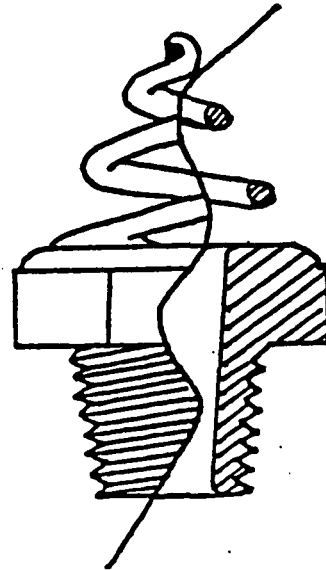
#### 3.4.2 Drop Formation Test Results

Comparison tests were run on the three alternative nozzles, along with the standard B&W 12/45 splashplate, CE swirl cone, and SS F-12 V-jet. Operating conditions were 75 C/60% solids (220 cP viscosity) and 89 C/56% solids (70 cP); nozzle pressures of 20 and 35 psig were used. Results are summarized in Table 3.8 and Fig. 3.17.

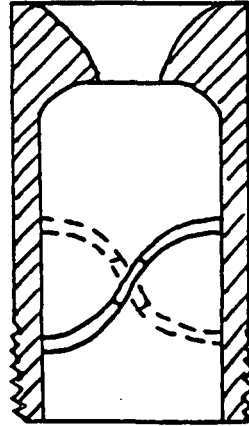
Looking at the mass median diameters for the four sets of experimental conditions shows that the only nozzle to give a significantly different diameter was the Delavan Raindrop. It gave values on the order of 50 - 80% greater than the average of the other five nozzles. Although this result looked encouraging at first, consideration of the drop size distribution proved otherwise.

# ALTERNATIVE COMMERCIAL NOZZLES

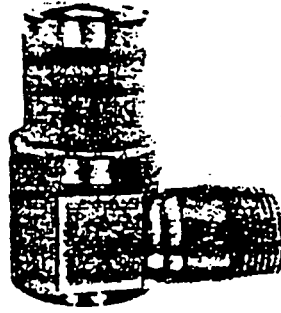
**BETE Spiral**



**BETE Whirl**



**Delavan Raindrop**



3/4"  
BASE PN36662-

FIG. 3.16

Table 3.8

## TESTS WITH DIFFERENT NOZZLES

TEST	NOZZLE	Dm	s/Dm <sup>.5</sup>	SOLID (%)	F1 (gpm)	P1 (psi)	T1 (C)	V1(@T2) (cP)
46E1	BT Spiral	2	0.205	59.8	10.6	20.9	74.6	221.4
46E2	BT Spiral	1.92	0.209	59.9	14.2	35.2	74.8	225.5
46J1	BT Spiral	1.26	0.171	55.6	11.3	18.4	87.7	61.5
46J2	BT Spiral	1.39	0.187	56	15.8	35.0	88.9	63.6
46F1	BT Whirl	2.58	0.199	60.1	24.9	19.3	77.1	214.0
46F2	BT Whirl	2.45	0.192	59.8	31.4	30.5	76.8	230.1
46I1	BT Whirl	1.814	0.180	54.9	27.9	19.1	90.0	70.3
46I2	BT Whirl	1.98	0.195	55.3	34.9	33.2	89.4	67.4
46A1	B+W 12/45	2.3	0.198	59.3	11.4	21.9	75.7	183.1
46A2	B+W 12/45	2.25	0.197	59.5	15.1	34.3	75.6	190.5
46N1	B+W 12/45	2.13	0.185	57.4	13.7	20.6	88.3	81.7
46N2	B+W 12/45	1.96	0.182	57.3	18.6	36.1	89.9	86.3
46B1	CE Swirl	2.15	0.211	60.2	10.3	19.1	76.7	204.4
46B2	CE Swirl	2.27	0.203	59.9	14.2	34.7	75.2	210.7
46M1	CE Swirl	1.96	0.196	57.1	11.0	18.9	87.6	76.0
46M2	CE Swirl	1.65	0.195	56.9	15.2	36.4	89.4	79.0
46C1	Del RA 200/140	3.62	0.198	60.5	11.7	21.4	76.7	212.7
46C2	Del RA 200/140	3.32	0.220	59.9	15.6	33.8	75.2	226.4
46L1	Del RA 200/140	3.33	0.208	56.7	12.2	18.4	89.4	72.2
46L2	Del RA 200/140	2.8	0.221	56.9	17.2	36.7	88.9	75.7
46D1	SS F-12	2.39	0.188	60.7	13.8	19.0	75.5	222.6
46D2	SS F-12	2.09	0.180	59.9	19.0	34.2	75.0	232.8
46K1	SS F-12	1.67	0.186	56.1	16.2	20.4	89.1	67.6
46K2	SS F-12	1.52	0.17	56.5	20.2	34.5	89.5	74.4

The six nozzles all fit the square root-normal distribution, and the normalized standard deviation showed all six nozzles to give the usual value of  $0.20 \pm 0.02$  (c.f. Fig. 3.18). Hence, while the Raindrop nozzle does indeed give a coarser spray, it gives the same size distribution about the median. Physically, once the spray issues from any of these nozzles, it is subject to the same inertial, viscous, and surface forces as all the others.

### **3.4.3 Conclusions**

No commercially available spray nozzles were identified which will allow control of mean drop diameter and size distribution width, independent of the normal operating parameters of nozzle diameter and liquor pressure, temperature, and per cent solids. A coarser-than-normal spray can be obtained with the Delavan Raindrop nozzle; this deserves consideration for boilers with unusually high carryover rates.

## **3.5 DEVELOPMENTAL NOZZLES**

A task was undertaken to develop new nozzle concepts in an effort to gain some degree of control over drop size and size distribution. One constraint always kept in view was that any new conceptual nozzle had to be easily implementable and very reliable. This latter limitation recognizes the need for the recovery boiler to remain on-line around the clock 350 days a year. One approach was to consider modifications to an existing splashplate nozzle which would change the nature of the sheet coming off the splashplate to reduce the randomness of the breakup process. A second approach has been to employ the principle of vibratory assist and apply it to an existing splashplate nozzle.

### **3.5.1 Dual Splashplate Nozzle**

Gaining some degree of control over the black liquor combustion unit operation would materialize if the balance between in-flight burning and char bed burning could be independently changed by the furnace operator. One conceptual way to accomplish this with a splashplate type of nozzle would be to use more than one nozzle per liquor feed port. Since the number of feed ports on a given boiler is fixed, one way to accomplish this would be to use a dual splashplate nozzle operating off of one liquor feed line. The droplet formation characteristics of the splashplate nozzle are now well known from earlier results in this study, so proper sizing of two nozzles should simultaneously give two different mass median diameters. In theory, this should result in a bimodal drop size distribution, with the fine fraction burning in suspension, and the coarse fraction falling to and burning on the char bed.

The way to accomplish two splashplates off of one feed line through one port opening is to configure the splashplates back-to-back (c.f. Fig 3.19). The liquor feed is divided into two branches, each having a control valve to adjust the flow through its branch. By using different diameter nozzles and different pressure drops in the two branches, two different sheet velocities, and hence two different drop size distributions, can be obtained. Interaction of the two liquor sheets coming off the splashplates can be varied by providing a spacer between the splashplates. By design, the spacer can not only control the distance between the sheets coming off the plates,

FIG. 3.17

## DROP SIZE FROM DIFFERENT NOZZLES

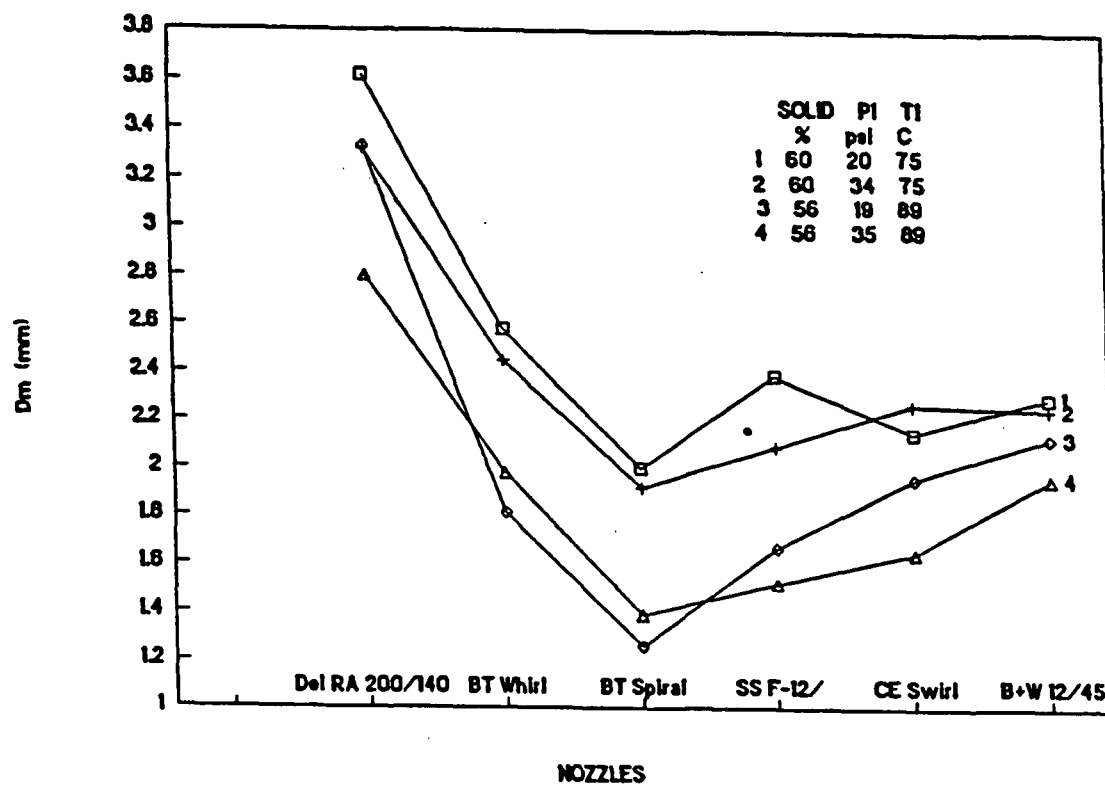
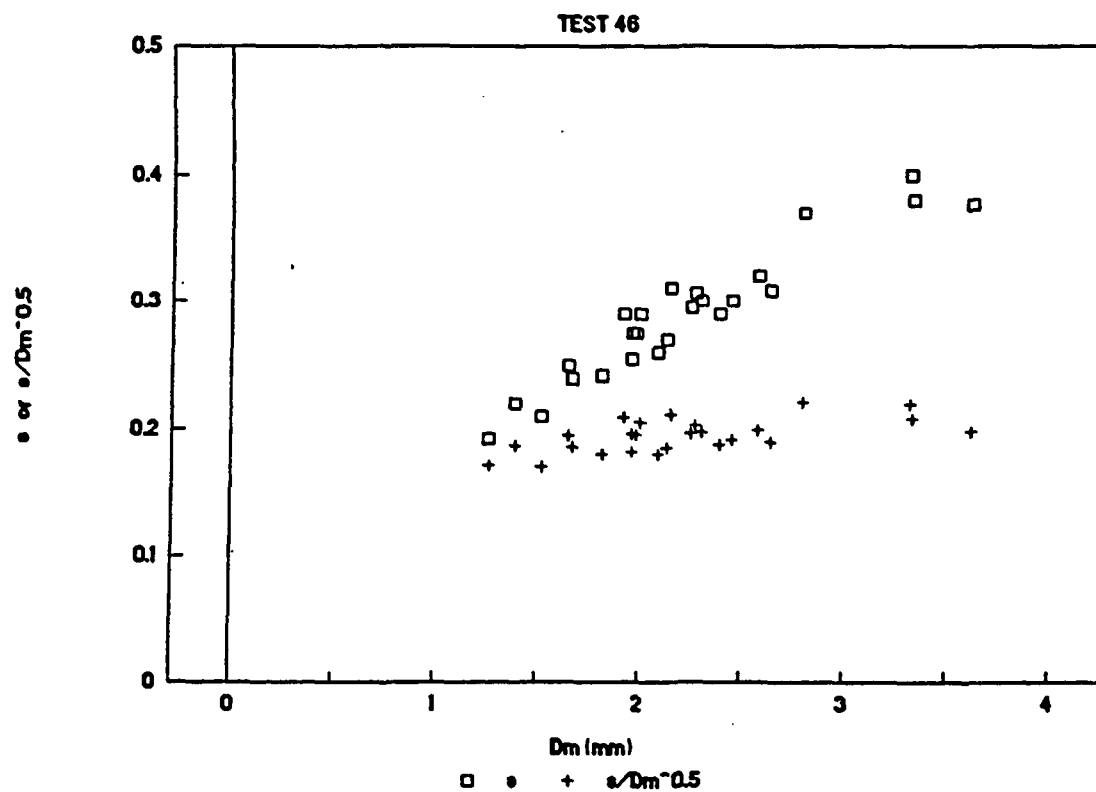


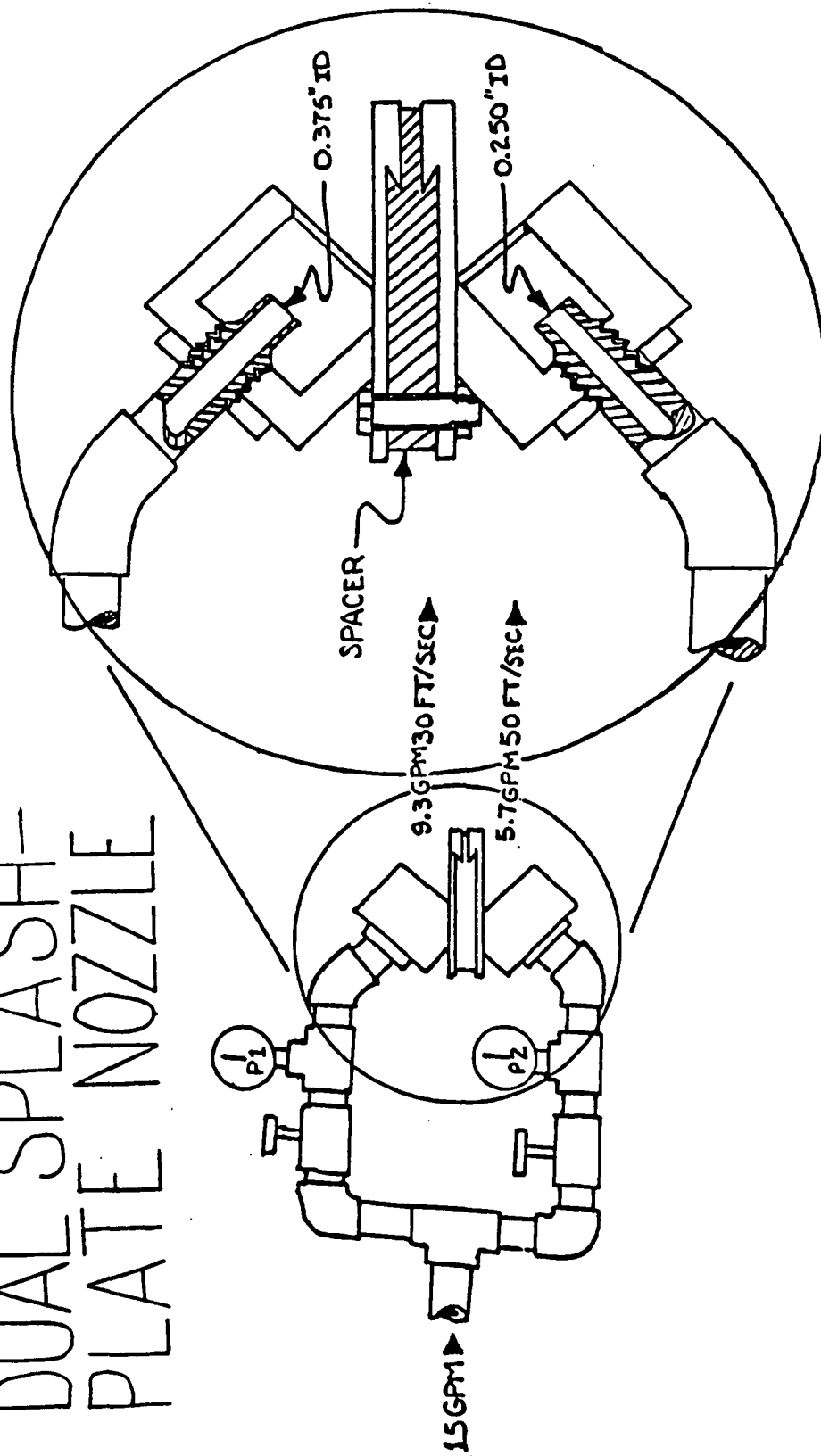
FIG. 3.18

## DROP SIZE DISTRIBUTION FROM DIFFERENT NOZZLES



# DUAL SPLASH- PLATE NOZZLE

FIG. 3.19



PARALLEL

DIVERGING

CONVERGING

DS 11/24/92



but also the angle between the sheets. The sheets can readily be made to converge or diverge, thereby maximizing or minimizing the degree of sheet interaction. Naturally, each branch will function like a typical splashplate nozzle, and hence operational reliability of the dual splashplate concept should not be a concern. Since fabrication of such a nozzle is straightforward, the implementation and reliability issues raised earlier are both positively addressed.

Test results for dual splashplate nozzles are summarized in Table 3.9. The test nozzle with parallel plates spaced one inch apart (Test 50A) gave two liquor sheets which interacted to form a single sheet a short distance from the nozzle. Image analysis of the videos gave a median drop diameter of 2.9 mm, which is about 25% greater than what would have formed from a single sheet at the same conditions, based on previous data (c.f. Table 3.1). Interestingly, the normalized standard deviation of 0.21 is within the expected value for a single sheet. Figures 3.20, 3.21, and 3.22 show the Cumulative Volume Fraction curves for the square root-normal distribution, and the fit in all three cases is very good. Hence, there is no evidence that a bimodal size distribution was achieved for the operating conditions of Test 50A.

The large median diameter and normal size distribution can be explained by physical reasoning. When two parallel liquid sheets run close together, the air between them is quickly drawn out, forming a region of low pressure. The sheets are thus pushed together by the ambient pressure, providing opportunity for droplet coalescence to occur. The sheets breakup under the same fluid dynamic forces as a single sheet, yielding an unchanged distribution.

In Test 51, nozzle orifice diameters were increased to allow lower, more normal operating pressures, while keeping liquor flow rate, temperature, and per cent solids (and hence viscosity) roughly constant. Median drop size and size distribution remained at the values of Test 50A. Each side of the dual splashplate nozzle was run with the other shut off to assess their individual performance (Tests 51D, 51E). Median drop size agreed with earlier single nozzle results where the median drop size was about 75% of the dual splashplate drop diameters. Again, the normalized standard deviation of 0.19 was within the expected range.

In Test 52, the distance between the parallel plates was increased from one inch to 2.5 inches in an attempt to reduce the amount of interaction between the two sheets. Comparison of median diameters with those of Tests 51A, 51B, and 51C shows no significant difference. The width of the distribution as quantified by the normalized standard deviation is 0.21, which is within the normal range for single nozzles. Hence, there appears to be significant coalescence phenomena occurring to give the larger-than-expected drop sizes.

In Test 53, the two splashplates were oriented 20 degrees to each other in a diverging mode, forcing the spray sheets to travel away from each other and have much less, if any, interaction. Note that the drop sizes were about 30% smaller than the comparable parallel plate cases, and in agreement with the single nozzle results. Hence, we conclude that sheet interaction for the diverging nozzle was negligible.

The question of whether or not a bimodal drop size distribution from the dual splashplate nozzles was ever achieved needs to be addressed. In general, the sprays from the dual splashplate nozzles were similar to those produced by a single nozzle. The distributions fit the square root-

Table 3.9

## DUAL SPLASHPLATE NOZZLES

TEST	Nozzle	Solids (%)	F1 (gpm)	P1 (psi)	TC2 (C)	V1 (cP)	Dm mm	s/Dm <sup>.5</sup>
50A1	SP-ab1	61.4	9.98	100	84	128	2.9	0.22
50A2	SP-ab1	60.3	10.24	100	94	80	2.9	0.21
50A3	SP-ab1	60.5	10.46	100	100	68	2.8	0.21
51A1	SP-ab2	60.0	10.4	33.0	83.2	146.0	3.65	0.225
51A2	SP-ab2	61.8	12.1	42.5	84.6	152.1	2.90	0.217
51A3	SP-ab2	62.0	14.2	35.5	85.2	159.0	3.00	0.202
51B1	SP-ab2	61.7	15.4	36.0	96.1	98.5	2.80	0.209
51B2	SP-ab2	62.0	13.5	36.2	96.9	100.5	2.86	0.207
51B3	SP-ab2	61.7	11.1	36.6	97.3	100.6	3.40	0.228
51C1	SP-ab2	58.4	11.6	36.3	97.1	59.1	2.90	0.211
51C2	SP-ab2	59.1	14.3	33.6	97.8	68.9	2.75	0.199
51D1	SP-a2	60.2	8.9	28.3	96.5	71.2	2.50	0.209
51D2	SP-a2	60.2	8.2	24.4	98.5	68.1	2.30	0.204
51D3	SP-a2	60.4	7.0	19.5	99.1	70.0	2.40	0.194
51E1	SP-b2	60.2	3.7	19.8	99.6	62.3	2.40	0.187
51E2	SP-b2	60.3	4.2	23.7	99.4	64.0	2.08	0.194
51E3	SP-b2	60.9	4.5	26.5	99.9	67.1	2.16	0.191
52A1	SP-bi2	60.1	9.1	16.4	92.0	110.1	2.95	0.210
52A2	SP-bi2	60.2	11.4	21.8	91.8	113.8	3.70	0.234
52A3	SP-bi2	61.0	9.2	34.2	92.1	126.6	3.40	0.217
52A4	SP-bi2	60.8	11.2	26.4	90.8	129.7	2.85	0.207
52B1	SP-bi2	60.5	10.3	32.2	100.8	86.6	2.85	0.207
52B2	SP-bi2	60.8	12.6	25.1	102.0	86.4	2.85	0.201
52B3	SP-bi2	60.6	12.3	25.9	100.9	87.1	2.70	0.216
52B4	SP-bi2	60.9	9.8	17.7	102.9	85.1	3.40	0.228
					TC1	V1(@T1)		
53A1	SP-	59.7	11.9	41.1	85.5	133.8	1.94	0.187
53A2	SP-	60.2	14.5	40.5	86.9	138.4	2.16	0.191

## Nozzle Key:

SP-ab1: plates parallel, one inch apart

SP-ab2: plates parallel, one inch apart

SP-a2: only one nozzle and plate

SP-b2: only one nozzle and plate

SP-bi2: plates parallel, 2.5 inches apart

SP-: plates at 20 diverging angle

FIG. 3.20

# NORMALIZED DISTRIBUTION, 50A1

$D_m = 2.90 \text{ mm}, s = 0.38$

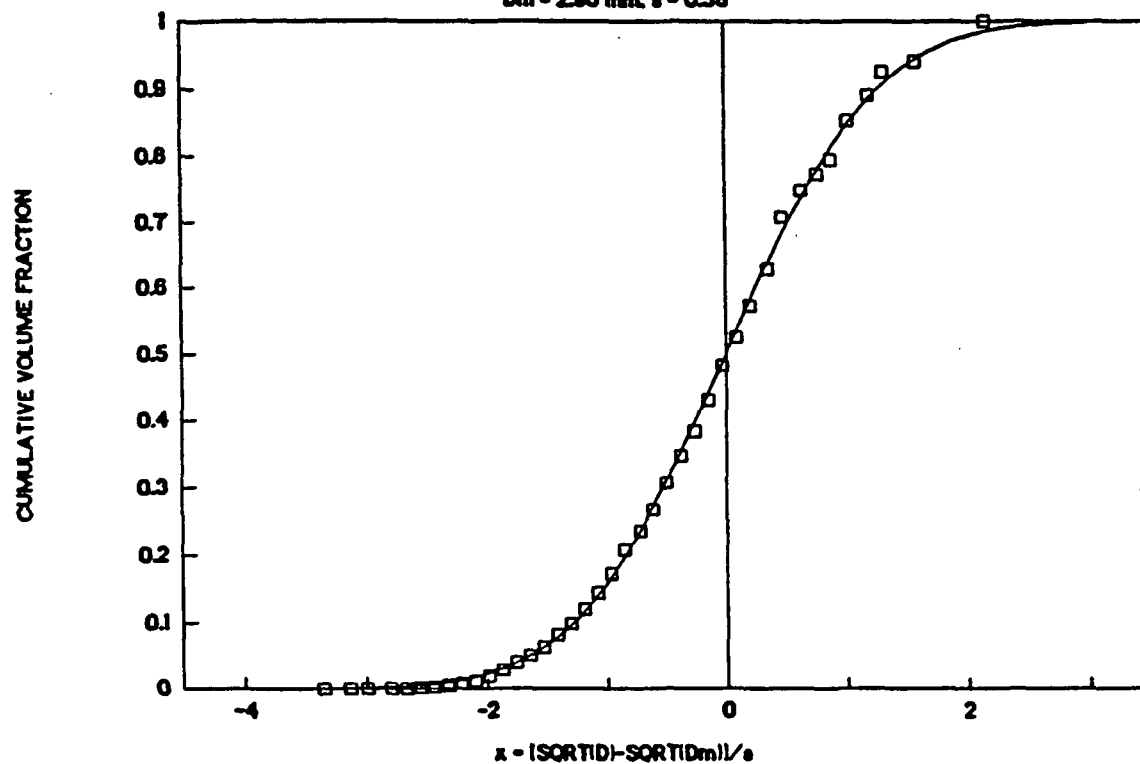


FIG. 3.21

# NORMALIZED DISTRIBUTION, 50A2

$D_m = 2.85 \text{ mm}, s = 0.36$

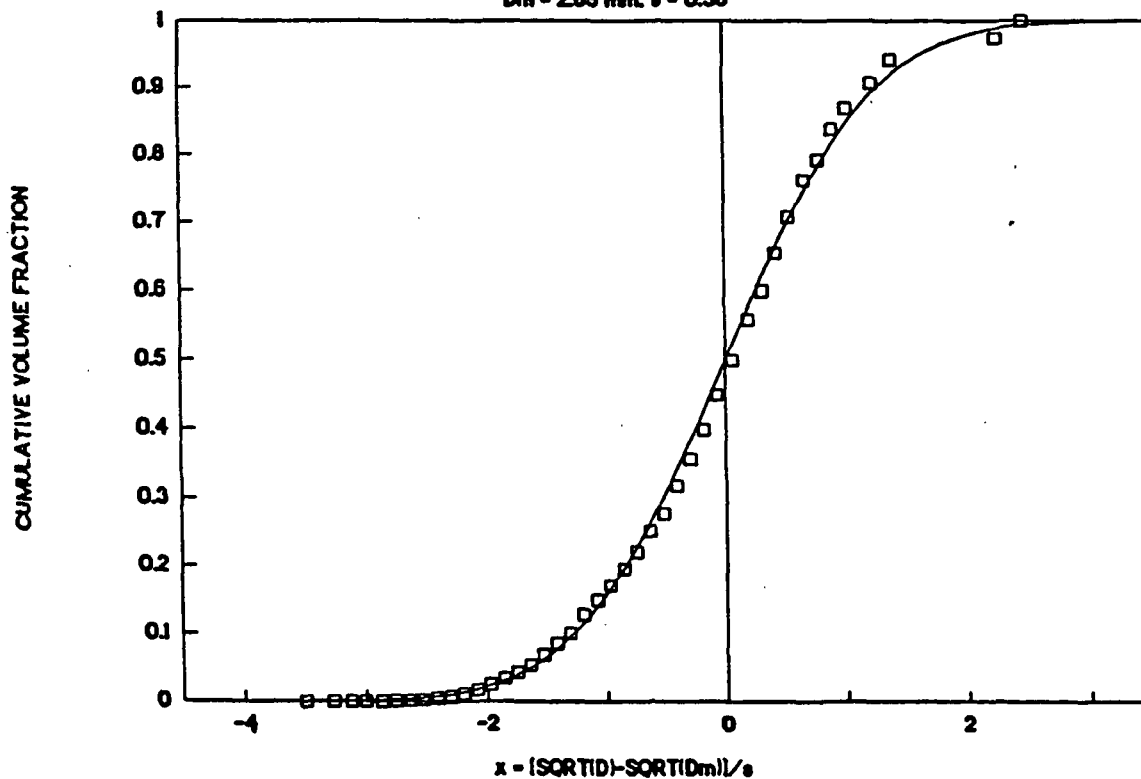
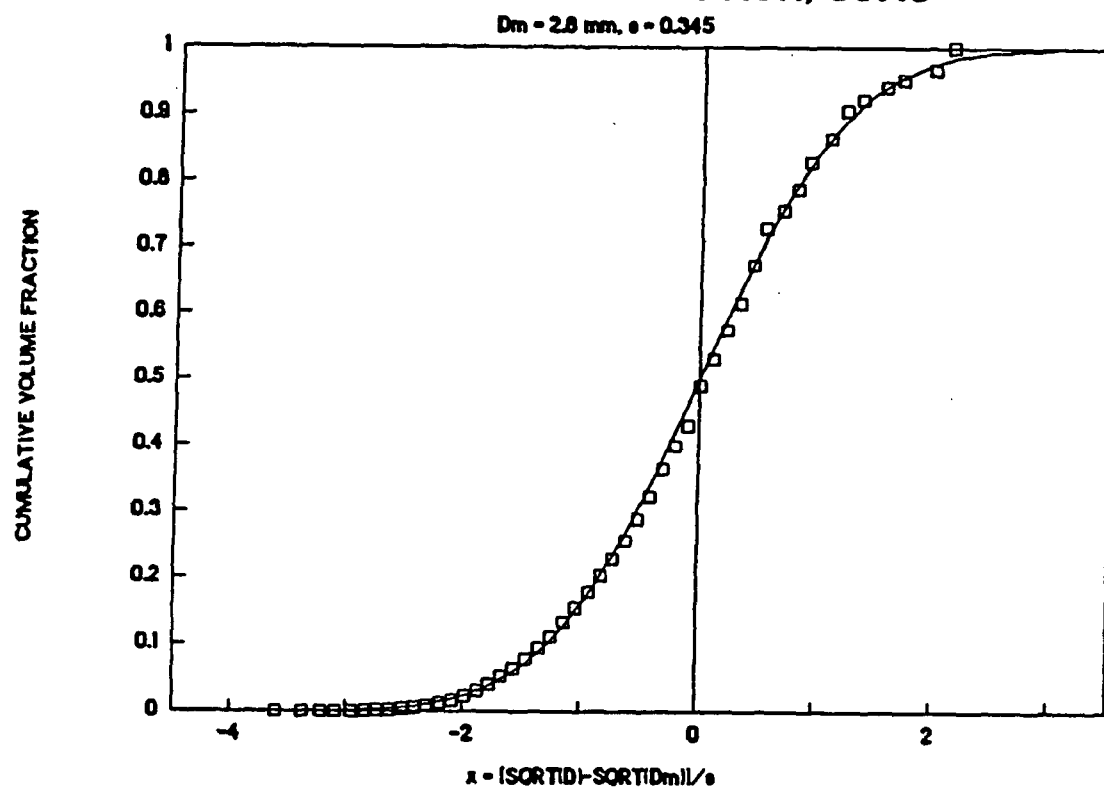


FIG. 3.22

# NORMALIZED DISTRIBUTION, 50A3



normal function well and gave the same distribution width, as expressed by the normalized standard deviation. It should be stressed that this does not imply that the distributions from both sides of the dual splashplate were the same. The fact is that when two different distributions are superimposed, the result can be represented under certain conditions, with negligible error, by another single distribution. Figure 3.23 demonstrates superimposition of the two distributions from Tests 51D1 and 51E2. The combined result is accurately described by a single distribution. If the difference between the two mass median diameters is not relatively large, it is difficult to generate a bimodal distribution with two distinctive probability density peaks.

Only when the difference between the medians is considerably larger than their standard deviations may the combination of two normal distributions result in a bimodal distribution with two distinct probability density peaks. To illustrate this, consider the hypothetical case of two different square root-normal distributions each having a normalized standard deviation of 0.2. The first distribution will be chosen to have a median diameter of 2.0 mm at a liquor flow rate of 40% of the total, while the second distribution will have a median diameter of 5.0 mm at a flow rate 60% of the total. Figure 3.24 shows the probability density curves for these two distributions. If these data are then combined and a single probability density curve constructed, the result shows a curve with two distinct peaks, and hence a bimodal distribution. For the combined data, the Cumulative Volume Fraction curve can be readily calculated and the result is also shown on Fig. 3.24. Note that these data points deviate from the square root-normal curve in a characteristic way. It should also be noted that the normalized standard deviation for the combined case is 0.29, or 50% higher than the values for the individual component distributions. This would signify that the combined case has a significantly broader distribution. By comparison with Fig. 3.23 where the individual median diameters were much closer together, the normalized standard deviation for that combined case was still within the normal range for a single distribution.

Hence, from this analysis, any truly bimodal distribution ought to show the characteristic deviation from the square root-normal Cumulative Volume Fraction curve and have a normalized standard deviation well above 0.2. The dual splashplate data did not show either of these properties; however the two individual median diameters were not enough different from each other that we should have expected to see a bimodal distribution. Run conditions need to be tried where the expected individual median diameters are far enough apart.

### 3.5.2 Modified Splashplate Nozzles

To gain some degree of control over black liquor drop size and size distribution, we must reduce the randomness of the sheet breakup process. Conceptually, one way to accomplish that would be to modify the smooth, flat surface of the splashplate on splashplate nozzles in such a way that the liquor sheet is no longer uniform, but has defined zones of alternating thick and thin cross-section. In this way, the sheet would initially tend to break at the thin spots, which would be governed by how the sheet thickness was perturbed by the surface characteristics of the modified splashplate. Hence, the initial breakup would no longer be random. Of course, subsequent breakup of the resulting individual "jets" into droplets would still be governed by fluid mechanical forces and the randomness that those forces introduce.

# BIMODAL DISTRIBUTION

TEST 51D1 AND TEST 51E2

FIG. 3.23

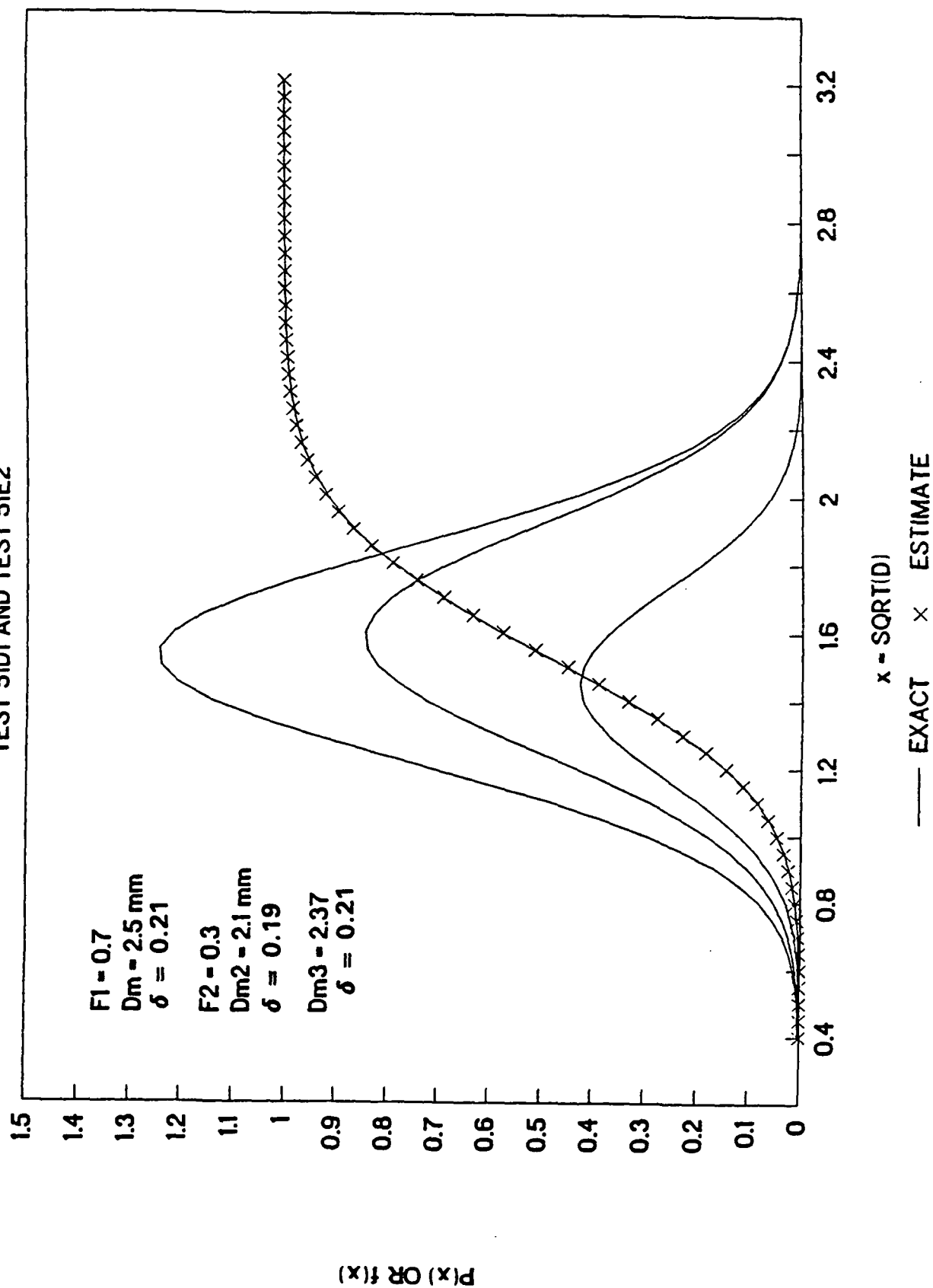
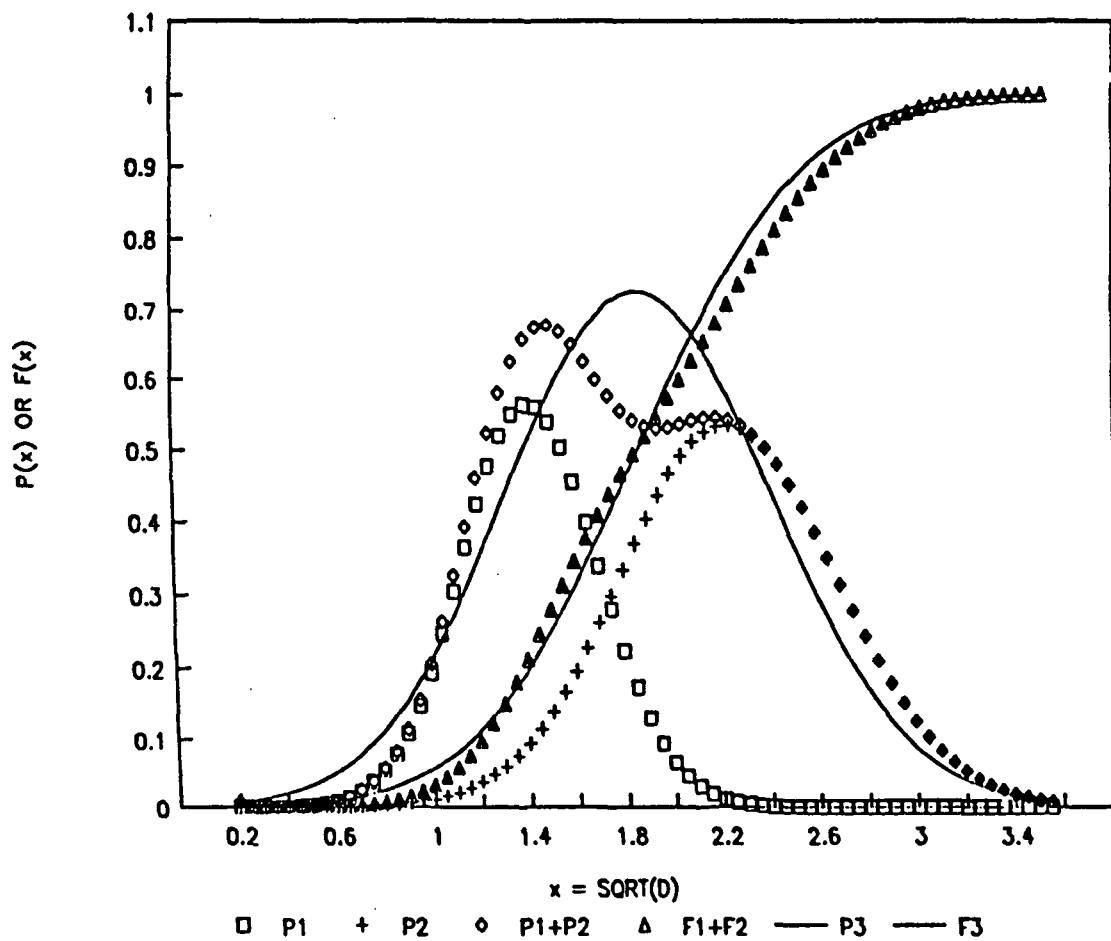


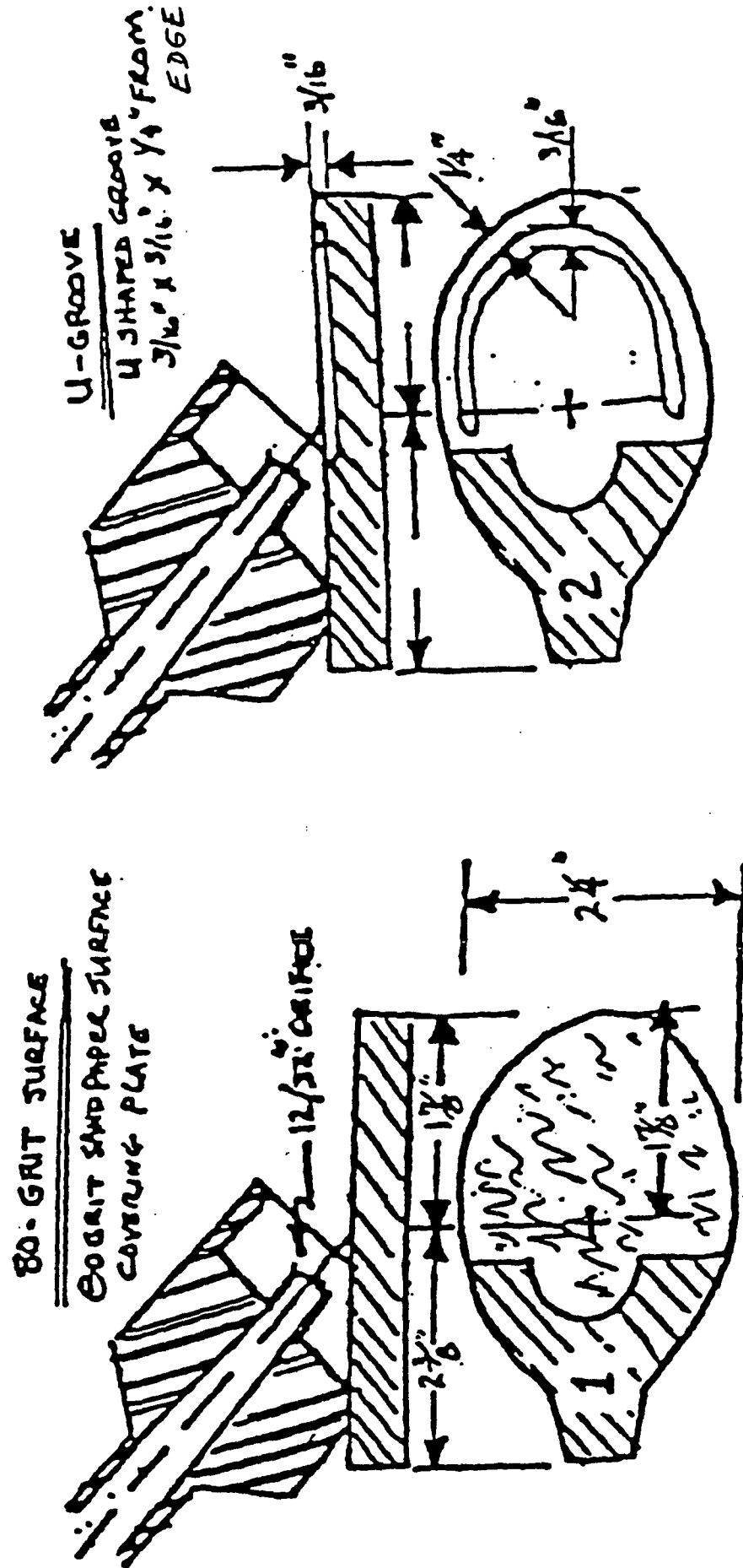
FIG. 3.24 BIMODAL DISTRIBUTION AND APPROXIMATION



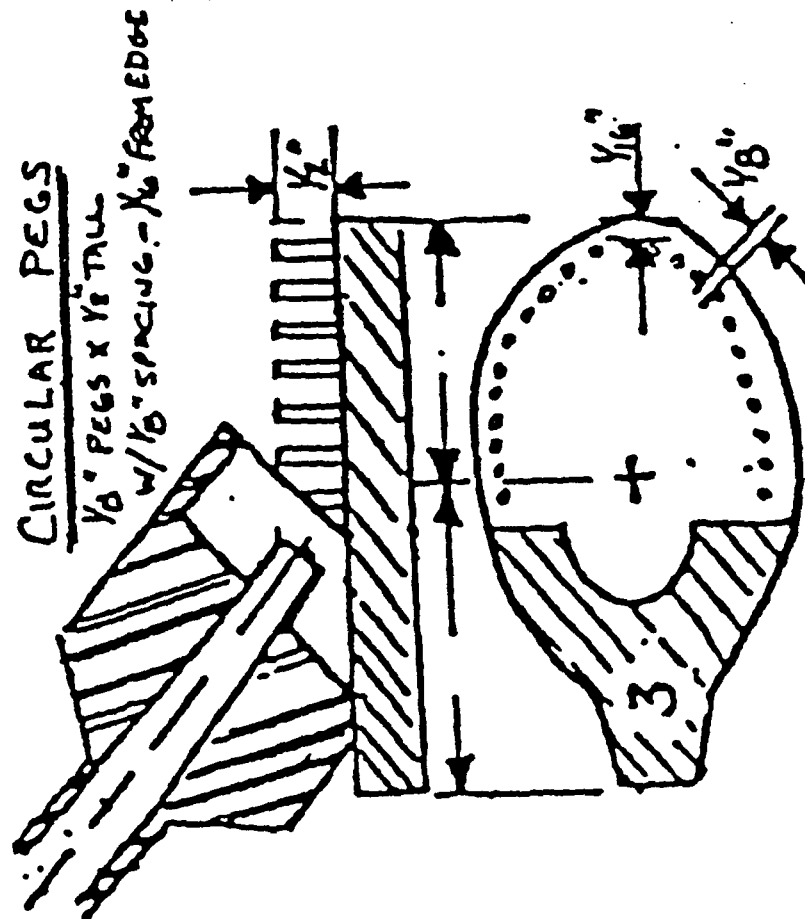
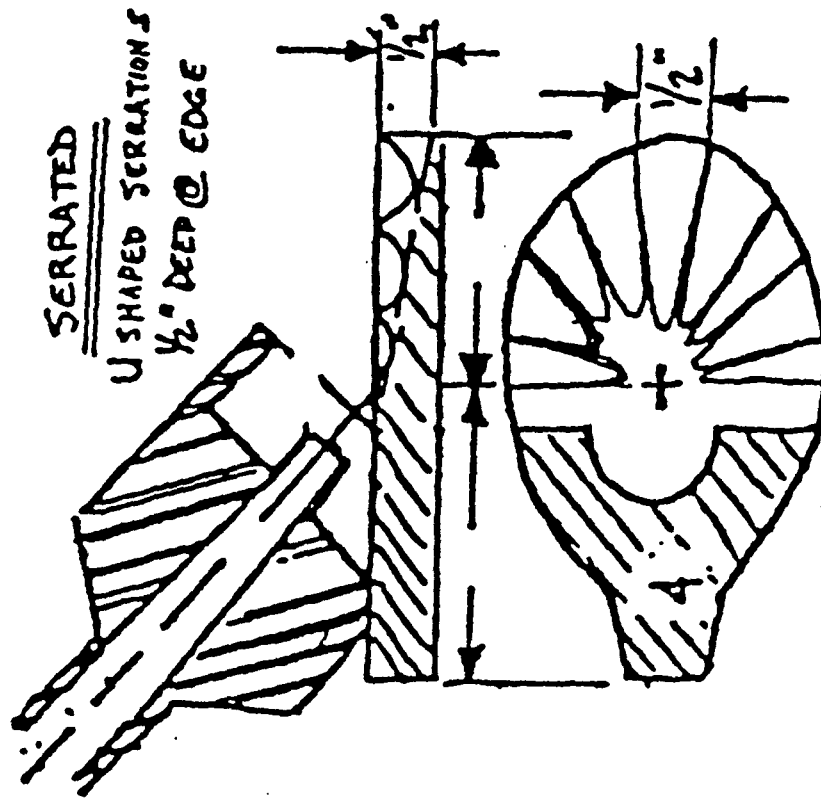
F1 =	0.4	F2 =	0.6	F3 =	1
Dm1 =	2	Dm2 =	5	Dm3 =	3.5
s1 =	0.283	s2 =	0.447	s3 =	0.55
s/Dm <sup>0.5</sup> =	0.2	s/Dm <sup>0.5</sup> =	0.2	s/Dm <sup>0.5</sup> =	0.294

# MODIFIED SPLASH PLATES

FIG. 3.25







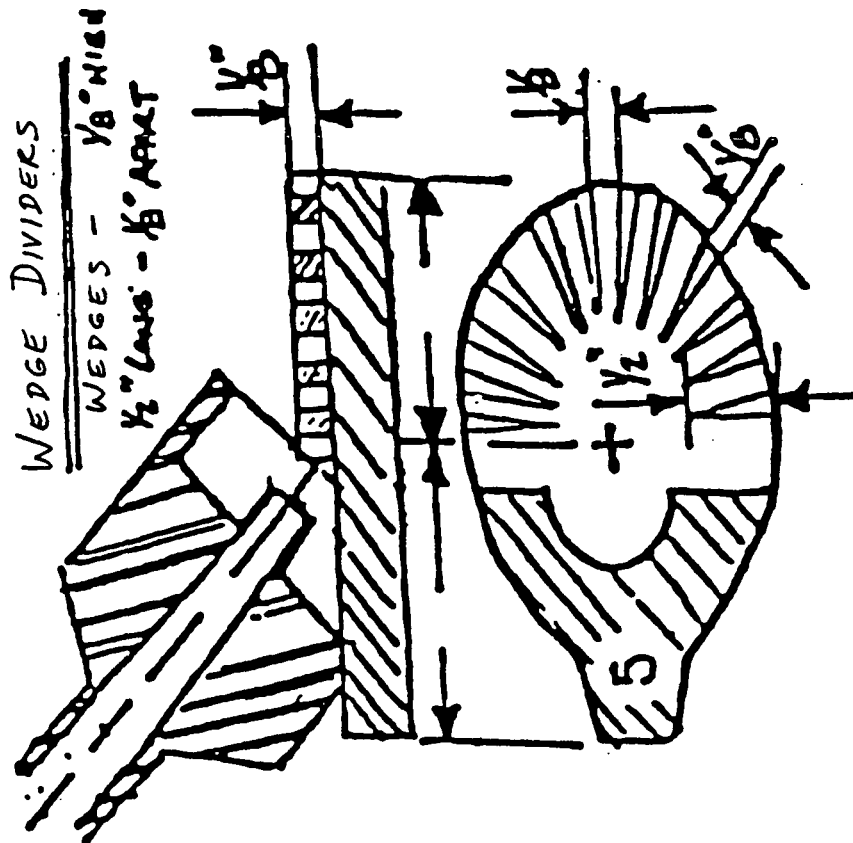
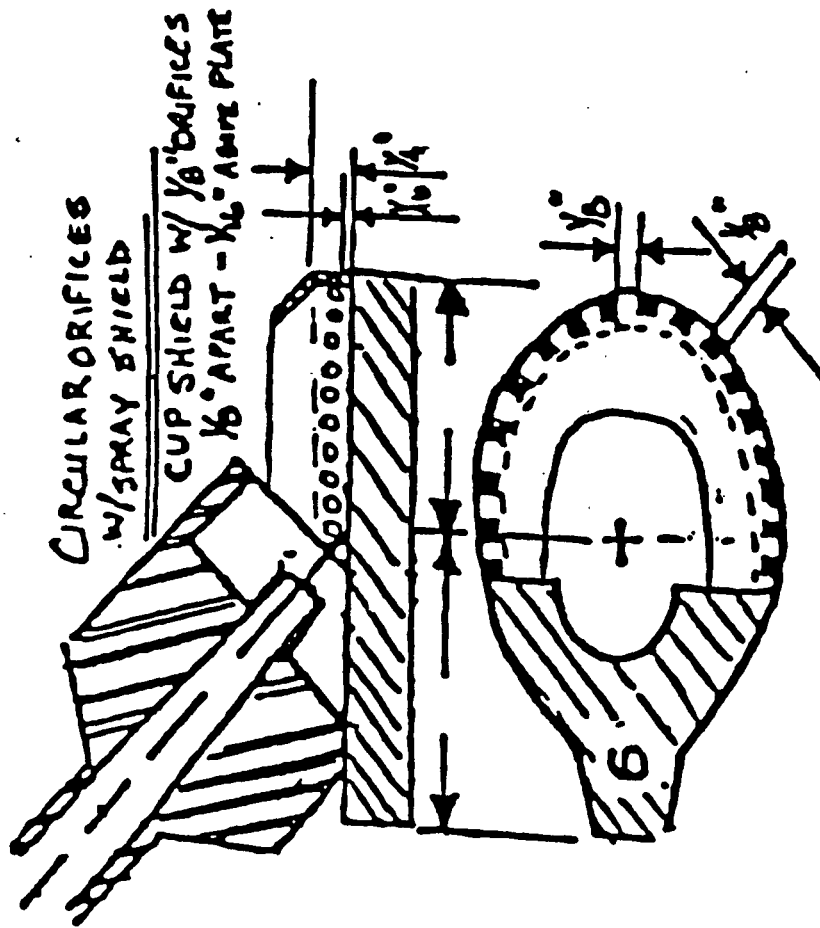


Table 3.10

## TEST CONDITIONS AND RESULTS FOR MODIFIED SPLASHPLATES

Test	Spray Nozzle	Solids (%)	F1 (gpm)	P1 (psi)	TC1 (C)	V1 (cP)	Dm mm	s/Dm <sup>.5</sup>
47A1	B&W	59.4	12.0	19.4	90	108	2.4	0.22
47A2	B&W	59.3	12.3	19.2	94	94	2.4	0.21
47A3	B&W	59.3	12.6	19.2	103	72	2.4	0.19
47A4	B&W	61.1	12.4	18.5	106	67	2.4	0.18
47A5	B&W	60.3	12.3	19.9	114	59	2.4	0.21
47A6	B&W	61.0	11.8	20.8	119	54	2.5	0.20
47A7	B&W	62.4	12.1	22.9	124	48	1.8	0.18
48I1	U-Groove	61.2	10.24	19.7	77	210	2.4	0.21
48I2	U-Groove	61.2	14.32	34.9	76	245		
48J1	80-Grit	61.8	10.07	19.7	81	205		
48J2	80-Grit	61.7	14.81	35.1	81	200		
48K1	Orifices	61.7	10.08	20.5	79	217	4.2	0.15
48L1	Orifices	59.6	11.54	18.0	98	77	1.6	0.20
48L2	Orifices	59.4	17.14	34.2	103	63	1.8	0.20
48M1	Wedges	59.6	17.08	34.6	102	62	1.9	0.20
48F1	Wedges	60.0	10.68	20.4	74	196	2.3	0.21
48N1	Serrated	60.0	12.35	20.0	102	62	1.7	0.21
48N2	Serrated	60.4	17.15	35.3	107	66	3.0	0.26
48O1	Cyl-Pegs	61.0	12.37	19.6	107	64	2.4	0.26
48H2	Cyl-Pegs	61.0	14.26	34.4	75	223	2.4	0.28
56A1	Cyl. pegs (1/16")	59.4	12.9	14.6	89	114	1.83	0.185
56A2	Cyl. pegs (1/16")	59.2	14.9	19.9	92	99	1.71	0.176
56A3	Cyl. pegs (1/16")	59.7	16.6	24.9	92	106	1.7	0.176
56B1	Cyl. pegs (1/4")	61.1	12.3	15.2	76	249	4.7	0.240
56B2	Cyl. pegs (1/4")	61.3	14.3	20.6	83	190	3.2	0.252
56B3	Cyl. pegs (1/4")	61.5	15.6	24.6	87	170	1.74	0.197

Proposed modified splashplate nozzles are subject to the same guidelines applied to the dual splashplate nozzle, namely any changes must be easily implemented and the modified nozzle must maintain near 100% operational availability. Six different modified splashplates were designed, fabricated, and tested in the black liquor spray chamber. These are shown in Fig. 3.25.

Table 3.10 summarizes the droplet formation data for the modified splashplate nozzles tested. Black liquor solids was maintained at 60% and nozzle pressures were 20 and 35 psig. Temperature was varied so that viscosities of about 70 and 210 cP were obtained. Several runs with the standard, unmodified splashplate nozzle are listed so that comparisons can readily be made.

The 80-Grit sanded splashplate (#1) had no noticeable change on the spray pattern. No drop size information was obtained on this nozzle due to the predominance of strands as opposed to drops. The splashplate with a U-groove (#2) 3/16" deep around the periphery of the plate 3/16" from the edge also had no noticeable effect on the spray pattern. Test 48I1 with #2 gave the same median diameter and normalized standard deviation as the standard B&W splashplate nozzle. The splashplate with wedge dividers (#5) 1/8" high, spaced 1/8" apart also gave no noticeable change. These three nozzles can be grouped as having a negligible effect on droplet characteristics.

The serrated splashplate (#4) contained U-shaped serrations distributed around the plate periphery in a fan-shaped manner. The depth and width of the serrations went from 0 at the center of the plate to 1/2" at the plate edge. The concept here was to form a liquor sheet with alternating thick and thin regions where initial breakup would be favored in the thin areas. Test results with this nozzle were inconclusive. Test 48N1 at 20 psig gave a 30% smaller median drop size than the B&W nozzle, but the same distribution width. On the other hand Test 48N2 at 35 psig gave a median diameter nearly twice that at 20 psig and a normalized standard deviation of 0.26, similar to what would be expected from a bimodal distribution.

Splashplate #6 was fitted with a 1/2" high cupped shield around the periphery of the plate. The shield was drilled with 1/8" orifice holes spaced 1/8" apart and 1/16" above the plate surface. As liquor flowed along the surface, it encountered the shield and flowed out through the orifice holes. The result was that the liquor came off the splashplate in the form of multiple cylindrical jets, which then broke up into droplets. Test 48K1 at low temperature gave an unusually large median diameter (4.2 mm) and did not fit the square root-normal model well. If the drop diameters larger than the median are fit to the square root-normal curve, an unusually small normalized standard deviation (0.15) results, as shown in Fig. 3.26. This means that the larger drops are narrowly distributed. If a normalized standard deviation of 0.2 is forced into the square root-normal model, the smaller droplets fit the model, but the larger drops distribute in a narrower range than would be expected by the model. This is shown in Fig. 3.27. At higher temperatures (still below the transition temperature), the median drop diameter fell to 1.7 mm, about 30% smaller than the standard splashplate nozzle, with the normal distribution width. At the higher temperature, nozzle pressure made no difference in drop diameter.

The most interesting modified splashplate nozzle (#3) tested had a series of cylindrical pegs mounted normal to the surface of the plate around the plate periphery 1/16" from the edge. The

FIG. 3.26

## NORMALIZED DISTRIBUTION, 48K1

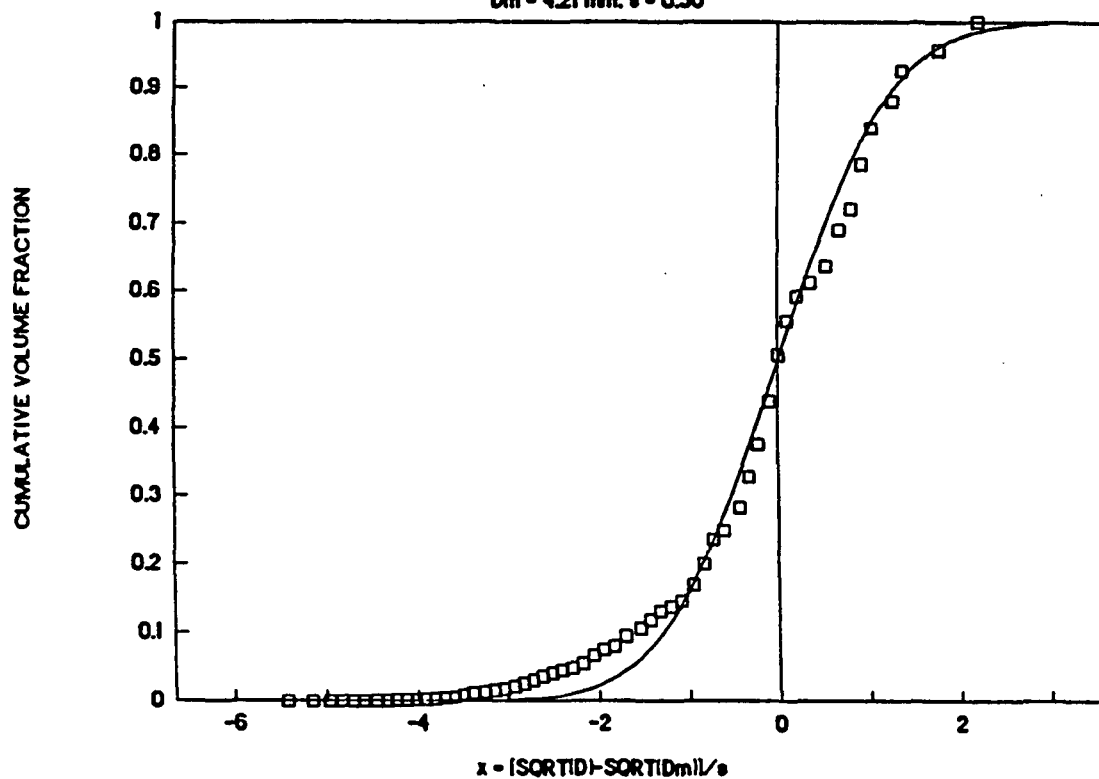
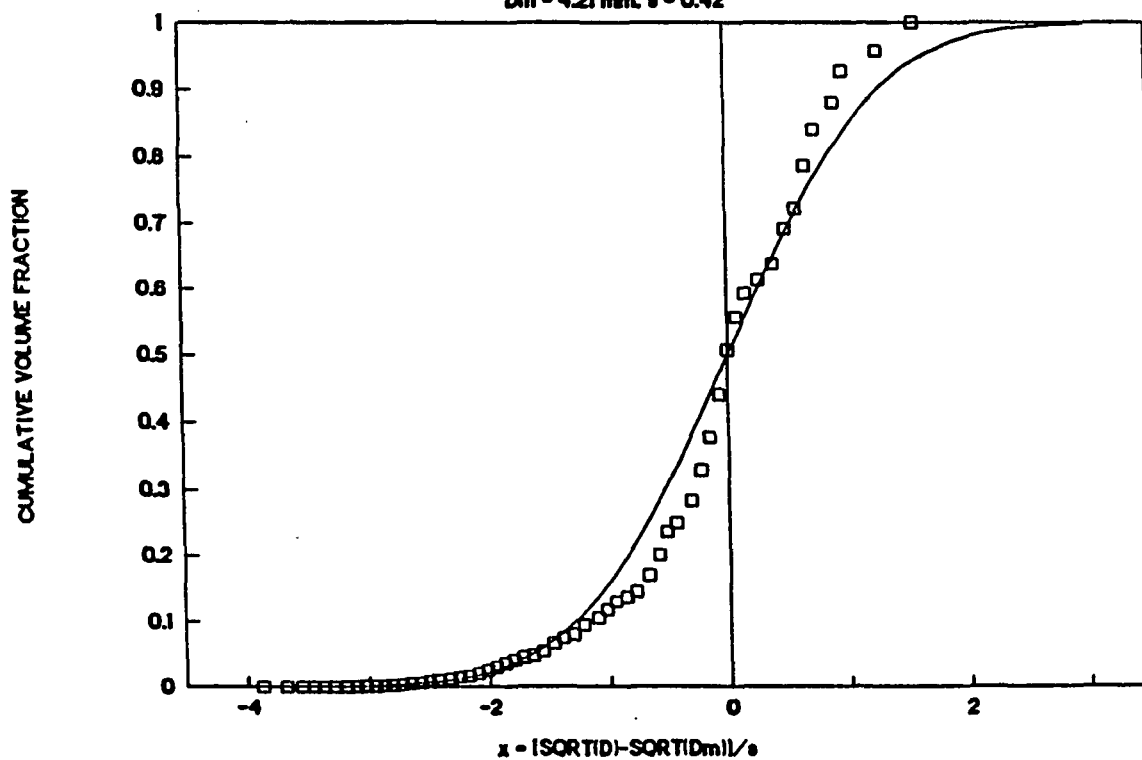
 $D_m = 4.21 \text{ mm}, s = 0.30$ 

FIG. 3.27

## NORMALIZED DISTRIBUTION, 48K1

 $D_m = 4.21 \text{ mm}, s = 0.42$ 

pegs were 1/8" in diameter, 1/2" long, and spaced 1/8" apart. With this configuration, the liquor flowed off the plate in the form of discrete jets. Hence, the mechanism of droplet formation in this case was different from nozzles that formed sheets. Tests 48O1 (107 C, 20 psig) and 48H2 (75 C, 35 psig) gave normal median drop sizes, but the normalized standard deviations were abnormally high, in the range expected for a bimodal distribution. Drop sizes for the two tests are plotted in Figs. 3.28 and 3.29, respectively. It is obvious that neither test gave droplets that fit the square root-normal model. Below the median diameter, the droplets fit the square root-normal distribution, but above it, they were narrowly distributed. In addition, there did not appear to be any effects of temperature or pressure.

Two more splashplate nozzles with 1/8" cylindrical pegs were tested to look at the effect of peg spacing. Test 56A used 1/16" spacing, while Test 56B used 1/4". With the smaller spacing and at low velocity, Test 56A1 produced a bimodal drop size distribution, in which the smaller sizes fit a square root-normal function (c.f. Fig 3.30). Similar to Tests 48H and 48O, some large drops formed from the jets. As the flow rate increased, some black liquor accumulated before the pegs, causing flow redistribution behind the pegs, resulting in a sheet of liquor coming off the plate. The sheet broke up quickly, and the subsequent drop size distribution fitted the square root-normal function perfectly (c.f. Figs. 3.31, 3.32), with the median diameters being 25% under those expected for a standard splashplate nozzle. With the larger spacing and low velocities (Tests 56B1, 56B2), the drop size distributions deviated from the square root-normal function (c.f. Figs. 3.33, 3.34). However, as the velocity increased (Test 56B3), the large strands disappeared and the drop size distributions again fitted the square root-normal function (c.f. Fig. 3.35).

### 3.5.3 Vibratory Assist

A number of studies have been carried out regarding the stability of thin liquid sheets moving in a gaseous environment. Inviscid theories of two-dimensional wave growth predict that, in the initial stages of growth, an optimum frequency exists where the growth rate is a maximum. Viscous theory, on the other hand, predicts the absence of a wave of maximum growth rate except at low velocities. Crapper, et al. (5) have claimed that dominant waves seen on a sheet must be of a frequency imposed by some external force. Hence, the role of vibratory assist is to obtain growth rates of low amplitude waves at any distance from the nozzle orifice. Crapper and Dombrowski (6) suggested that drop size may be effected by both nozzle amplitude and frequency. Since these factors may depend upon natural frequencies in the apparatus, drop sizes in industrial settings could well turn out to be different from those given by the same nozzle in the laboratory.

The effects of external vibrations on the disintegration of liquid jets has been investigated by many, with the finding that atomization can be induced only in widely separated narrow bands of frequency (7,8,9). If a sinusoidal perturbation is applied to a jet of liquid, the jet rapidly decomposes into a sequence of droplets whose diameters are determined by the wave length of the original disturbance. The wave length of the disturbance can easily be varied, and thus, in principle, the size of the droplets can be controlled (9). A similar analysis applied to droplet formation from liquid sheets showed different behavior than that exhibited by jets (10). For perturbations driven solely by capillary forces, the sheet of fluid was found to be stable for all

FIG. 3.29

# NORMALIZED DISTRIBUTION, 48H2

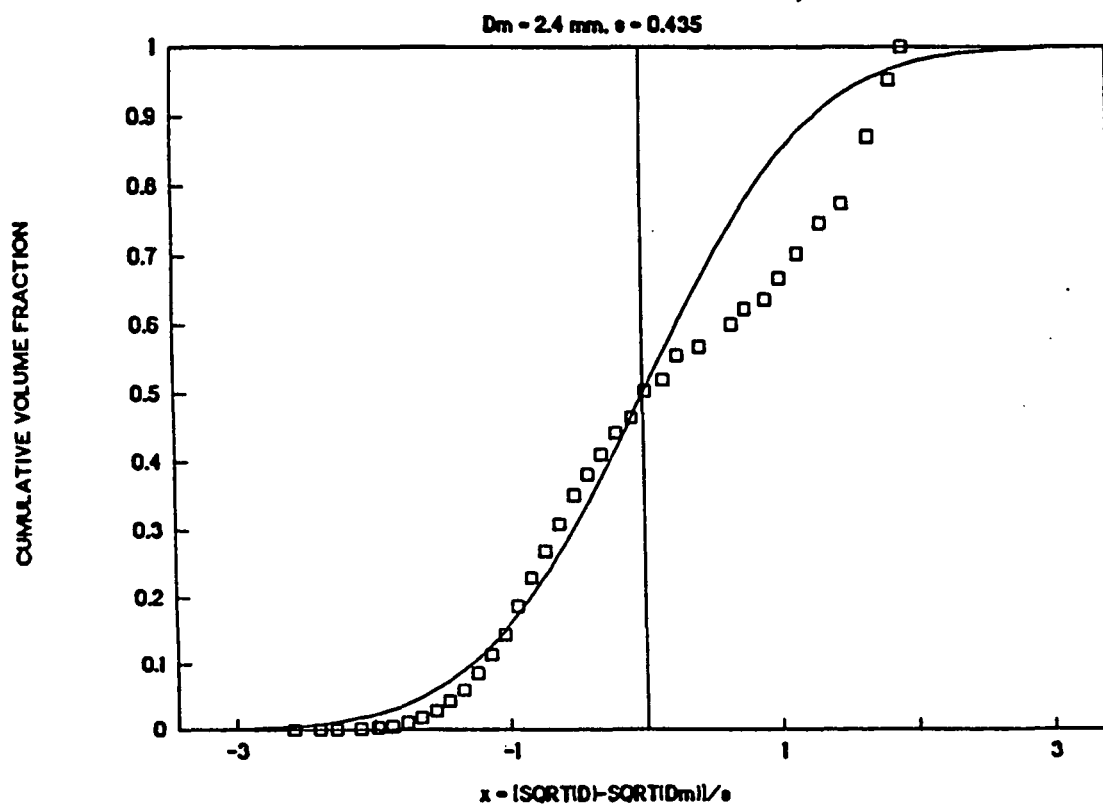


FIG. 3.28

# NORMALIZED DISTRIBUTION, 4801

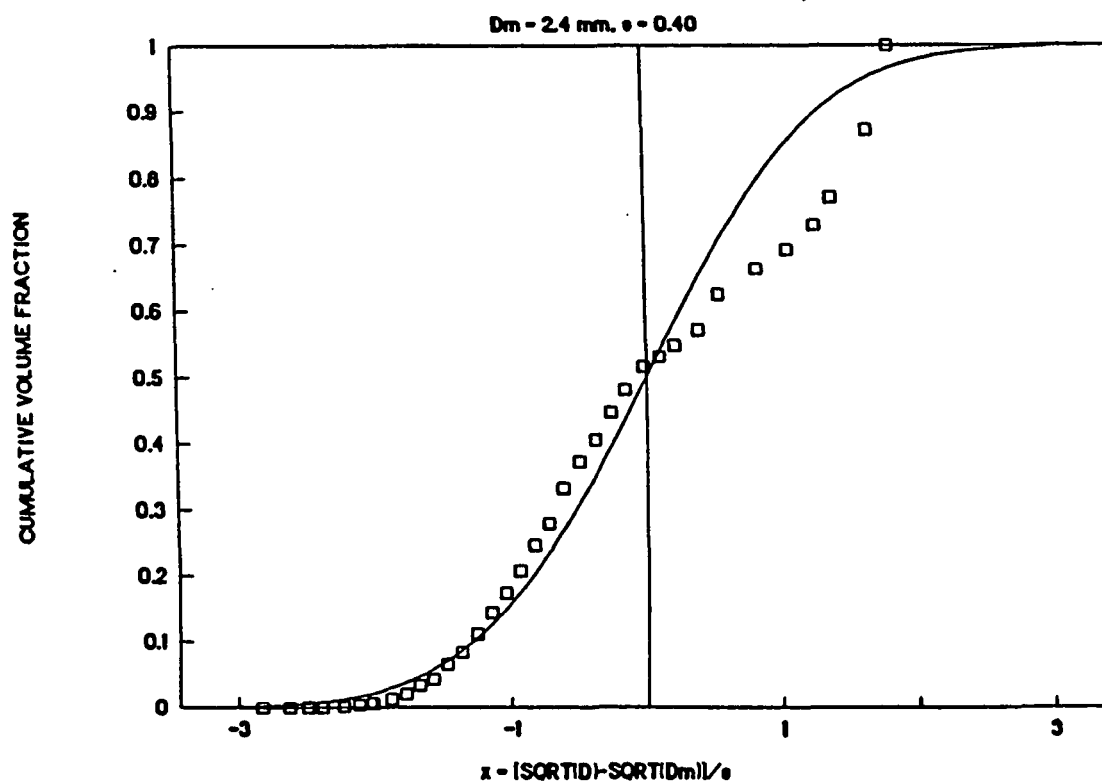


FIG. 3.30

# NORMALIZED DISTRIBUTION, 56A1

$D_m = 1.83 \text{ mm}$ ,  $\sigma = 0.25$

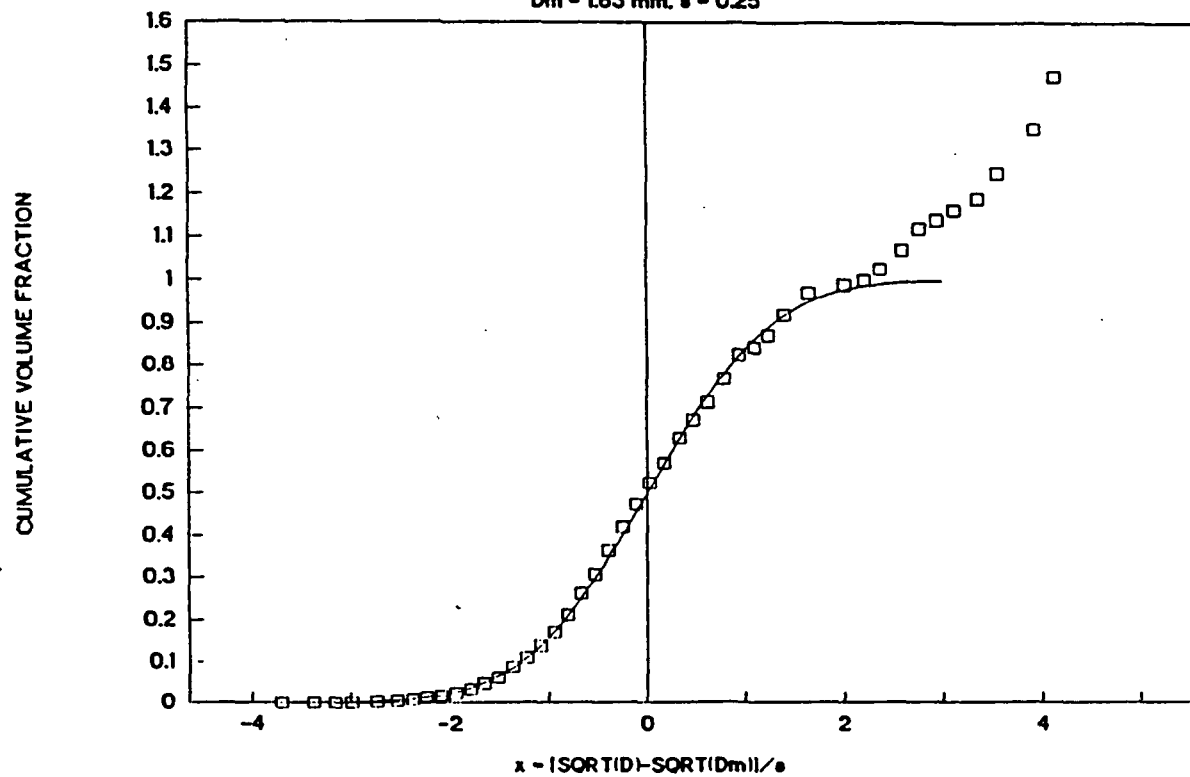




FIG. 3.31

# NORMALIZED DISTRIBUTION, 56A2

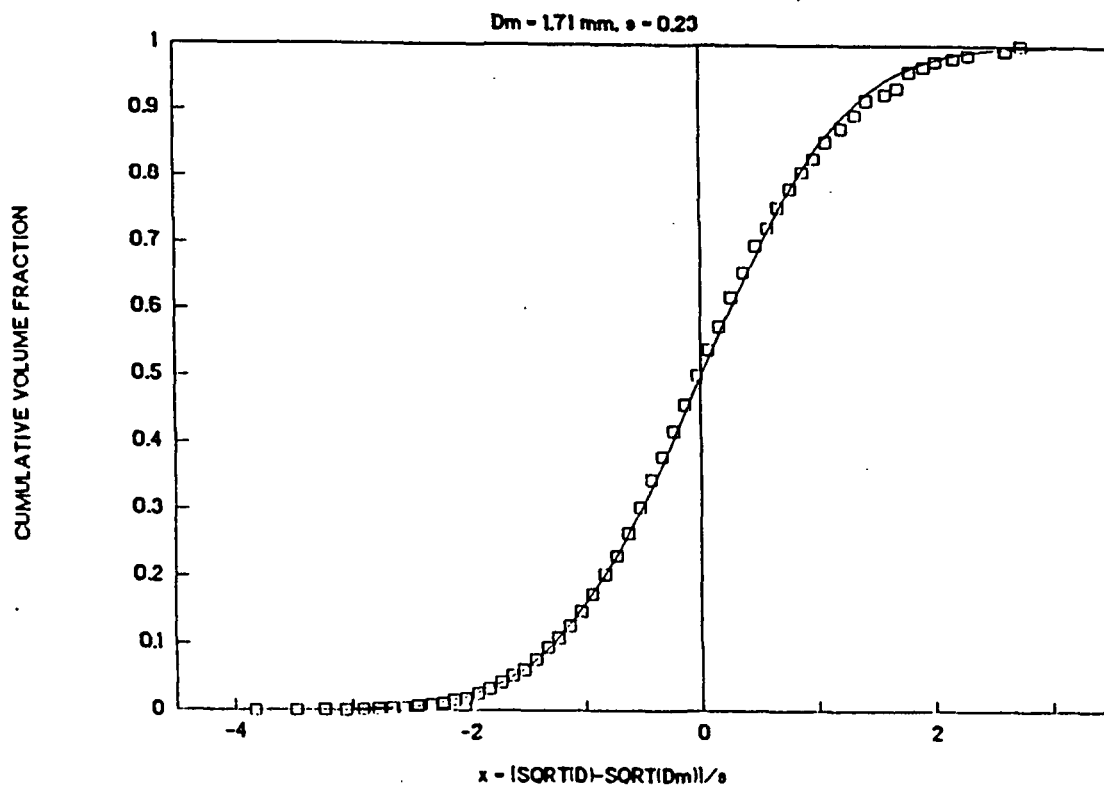


FIG. 3.32

# NORMALIZED DISTRIBUTION, 56A3

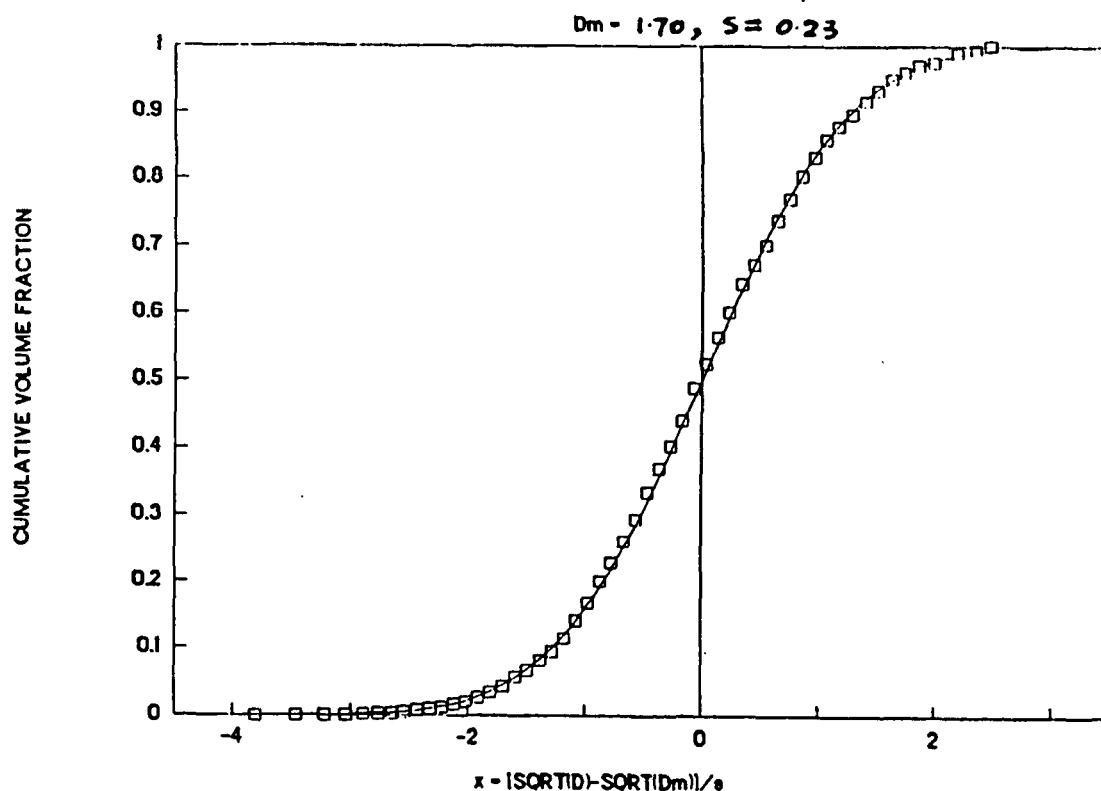


FIG. 3.33

# NORMALIZED DISTRIBUTION, 56B1

$D_m = 4.7 \text{ mm. } s = 0.52$

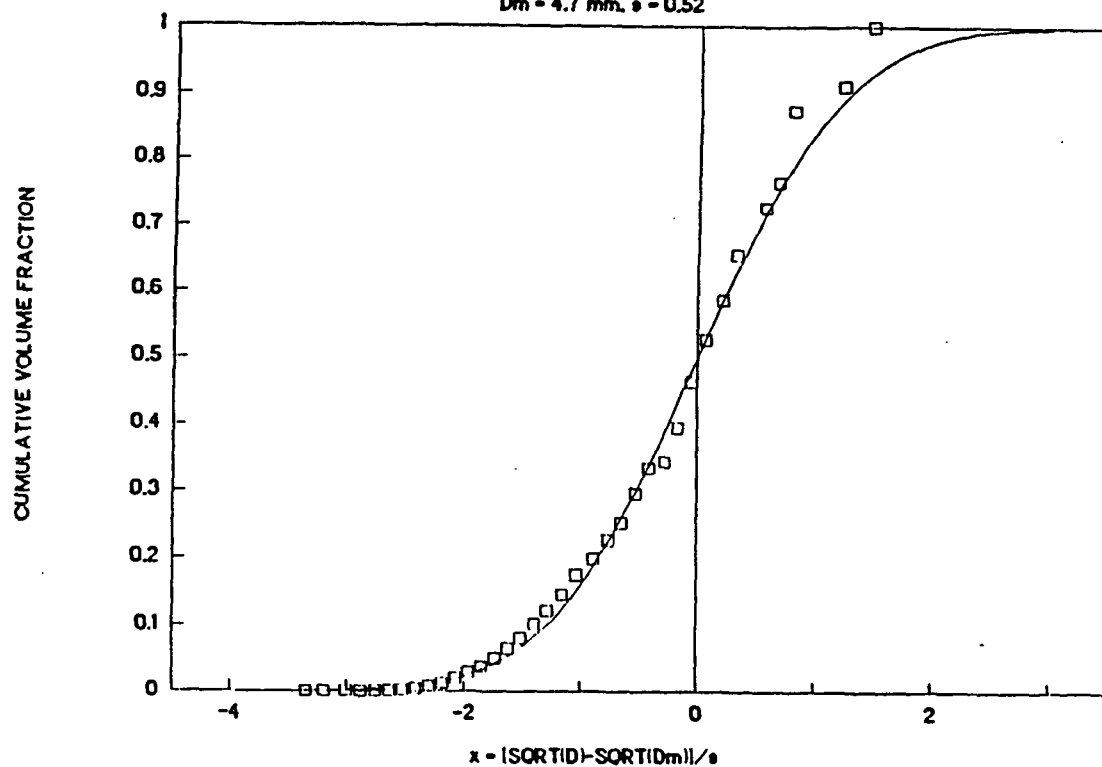


FIG. 3.34

# NORMALIZED DISTRIBUTION, 56B2

$D_m = 3.2 \text{ mm. } s = 0.45$

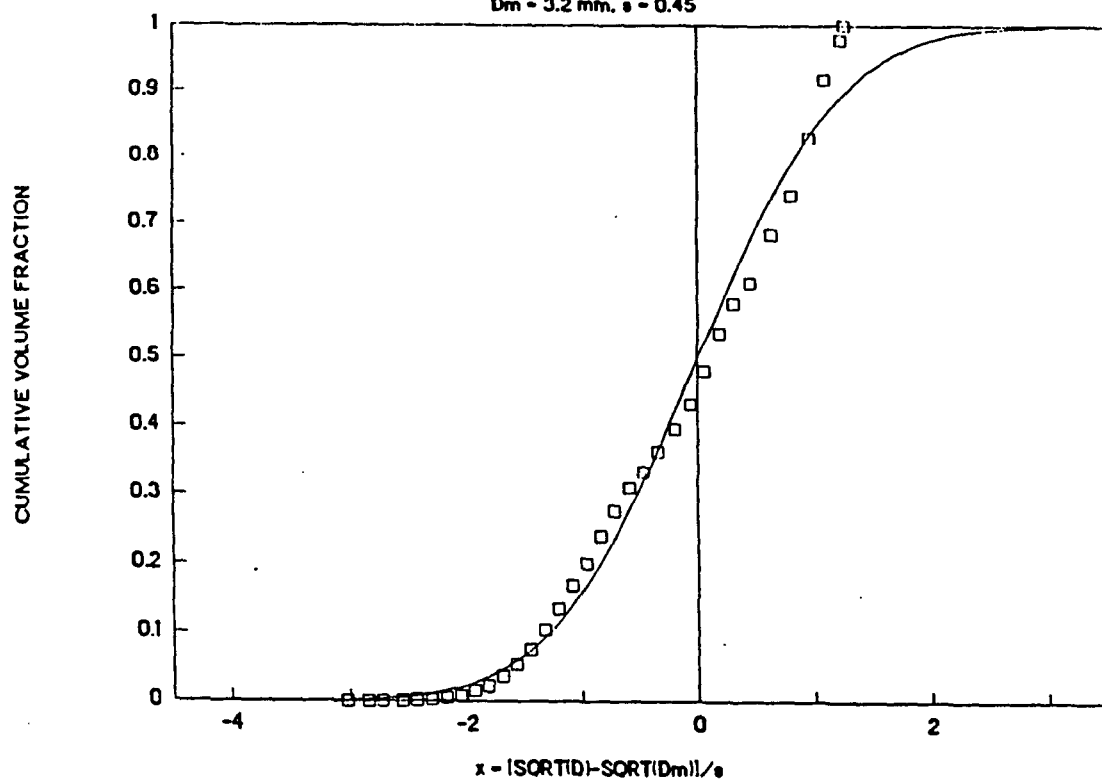
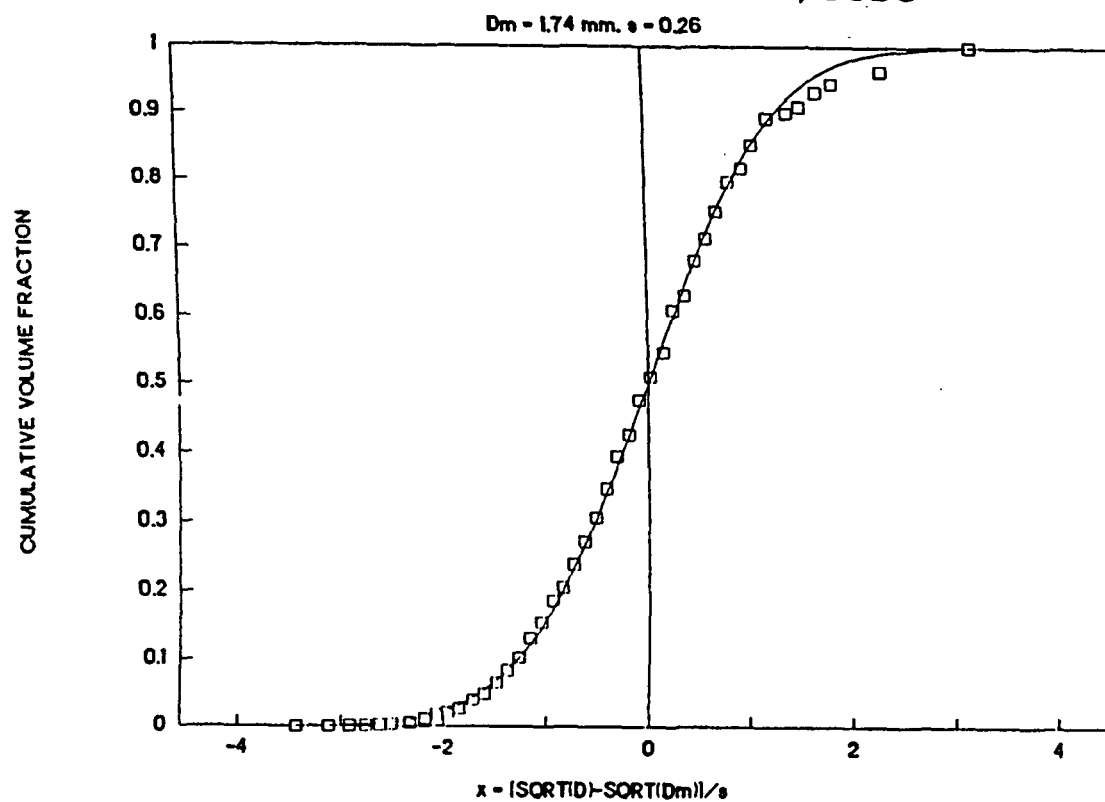


FIG. 3.35

# NORMALIZED DISTRIBUTION, 56B3



perturbations. Hence, the technique of inducing controlled atomization with a small perturbation works only for circular jets and not for sheets.

On the other hand, it has been reported that a high amplitude acoustic signal can achieve some control over the drop size from fans, cones, cylinders, and sheets (10). An acoustically driven atomizer gave a sheet comprised of dilational waves, which subsequently broke up into ligaments which then broke up into uniform drops; a sheet with sinuous waves ejected small drops from the sides of the sheet.

### 3.5.3.1 Frequency of a Vibrating Nozzle

For vibratory assist to work effectively, it must be done at the proper frequency and amplitude. Otherwise the natural frequency of the sheet will dominate, giving a normal distribution of drop sizes. It would be instructive to estimate the operating frequency for desired drop size and specified operating conditions.

Assuming that the velocity ( $v$ ) and the thickness ( $h$ ) of the sheet are uniform at a given distance from the nozzle, wave theory stipulates that an unstable sheet breaks at every half wave length ( $w$ ). The bands of liquor thus formed then break up into droplets. Knowing the volumetric liquor flow rate ( $F$ ), the subtended angle of the spray sheet ( $\theta$ ), the breakup distance ( $L$ ) from the nozzle, and the desired radius ( $R$ ) of the bands of liquor (ligaments), we can calculate the thickness and length ( $l$ ) of a ligament:

$$l = (2 \pi \theta L) / 360 \quad (1)$$

$$h = F / (v l) \quad (2)$$

At the point of sheet breakup, a ligament will have width  $w$  and thickness  $h$ ; this ligament will then assume an approximate circular cross section having an area of  $\pi R^2$ . Therefore,

$$w = \pi R^2 / h \quad (3)$$

Substituting (2) into (3),

$$w = \pi R^2 v l / F \quad (4)$$

From the wave equation,

$$\begin{aligned} f &= v / (2w) \\ &= F / (2\pi R^2 l) = 90 F / (\theta L (\pi R)^2) \end{aligned} \quad (5)$$

Rayleigh's instability theory predicts that the wave length for which the instability occurs in the minimum time is given approximately by  $w = 9R$  (11). Using this, the diameter of a resulting droplet ( $D$ ) can be calculated from a mass balance:

$$D = 3.8 R \quad (6)$$

Substituting Eq.(6) into Eq.(5),

$$f = 132 F / (0 L D^2) \quad (7)$$

Assuming typical values for the process parameters ( $F = 20$  gpm,  $L = 1$  m,  $0 = 120$ ,  $D = 2.5$  mm), the estimated vibrational frequency is:

$$\begin{aligned} f &= (132 \times 20 / (120 \times 1 \times 6.25)) \times 68.2 \\ &= 240 \text{ Hz} \end{aligned}$$

The analysis above is highly simplified, with a key assumption being that the sheet breaks up into discrete uniform bands with no interactions between adjacent bands. Also, if the ligament (or band) is wide and irregular, it may subdivide into several smaller ligaments. Nonetheless, the model does point out the important physical parameters and how they interact. There is no easy way to estimate the desired vibrational amplitude because it is related to complicated stability theories. Experimentation should be the rule here.

### 3.5.3.2 Transverse Vibrations

Vibration of the liquor flow can be done either in the direction of or normal to the flow. The resulting waves in the liquor sheet issuing from the nozzle should be in the dilational and sinuous modes, respectively. Fig. 3.36 characterizes the dilational and sinuous wave modes.

Conceptually, the dilational mode would be expected to give a narrower drop size distribution, since the breakup of the sheet into ligaments should occur at the points of minimum thickness. These are not randomly placed because of the vibrations imposed on the system. The subsequent breakup of ligaments into drops will still be random events. On the other hand, the sinuous wave mode maintains a constant sheet thickness, implying that sheet breakup will be a random phenomenon going to the ligaments, which then randomly break up into drops.

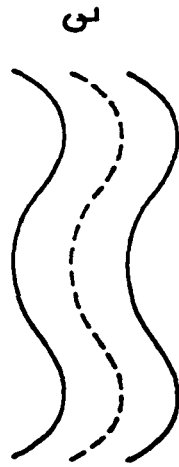
The sinuous wave mode was examined first because, conceptually, it is generated by vibrations normal to the flow (transverse), and it is easier to accomplish. A splashplate nozzle was vibrated by a two-knobbed cam rotating with a motor shaft. Vibrational frequency was varied from 0 to 93 Hz. Splashplate displacements (i.e. vibrational amplitudes) were about 0.1 and 0.2 mm.

Experimental conditions and results are listed in Table 3.11. Tests 54A and 54B employed a 0.1 mm displacement and showed no significant change in median drop size or normalized standard deviation with changes in vibrational frequency. We did, however, observe that vibrations caused the liquor sheets to break up sooner than without vibration. Test 54C, which had a 0.2 mm vibrational amplitude, did form liquor bands whose width decreased with increasing frequency. Nonetheless, median drop size was unaffected.

FIG. 3.36

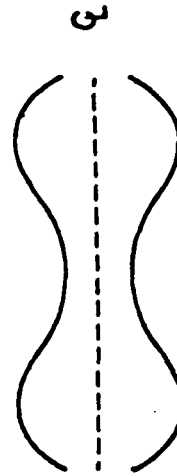
# VIBRATORY ASSIST

Sinusous Wave Generation – Wave-like Disturbances to Upper and Lower Surfaces of the Sheet Are in Phase



– Vibration in Direction Normal to Plane of the Sheet

Dilational Wave Generation – Wave-like Disturbances to Upper and Lower Surfaces of the Sheet Are Out of Phase



– Vibration in Direction of Liquor Flow (i.e. pulsation of Liquor flow)

An alternative mode of generating transverse waves was examined using an air-driven vibrator (Test 55). Frequencies up to 130 Hz were tried with the splashplate nozzle. Results showed a significant effect on the liquor sheet, but not on the drop size distribution. At 130 Hz, bands of liquor formed. The width of the bands was inversely proportional to the vibrational frequency. The bands broke into smaller pieces, resulting in the usual wide range of drop sizes.

Table 3.10 lists results for median drop size using the air-driven vibrator. Median drop size increased by 12 to 30%, and the width of the size distribution increased by 16 to 30%, as measured by the normalized standard deviation. The trend here is not what we would have expected and remains unexplained.

### **3.5.3.3 Axial Vibrations**

The dilational wave mode was examined by imposing axial vibrations (i.e. pulses) on the liquor flow. This mode is very difficult to accomplish experimentally, as evidenced by the lack of results reported in the literature (10). We conceptualized, designed, and built an apparatus to mechanically pulse the liquor flow to a commercial splashplate nozzle under controlled conditions of vibrational frequency and amplitude. A detailed sketch of the vibrator assembly is shown in Fig. 3.37.

Black liquor is fed through a tee which precedes the nozzle. At the other end of the run of the tee (opposite the nozzle) is the vibrator assembly. Between the tee and the vibrator assembly is a variable volume section which seals the vibrator from the liquor in the tee and which can vary the volume of liquor present in the tee at any instant in time. This variable volume section is a section of 3/4-inch CT Flex @ corrugated tubing. Vibration (i.e. reciprocating motion of the connector rod) is accomplished with a rotating triangular cam. A rectangular slot is machined in the rod so that the cam can rotate within it. The slot is so dimensioned that a vertex of the cam will displace the rod by a small distance, effectively giving the amplitude in flow variation. As the cam rotates, the preceding vertex pushes the rod (slot) in the opposite direction, by the same distance. This gives the negative variation in amplitude. The amplitude that is achieved is dependent upon the volume change in the variable volume section and the liquor feed rate. The speed of rotation of the cam by a variable speed motor determines the frequency of pulsation (vibration) of the black liquor flow.

A key feature of this method of pulsing the flow is that the operator can positively control the amplitude and frequency of variation. One does not have to rely on a "spring constant" which most other mechanical vibratory methods do. Also, larger amplitudes can be accomplished than what is normally achieved with traditional acoustic or pneumatic vibrators.

Test results with this new nozzle concept are forthcoming and will be reported in the next annual report.

Table 3.11

## TRANSVERSE VIBRATORY ASSISTED SRRAYS

Test	Solids (%)	Flow F1 (gpm)	Pres. P1 (psi)	Temp TC1 (C)	Visc @ T1 (cP)	Splateplate Mode	Nozzle Freq (min -1)	Vibrations Displacement (mm)	Dm mm	s/Dm <sup>1.5</sup>
54A1	60.6	11.0	19.7	86.4	149.1	Std cam	0	0	2.05	0.203
54A2	60.7	10.9	19.8	86.4	152.2	Std cam	900	0.1	2.3	0.211
54A3	60.8	10.9	19.8	87.0	150.5	Std cam	1900	0.1	2.27	0.199
54A4	61.3	10.9	19.8	87.2	161.0	Std cam	3300	0.1	2.25	0.203
54A5	60.9	10.9	20.0	88.0	146.6	Std cam	4500	0.1	2.28	0.205
54A6	61.2	10.9	20.1	88.3	153.0	Std cam	5600	0.1	2.42	0.219
54B1	56.9	12.0	18.7	88.5	78.1	Std cam	0	0	2.12	0.185
54B2	56.9	12.0	18.9	89.7	75.2	Std cam	900	0.1	2.1	0.186
54B3	57.0	12.0	19.0	89.6	76.6	Std cam	1900	0.1	2.1	0.193
54B4	57.4	12.0	18.9	89.7	80.2	Std cam	3300	0.1	2.47	0.204
54B5	57.4	12.0	19.0	89.8	79.8	Std cam	4500	0.1	2.21	0.188
54B6	57.4	11.9	19.0	90.0	80.3	Std cam	5600			
54C1	60.1	12.1	19.0	92.6	65.6	Std cam	0	0	1.88	0.165
54C2	60.1	12.1	18.9	92.4	65	Std cam	900	0.2	2.27	0.219
54C3	60.2	12.0	19.0	93.6	67	Std cam	1900	0.2	1.96	0.168
54C4	60.3	12.0	19.0	93.8	70	Std cam	3300	0.2	1.96	0.220
54C5	60.1	11.9	19.2	92.3	73	Std cam	4500	0.2	1.93	0.193
54C6	60.1	11.8	19.3	92.3	76	Std cam	5600	0.2	1.90	0.172
55A	57.5	13.0	15.1	89.3	79.7	Std Air	0		2.46	0.217
55B	59.2	12.8	15.2	91.0	87.1	Std Air	4200		2.89	0.270
55C	60.4	12.8	15.4	93.6	97.1	Std Air	5400		2.74	0.253
55D	61.1	12.1	15.1	91.6	121.3	Std Air	6600		3.20	0.280





## 4.0 CONCLUSIONS

Black liquor spraying characteristics are not sensitive to the type of liquor at the same viscosity. Mass median diameter was shown to depend most strongly upon nozzle type and pressure, along with liquor viscosity. A weak dependence upon nozzle diameter was also observed.

There exists a transition temperature 6-9 C above the atmospheric boiling point of black liquor above which median droplet size exhibits a 20% stepwise decrease; the normalized standard deviation remains unchanged at 0.20. This effect is accompanied by a noticeable change in the physical appearance of the spray. The normally planar spray sheet becomes oval in cross-section, and, for a splashplate nozzle, the central plane of the sheet comes off the plate at a 20 to 40 degree angle, rather than at zero degrees. Correlations for the flow/pressure drop characteristics of nozzles operating above the transition temperature must be based on liquor vapor pressure instead of atmospheric pressure.

Consideration of alternative commercial nozzles uncovered none which featured improved control over median diameter and width of the diameter distribution. The Delavan Raindrop® did give a coarser-than-normal spray.

Configuration of a splashplate type nozzle to give two parallel liquor sheets, which subsequently break up into two distinct droplet distributions, gave a larger median drop size than a single splashplate nozzle, if there was sheet interaction. If there was little or no sheet interaction, drop size and size distribution were unchanged from the single nozzle case. Under the conditions run, no bimodal drop size distributions were detected.

Geometric modification of the surface of a splashplate nozzle to alter drop size and size distribution at near-normal spraying temperatures proved ineffective. However, using multiple cylindrical pegs mounted normal to the splashplate surface gave a 25% reduction in median diameter, with a 0-30% increase in the width of the distribution. These were attributed to the formation and breakup of multiple jets rather than a sheet of liquor.

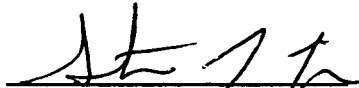
The use of vibratory assist with vibrations transverse to the liquor flow resulted in a shortening of the breakup length of the liquor sheet. For mechanically induced vibration by a cam, little or no change in drop diameter or size distribution resulted. Using an air vibrator actually gave a 15-30% increase in diameter and distribution width, counter to expectation.

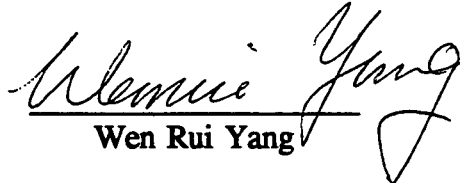
Use of axial vibrations is expected to be more effective in reducing the randomness of droplet formation, resulting in a narrower distribution. Achieving this mode of operation will require an "invention", and this is presently being pursued.


## 5.0 REFERENCES

1. Empie, H.J., Lien, S.J., Yang, W., Samuels, D.B., and Adams, T.N., "Kraft Black Liquor Delivery Systems Report No. 3," US DOE Contract No. DE-FC02-88CE40839, IPST (Dec. 1991).
2. Adams, T.N., Empie, H.J., Lien, S.J., and Spielbauer, T.M., "Kraft Black Liquor Delivery Systems Report No. 2," US DOE Contract No. DE-FC02-88CE40839, IPST (Dec. 1990).
3. Adams, T.N., Empie, H.J., Obuskovic, N., and Spielbauer, T.M., "Kraft Black Liquor Delivery Systems Report No. 1," US DOE Contract No. DE-FC02-88CE40839, IPST (Feb. 1990).
4. Fricke, A.L., "Physical Properties of Kraft Black Liquors: Final Report -- Phase I and II," DOE Report No. DOE/CE40606-T5 (DE88002991), 1987.
5. Crapper, G.D., Dombrowki, N., and Pyott, G.A.D., Proc. Roy. Soc. London A342, 209-224 (1975).
6. Crapper, G.D., and N. Dombrowski, Int. J. Multiphase Flow 10 (6), 731-736 (1984).
7. Mason, B.J. and Brownscombe, J.L., "Product of Uniform Size Drops at a Controllable Freq. & Spacing from a Vibrating Capillary," J. Sci. Instr. 41 (1964).
8. Lin, S.P. and Woods, D.R., "Induced Stomizn," ICLASS-91 (Gaithersburg, MD), 383 (1991).
9. Schneider, J.M. and Hendricks, "Source of Uniform-Sized Liquor Droplets," Rev. Sci. Instr. 35 (10), 1349 (1964).
10. Dressler, J.L., "Stomization of Liquid Cylinders, Cones, and Sheets by Acoustically-Driven, Amplitude-Dependent Instabilities," ICLASS-91 (Gaithersburg, MD), 397 (1991).
11. Rayleigh, L., Proc. Lond. Math. Soc. 10, 4 (1878).
12. Bennington, C.P.J., and Kerekes, R.J., "Effect of Temperature on Drop Size of Black Liquor Sprays," Proc. Int'l Chem. Recov. Conf. (New Orleans), TAPPI/CPPA, 345-354 (1985).
13. Hough, G. (ed.), Chemical Recovery in the Alkaline Pulping Processes, TAPPI Press, Atlanta, (1985).
14. Ruiz, F. "A Few Useful Relations for Cavitating Orifices," ICLASS-91 (Gaithersburg, MD), paper 65, 595-601 (1991).

  
H. Jeff Empie

  
Steven J. Lien

  
Wen Rui Yang

  
Douglas B. Samuels

IPST HASELTON LIBRARY



5 0602 01055576 3